A scaling theory of trait evolution

W. Bryan Jennings*

Department of Evolution, Ecology, & Organismal Biology, University of California, Riverside, United States

*Correspondence: bryan.jennings@ucr.edu

Abstract

A graphical scaling model, named the "geometric-similarity-first model," is developed to explain allometric trait divergence over recent evolutionary time. According to the model, traits first undergo geometric scaling with body size changes. In step two, traits go through evolutionary allometric scaling owing to a "re-optimization" process caused by directional selection. Three predictions of the model are: geometric similarity precedes evolutionary allometry, geometric similarity is a temporary phase, and all allometric traits undergo geometric scaling during initial divergence. All predictions were supported by data for three locomotor traits in pygopodid lizards. An implication of these results is that geometric scaling, driven by natural or sexual selection, may be a mechanism for peak shifts on an adaptive landscape. Given the ubiquity of body size variation in nature, this hypothetical process, termed "niche scaling," may be important to ecological diversification. Applications of the model to Darwin's finches and the Irish Elk are discussed.

Introduction

Since Darwin, evolutionary biologists have attempted to understand the mechanisms and consequences of functional trait divergence because this process has played a major role in creating the diversity of life (Darwin 1859; Lack 1947; Simpson 1944, 1953; Grant 1986; Schluter 2000; Grant and Grant 2008; Losos 2009; Gillespie et al. 2020; Tobias et al. 2021; Grant and Grant 2024). Although these and many other studies have demonstrated natural selection's importance as a mechanism driving trait divergences, parts of this process—especially details of the initial stage of trait divergence—remain obscure (Schluter 2000; Stroud and Losos 2020). The "problem of initial divergence" is far-reaching in evolutionary biology. For example, while we understand that traits must first undergo divergence in isolated populations before they can become adaptations that permit species to occupy new peaks on adaptive landscapes, we still know little about the mechanisms that drive such peak shifts (Simpson 1944, 1953; Schluter 2000). Moreover, there is widespread disagreement among studies about which mechanisms are most important for driving initial divergence in functional traits.

Bivariate allometric analyses of morphological data for conspecific populations and closely related species can reveal distinctive trait divergence patterns, each with its own biomechanical and macroevolutionary implications (Kurtén 1954, 1955; Meunier 1959a, 1959b; Gould 1966, 1971; Klingenberg 1998). For example, if hormonal or genetic changes unlock the usual correlation of growth and development, then a population can evolve a smaller or larger body size without alterations to the shapes of allometric traits; when this occurs, a pair of ontogenetic growth trajectories for traits that exhibit positive ontogenetic allometry will exhibit a 2-D pattern known as "geometric similarity" (Gould 1971; Figure 1A). If the traits instead display negative ontogenetic allometry, then a pair of trajectories can still exhibit geometric

similarity, but it will be a different spatial pattern (Figure 1B). Geometric scaling is considered necessary for phyletic size changes when traits exhibit strong allometry otherwise scaling up or down an ancestral ontogeny in body size may produce maladaptive proportions (Kurtén 1954, 1955; Gould 1966, 1971). While a population or species can evolve smaller or larger body sizes that results in geometric scaling of allometric traits, biomechanical analysis indicates that if a trait changes in size but retains its shape, there may be a reduction in its function (Gould 1971). On the other hand, the evolution of a potentially suboptimal trait shape may be offset by the physiological or ecological advantages associated with attaining a new body size (e.g., Szarski 1964; Gould 1966, 1971; Lande 1979). The co-evolution of body and brain sizes in mammals may be such an example because evolutionary increases in body size result in concomitant increases in brain size, thus bestowing associated advantages (Gould 1966, 1971; Lande 1979). In another example, Sweet (1980) argued that evolutionary downsizing of desmognathine salamanders into new species that are geometrically similar to larger relatives conferred anti-predator benefits to the smaller species thereby facilitating their occupation of novel habitat niches.

Another allometric pattern called “ontogenetic scaling,” which is a form of evolutionary allometry, is thought to occur when an allometric trait scales up or down an ancestral ontogeny (Gould 1971; Klingenberg 1998). An ontogenetic scaling pattern reflects positive evolutionary allometry when the trait exhibits positive ontogenetic allometry (Figure 1C), or it can reflect negative evolutionary allometry when the trait exhibits negative ontogenetic allometry (Figure 1D). Positive and negative evolutionary allometry can also arise when a pair of trajectories become transposed in 2-D space, though the scaling pattern depends on whether the trait shows positive (Figure 1E) or negative (Figure 1F) ontogenetic allometry. When traits undergo a

reorganization of proportions, this can cause ontogenetic trajectories to become independent from the ancestral trajectory and hence exhibit other types of scaling patterns on log-log plots (Gould 1971), a phenomenon later termed “allometric escape” by Tonini et al. (2020). By reorganizing trait proportions at the start of allometric growth, the resulting novel trait shapes may evolve new functions that enable lineages to occupy completely different niches than their closest relatives (Gould 1971; Grant 1986; Tonini et al. 2020). However, this type of trait evolution appears to only occur between highly divergent lineages (Gould 1971; Tonini et al. 2020) and thus may not occur during initial divergence.

Many studies in the literature used the comparative allometric trajectory approach to infer the evolutionary significance of morphological trait divergences among closely related species. Among these studies whose focus was adaptive radiation, the earliest appears to be Boag (1984), who studied the allometries for seven morphological traits in four species of Galápagos ground finches in the genus *Geospiza*. Observing that at least some of the traits (i.e., beak traits) exhibited strong ontogenetic allometry, the author suggested that the 19 (the actual number was 20) statistically significant transpositions found in the results (see Table VIII in Boag, 1984) may have been required to avoid the evolution of maladaptive trait proportions through ontogenetic scaling. However, Boag didn’t discriminate between transpositions that reflected geometric similarity versus those that indicated evolutionary allometry via transposition, which is important because not all the statistically supported transpositions in Boag’s analysis reflected geometric similarity. For example, according to Table VIII in Boag (1984) the *G. scandens* vs. *G. fuliginosa* comparison for the bill length on body weight regression showed a transposition, yet the spatial pattern exhibited by regression lines in Figure 3 of that paper clearly shows evolutionary allometry via transposition, not geometric similarity. Thus, some confusion exists in this paper

pertaining to the author's evolutionary interpretations of the transpositions and therefore it is not clear which scaling pattern best characterizes initial trait divergences in Darwin's finches.

Since Boag's study, there has been a surge in comparative allometry studies that focused on elucidating trait divergence patterns in Australasian lizard and snake radiations. In a study of pygopodid lizards, a group that contains 48 species of elongated and limb-reduced lizards in Australia and New Guinea (Pepper et al. 2025), Jennings (2002) examined scaling patterns in tail length, which is a key locomotor trait for these snake-like lizards that is related to their habitat specializations. Pygopodids showed a strong trend of positive ontogenetic allometry for tail length, and their ontogenetic trajectories exhibited many transpositions most of which reflected positive evolutionary allometry (Jennings 2002). In a later study of pythons, a group of 44 species, Esquerré et al. (2017) found that evolutionary allometry through ontogenetic scaling of body and head traits—important for trophic niches—mainly explained body size and trait divergence in this group at both recent and deep timescales. Similarly, Gray et al. (2019) observed a prevalence of ontogenetic scaling involving traits that characterized body size and cranial shape among species of Australian agamid lizards, a monophyletic group containing at least 108 species. Lastly, a study on monitor lizards and allies by Pavón-Vázquez et al. (2022), who focused on head and limb traits important for diet and habitat specializations, also concluded that ontogenetic scaling was the major mode of trait divergence in this group of 82 species. How can we reconcile the differences in scaling patterns for trait divergences within and among the studies cited above?

During June to August 2020, the present author uncovered preliminary evidence suggesting that initial tail length divergences in pygopodid lizards were the result of geometric scaling—a feature of pygopodid trait divergence that was overlooked in his Ph.D. dissertation

(Jennings 2002). The first line of new evidence concerned the observation of a geometric-similarity-like scaling pattern for relative tail length between two populations of *Pygopus lepidopodus* using data from the dissertation (Appendix 1). The second line of evidence consisted of three additional possible cases of geometric similarity in relative tail length involving recently diverged populations using data from the literature on pygopodids (Appendix 2). The idea that geometric similarity constitutes the initial phase of trait divergence was further corroborated by the present author's discovery that the only conspecific pair of Ground finch populations (i.e., *G. fortis*) in Boag's (1984) Figure 3 also exhibited geometric similarity-like scaling patterns for all three beak traits when they were regressed against body weight—an observation that was not reported in the paper. The resemblance between the tails of pygopodid lizards and beaks of Darwin's finches in terms of their scaling patterns may not be a coincidence. If Gould (1971) was right, then geometric scaling should have produced tails and beaks that were smaller or larger in size than predicted by mechanical analysis when body size increased or decreased, respectively. Thus, one way to account for these results is to hypothesize that, following geometric scaling of these traits, directional natural selection re-optimized the functionality of these traits by increasing their sizes when it was body size that initially increased, or by decreasing their sizes when body size had originally decreased; in short, it is hypothesized that these traits underwent geometric scaling first (Figure 1A) followed by positive evolutionary allometric scaling (Figure 1E). If this is correct, then traits that show negative ontogenetic allometry should first undergo geometric scaling (Figure 1B) followed by negative evolutionary allometric scaling (Figure 1F). This trait divergence hypothesis may be of general interest in evolutionary biology because it can potentially explain the variation in trait scaling patterns observed within and among empirical studies.

Although the present author independently developed this hypothesis, Szarski (1964) proposed a similar hypothesis in a comparative study of amphibian metabolism (Gould 1971, p. 132). Szarski (1964, pp. 124-125) hypothesized that if one species changed in body size while a closely related species remained unchanged, then the following trait divergence scenario would unfold. First, the trait under study—surface area of respiratory organs—would undergo geometric scaling in the former species, meaning that the interspecific regression slope would attain a value of 0.66 for the metabolism-body size scaling relationship. For the second step, Szarski argued that the trait would subsequently evolve compensatory changes in its shape by increasing its area of respiratory surfaces, leading to a higher level of metabolism. Although Szarski's hypothesis aligns with the first (i.e., geometric similarity) step of the present author's hypothesis, the two hypotheses make opposite predictions in the second (i.e., evolutionary allometry) step. Because most of the amphibian species in Szarski's study displayed negative ontogenetic allometry in metabolism (see Figure 3 in Szarski 1964), the present author's hypothesis predicts that the trait would undergo *negative* evolutionary allometric scaling to compensate for changed body size (i.e., evolve an interspecific slope < 0.66). In contrast, Szarski suggested that *positive* evolutionary allometry would occur (i.e., evolve an interspecific slope > 0.66), which would not re-optimize the trait's shape and thus restore its ideal performance level according to biomechanical analysis.

In this paper, we present a new graphical model of the allometric trait divergence process. We then test three of the model's key predictions using an expanded dataset of locomotor-relevant trait data for pygopodid lizards. The results of this study supported the model's predictions and strongly disagreed with the second step of Szarski's (1964) trait divergence

hypothesis. The results also revealed additional insights about the trait divergence process in pygopodids and other well-studied species.

Model

We can concretize the new hypothesis for trait divergence into a graphical model, here called the geometric-similarity-first model or "GSF model." As noted above, how a trait undergoes divergence depends in part on its ontogenetic scaling pattern (positive or negative). Another determinant of how a trait evolves is the direction of body size change (increasing or decreasing) in a population by reference to an ancestral population. Thus, there are four different trait divergence scenarios of the model depending on the trait allometry and the direction of body size change.

Scenario 1: positive ontogenetic (or static) allometry and body size increase.—Gould (1966, 1971) presented many examples of geometric similarity between closely related species, an observation that is consistent with Szarski's (1964, p. 124) view that geometric scaling occurs between established species, not conspecific populations. However, evidence from pygopodid lizards and Darwin's finches cited above suggested that geometric scaling begins before speciation. Additional evidence for this comes from Teissier (1936), who showed that the adults in two lobster populations underwent geometric scaling in claw length (see Figure 7 in Gould 1971). Accordingly, we can hypothesize that when an ancestral population gives rise to two descendant populations, one of which (i.e., population B) evolves a *larger* body size, the model predicts that there will be no change in trait shape in population B; that is, the slope between comparable individuals on the two populational trajectories will reflect geometric similarity

(Phase 1, Figure 2A). The geometric similarity phase is expected to continue beyond the time at which populations A and B become reproductively isolated from each other and thus evolve into species A and B, respectively (Phase 2, Figure 2A). However, because species B presumably experiences a loss of performance in the trait to some degree as a consequence of geometric scaling, it is expected that directional natural selection will favor the evolution of a compensatory *increase* in trait size. This process of trait re-optimization through positive evolutionary allometric scaling characterizes the third and fourth phases of trait divergence. The model predicts that at some point in time the trajectory of species B should partially eclipse or overlap the trajectory of species A thereby exhibiting a "pseudo-ontogenetic scaling" pattern (Phase 3, Figure 2A). However, as was noted above, the predominant scaling pattern among pygopodid lizards and Darwin's finches was positive evolutionary allometry via transposition, which implies that pseudo-ontogenetic scaling must be a transitional form of evolutionary allometry. Thus, the strength of the positive evolutionary allometric relationship is expected to further increase as the trajectory of species B continues *upwards* in trait space until the trait attains an optimal shape for its current ecological utility (Phase 4, Figure 2A). At this stable stopping point the trajectory of species B will be transposed above and to the right of the trajectory of species A (Phase 4, Figure 2A).

Scenario 2: positive ontogenetic (or static) allometry and body size decrease—When an ancestral population gives rise to two descendant populations, one of which (population B) evolves a *smaller* body size, the model predicts that there will be no change in trait shape in population B (Phase 1, Figure 2B). Like Scenario 1, this model predicts that the geometric similarity phase will continue beyond the time at which the populations evolve into different species (Phase 2, Figure 2B), and that Phase 3 is characterized by a pseudo-ontogenetic scaling

pattern at some point during the trait optimization process. However, this scenario predicts that trait size will undergo an evolutionary size decrease, resulting in partially overlapping trajectories (Phase 3, Figure 2B). In the final stage of trait divergence, this scenario predicts that the strength of positive evolutionary allometric scaling will further increase, as the trajectory of species B continues to shift *downwards* until the trait size has been optimized by directional natural selection (Phase 4, Figure 2B).

Scenario 3: negative ontogenetic (or static) allometry and body size increase—Like Scenario 1, when an ancestral population gives rise to two descendant populations, one of which (population B) evolves a larger body size, this model predicts that there will be no change in trait shape in population B (Phase 1, Figure 2C). This model also predicts that the geometric similarity phase will continue beyond the time at which the populations evolve into different species (Phase 2, Figure 2C). Like the previous two scenarios, Phase 3 is characterized by a pseudo-ontogenetic scaling pattern at some point during the trait optimization process. However, this model predicts that trait size will undergo an evolutionary size *decrease*, resulting in partially overlapping trajectories (Phase 3, Figure 2C). In the final stage of trait divergence, this model predicts that the strength of negative evolutionary allometric scaling will further increase, as the trajectory of the larger species continues to shift *downwards* in trait space until the trait size has been optimized (Phase 4, Figure 2C).

Scenario 4: negative ontogenetic (or static) allometry and body size decrease—Like Scenario 2, when an ancestral population gives rise to two descendant populations, one of which (population B) evolves a smaller body size, this version of the model predicts that there will be no change in trait shape in population B (Phase 1, Figure 2D). As with the previous three scenarios, the geometric similarity phase is expected to continue beyond the time at which the populations

evolve into different species (Phase 2, Figure 2D). Phase 3 is characterized by a pseudo-ontogenetic scaling pattern at some point during the trait optimization process. However, this scenario predicts that trait size will undergo an evolutionary size *increase*, resulting in partially overlapping trajectories (Phase 3, Figure 2D). In the final stage of trait divergence, this scenario predicts that the strength of negative evolutionary allometry will further in increase as the trajectory of the larger species continues to shift *upwards* until the trait size has been optimized (Phase 4, Figure 2D).

There are several predictions that can be deduced from the GSF model. The most critical prediction of the model is that initial trait divergence between conspecific populations is characterized by geometric scaling. A second prediction holds that geometric similarity is a temporary phase of trait divergence, which begins prior to speciation and ends soon after speciation. A third prediction is that all allometric traits should undergo geometric scaling at the outset of trait divergence whenever body size changes in a population. Testing the predictions of the GSF model can be readily accomplished using trait data for fossils, contemporary species, or a combination of the two. Paleontological data have the advantage that fossils are often dated, which means that investigators can readily determine the direction of body size change (e.g., Kurtén 1954) and therefore distinguish between trait divergence scenarios that only differ in the direction of body size change (i.e., between Figure 2A and B, and between Figure 2C and D). Although neontological data are more challenging in this regard, comparative methods (Harvey and Pagel 1991) can be used to infer the body size of the most recent common ancestor for each pair of contemporary conspecific populations or closely related species in a pairwise comparison of allometric trajectories. Note that it is not necessary to know the direction of body size change to test the predictions of the GSF model. What is required to test the model, however, is that the

maximum body size attained by each population or species in a pairwise comparison must be known or estimated.

Results

Maximum body sizes of pygopodid lizards

Table 1 shows two measures of maximum body size—maximum known *SVL*s and $\overline{BW}$s—for 35 pygopodid lizard OTUs. These data suggest that most of the maximum $\overline{BW}$ estimates underestimated the true population values because their associated *SVL* values are less than the maximum known *SVL* for that species. Maximum *SVL* may therefore be a more reliable indicator of maximum body size than maximum $\overline{BW}$.

Testing the null hypothesis of ontogenetic isometry

Another requirement of the geometric-scaling-first model is that functional traits of interest must display positive or negative ontogenetic allometry. The results of three ontogenetic scaling relationships (i.e., ln*Tail* on ln*SVL*, ln*Tail* on ln$\overline{BW}$, and ln$\overline{BW}$ on ln*SVL*) that are relevant to the locomotor abilities of snake-like pygopodid lizards show this to be generally true as detailed below.

The average slope across 32 OTUs in the ln*Tail* on ln*SVL* regressions was 1.28 with a range of 0.88 to 1.56 (Table 2). Only two of the 32 slopes were less than or equal to the null value of 1.00 (i.e., isometry). When the slopes were tested against the null hypothesis of

isometry, 25 (78%) of them reflected statistically significant positive allometry. Average R^2 for the sample was 0.89 (range 0.52 - 0.99). These results showed a marked tendency towards positive ontogenetic allometry in tail length when *SVL* was used as the body size measure. All OTUs in *Delma*, *Lialis*, and *Pygopus* except for *D. hebesa* showed significant positive allometry. In contrast, six of the seven *Aprasia* OTUs had non-significant slopes. *Aprasia* OTUs tended to show a poorer fit between regression lines and data points (average $R^2 = 0.80$) compared to OTUs in *Delma*, *Lialis*, and *Pygopus* (average R^2 values for these genera were 0.90, 0.94, and 0.95, respectively). Despite *A. striolata* having a slope of 1.12 and a reasonably large sample size (n = 39), the slope for this OTU was non-significant though its *p*-value of 0.05 was on the cutoff for significance.

The average slope across 32 OTUs in the ln*Tail* on ln$\overline{BW}$ regressions was 1.44 with a range of 0.81 to 1.87 (Table 3). Only two of the 32 slopes were less than or equal to the null value of 1.00. When the slopes were tested against the null hypothesis of isometry, 26 (81%) of them showed significant positive allometry. Average R^2 for the sample was 0.83 (range 0.57 - 0.98). These results showed pronounced positive allometry in tail length when average $\overline{BW}$ was used as the body size measure. With only two exceptions (*D. hebesa* and *D. desmosa*), OTUs in *Delma*, *Lialis*, and *Pygopus* showed significant positive allometry. In contrast, four of the seven *Aprasia* OTUs had non-significant slopes. *Aprasia* OTUs tended to show a poorer fit between regression lines and data points (average $R^2 = 0.69$) compared to OTUs in *Delma*, *Lialis*, and *Pygopus* (average R^2 values for these genera were 0.84, 0.86, and 0.92, respectively). Despite having a slope that reflected positive ontogenetic allometry (slope = 1.19) and a reasonably large sample size (n = 39), the slope for *A. striolata* was not significantly different from isometry (p = 0.13).

The average slope across 35 OTUs in the ln$\overline{BW}$ on ln*SVL* regressions was 0.76 with a range of 0.45 to 0.90 (Table 4). All OTUs had slopes that showed negative ontogenetic allometry, of which 33 were statistically significant. Only *D. australis* and *D. petersoni* had non-significant slopes, though the *p*-values for both OTUs (p = 0.06 and 0.05, respectively) were nearly significant. Average R^2 for the sample was 0.83 (range 0.57 - 0.95). However, as with the tail length scaling results, *Aprasia* OTUs tended to show a poorer fit between regression lines and data points (average R^2 = 0.73) compared to OTUs in *Delma*, *Lialis*, and *Pygopus* (average R^2 = 0.85, 0.88, and 0.91, respectively). These results showed a strong trend of negative allometry in average body width.

Scaling relationships in pairwise OTU comparisons

Figure 3 shows 21 pairwise comparisons of ontogenetic trajectories for the three different scaling relationships (i.e., ln*Tail* on ln*SVL*, ln*Tail* on ln$\overline{BW}$, and ln$\overline{BW}$ on ln*SVL*) involving OTUs in the *Aprasia repens* group. Of these, 18 plots yielded unambiguous scaling patterns when *SVL* was used as the criterion of body size (Figure 3; Table 5). Eight plots (Figure 3A-C, F, and N-Q) showed statistically supported geometric similarity (all ages) patterns, two (Figure 3J and K) reflected geometric similarity (adults) patterns, six (Figure 3D-E, L-M, R, and T) exhibited evolutionary allometry overlap (slopes equal) patterns, and two (Figure 3S and U) demonstrated evolutionary allometry transposition (all ages) patterns. The predominant scaling pattern was geometric similarity (10/18 pairs) followed by evolutionary allometry overlap (6/18 pairs) and then evolutionary allometry transposition (2/18 pairs). Note that all three *A. repens* vs. *A. rostrata* comparisons showed statistically significant transpositions (Figure 3G-I), but they could

not be interpreted because both OTUs had the same maximum *SVL* (see Table 1) and so could not be classified as geometric similarity or evolutionary allometry transposition (all ages). In contrast, plots Figure 3R and T did not have ambiguous interpretations in this regard (i.e., they are evolutionary allometry overlap regardless) even though it is not clear which body size metric (i.e., *SVL* or $\overline{BW}$) may be more appropriate to use in these cases. If we exclude the plots in Figure 3G-I, S, and U because of their uncertainties as to which OTU is the larger OTU in a pairing, then the distribution of observed scaling pattens becomes 8/16 pairs exhibited geometric similarity (all ages) 2/16 pairs showed geometric similarity (adults), and 6/18 pairs reflected evolutionary allometry overlap (slopes equal). The results of this more conservative analysis are like the first analysis with all data included except that they do not include two plots (Figure 3S and U) with uninterpretable transpositions. Note that many pairwise comparisons involving tail length (i.e., Xs in Table 5) were not possible because one or both OTUs lacked sufficient tail length data (i.e., too many specimens had missing or regenerated tails).

Figure 4 shows 18 pairwise comparisons of ontogenetic trajectories for the three different scaling relationships (i.e., ln*Tail* on ln*SVL*, ln*Tail* on ln$\overline{BW}$, and ln$\overline{BW}$ on ln*SVL*) involving OTUs in the southeastern Australia *Aprasia* group. All plots yielded unambiguous scaling patterns when *SVL* was used as the criterion of body size (Figure 4; Table 6). Two plots (Figure 4C and G) showed statistically supported geometric similarity (all ages) patterns, two (Figure 4D and H) exhibited evolutionary allometry overlap (slopes equal) patterns, one (Figure 4B) exhibited an evolutionary allometry overlap (slopes not equal) pattern, ten (Figure 4A, F, and I-P) showed evolutionary allometry transposition (all ages) patterns, two (Figure 4Q and R) exhibited evolutionary allometry transposition (adults) patterns, and one (Figure 4E) showed an evolutionary allometry transposition (juveniles) pattern. The predominant scaling pattern was

evolutionary allometry transposition (13/18 pairs) followed by evolutionary allometry overlap (3/18 pairs) and then geometric similarity (2/18 pairs). In 12 of the plots (Figure 4G-R; Table 6) it was not clear which body size metric may be more appropriate to use in these cases. Thus, if we exclude these plots from consideration, then the distribution of observed scaling patterns becomes one geometric similarity (all ages), one evolutionary allometry overlap (slopes equal), one evolutionary allometry overlap (slopes not equal), two evolutionary allometry transposition (all ages), and one evolutionary allometry transposition (juveniles). Like the full-data results, evolutionary allometry transposition was the most prevalent scaling pattern (3/6 pairs) followed by evolutionary allometry overlap (2/6 pairs) and then geometric similarity (1/6 pairs). Overall, the relative proportions of each scaling pattern type are roughly similar between the full-data and reduced-data analyses with the exception that evolutionary allometry transposition was conspicuously the most prevalent pattern in the full-data analysis.

Figure 5 shows 15 pairwise comparisons of ontogenetic trajectories for the three different scaling relationships (i.e., ln*Tail* on ln*SVL*, ln*Tail* on ln$\overline{BW}$, and ln$\overline{BW}$ on ln*SVL*) involving OTUs in the *Delma australis*, *D. fraseri*, and *D. impar* groups. When *SVL* was used as the criterion of body size, scaling patterns could be deduced from twelve of the plots (Figure 5A-C and G-O; Table 7). In contrast, scaling patterns for Figure 5D-F could not be determined because *D. petersoni* and *D. fraseri* displayed the same maximum *SVL*. Of the 12 plots that had unambiguous scaling patterns, four (Figure 5A, I, and M-N) showed an evolutionary allometry overlap (slopes equal) pattern, four (Figure 5B-C, L, and O) reflected an evolutionary allometry overlap (slopes unequal) pattern, three (Figure 5G-H and J) depicted an evolutionary allometry transposition (all ages) pattern, and one (Figure 5K) exhibited an evolutionary allometry transposition (adults) pattern. Thus, 8/12 plots showed some form of evolutionary allometry

overlap while the other four plots exhibited evolutionary allometry transposition. In all 18 plots, it was not clear which body size metric may be more appropriate to use in these cases therefore it was not possible to examine a reduced dataset for these groups.

Figure 6 shows 30 pairwise comparisons of ontogenetic trajectories for the three different scaling relationships (i.e., ln*Tail* on ln*SVL*, ln*Tail* on ln$\overline{BW}$, and ln$\overline{BW}$ on ln*SVL*) involving OTUs in the *Delma nasuta* group. All plots yielded unambiguous scaling patterns when *SVL* was used as the criterion of body size (Figure 6; Table 8). Eleven plots (Figure 6A-C, M-N, P-Q, S-T, and Y-Z) showed statistically supported geometric similarity (all ages) patterns, one (Figure 6J) exhibited a geometric similarity (juveniles) pattern, seven (Figure 6G-I, K, X, AA, and DD) reflected evolutionary allometry overlap (slopes equal) patterns, nine (Figure 6E-F, L, O, R, U, W, and BB-CC) depicted evolutionary allometry transposition (all ages) patterns, and two (Figure 6D and V) showed evolutionary allometry transposition (adult) patterns. The predominant scaling pattern was geometric similarity (12/30 pairs) closely followed by evolutionary allometry transposition (11/30 pairs) and then evolutionary allometry overlap (7/30 pairs). In three of the plots (Figure 6BB-DD; Table 8) it was not clear which body size metric may be more appropriate to use in these cases. If we exclude these plots from consideration, then the distribution of observed scaling patterns stays essentially the same as the full-dataset results, only with the minor exceptions that six evolutionary allometry overlap (slopes equal) and seven evolutionary allometry transpositions (all ages) were counted instead of seven and nine, respectively.

Figure 7 shows 9 pairwise comparisons of ontogenetic trajectories for the three different scaling relationships (i.e., ln*Tail* on ln*SVL*, ln*Tail* on ln$\overline{BW}$, and ln$\overline{BW}$ on ln*SVL*) involving OTUs in the *Delma tincta* group. When *SVL* was used as the criterion of body size, scaling

patterns could be determined from six of the plots (Figure 7A-C and G-I; Table 9). In contrast, scaling patterns for Figure 7D-F could not be determined because *D. borea* and *D. pax* had the same maximum *SVL*. Of the six plots that had unambiguous scaling patterns, four (Figure 7A, G-I) showed geometric similarity (all ages) patterns, one (Figure 7C) exhibited an evolutionary allometry overlap (slopes equal) pattern, and one (Figure 7B) reflected an evolutionary allometry overlap (slopes not equal) pattern. Thus, the predominant pattern was geometric similarity (4/6 plots) followed by evolutionary allometry overlap (2/6 plots).

Figure 8 shows 12 pairwise comparisons of ontogenetic trajectories for the three different scaling relationships (i.e., ln*Tail* on ln*SVL*, ln*Tail* on ln$\overline{BW}$, and ln$\overline{BW}$ on ln*SVL*) involving OTUs in the *Lialis* and *Pygopus lepidopodus* groups. All plots yielded unambiguous scaling patterns when *SVL* was used as the criterion of body size (Figure 8; Table 10). Six plots (Figure 8A-B, F, and J-L) showed statistically supported geometric similarity (all ages) patterns, three (Figure 8C and E) exhibited geometric similarity (adults) patterns, two (Figure 8H and I) depicted evolutionary allometry transposition (all ages) patterns, and one (Figure 8G) exhibited an evolutionary allometry transposition (adult) pattern. The predominant scaling pattern was geometric similarity (9/12 pairs) followed by evolutionary allometry transposition (3/12 pairs). In the three *L. jicari* vs. *L. burtonis* (dry biome) plots (Figure 8G-I) it was not clear which body size metric may be more appropriate to use in these cases. If we exclude these plots from consideration, then all observed scaling patterns reflected one form of geometric similarity or another.

Figure 9 shows 30 pairwise comparisons of ontogenetic trajectories for the three different scaling relationships (i.e., ln*Tail* on ln*SVL*, ln*Tail* on ln$\overline{BW}$, and ln$\overline{BW}$ on ln*SVL*) involving OTUs in the *Pygopus nigriceps* group. All plots yielded unambiguous scaling patterns when *SVL*

was used as the criterion of body size (Figure 9; Table 11). Eight plots (Figure 9B-D, J-K, O, V, and BB) showed statistically supported geometric similarity (all ages) patterns, three (Figure 9A, L, and N) exhibited geometric similarity (adults) patterns, four (Figure 9M, S, Y, and CC) depicted EA overlap (slopes equal) patterns, two (Figure 9G and P) showed EA overlap (slopes not equal) patterns, eleven (Figure 9E-F, I, Q-R, T-U, W-X, AA, and DD) reflected evolutionary allometry transposition (all ages) patterns, and two (Figure 9H and Z) exhibited evolutionary allometry transposition (juveniles) patterns. The predominant scaling pattern was evolutionary allometry transposition (13/30 pairs) closely followed by geometric similarity (11/30 pairs) then evolutionary allometry overlap (6/30 pairs). In 15 of the plots (Figure 9P-DD); Table 11) it was not clear which body size metric may be more appropriate to use in these cases. Thus, if we exclude these plots from consideration, then the distribution of observed scaling patterns among the remaining 15 plots becomes six geometric similarity (all ages), three geometric similarity (adults), one EA overlap (slopes equal), one evolutionary allometry overlap (slopes not equal), three evolutionary allometry transposition (all ages), and one evolutionary allometry transposition (juveniles).

Testing the predictions of the GSF model

Prediction 1: geometric similarity precedes evolutionary allometry

Figure 10 shows the prevalence of scaling patterns for ln*Tail* on ln*SVL* relationships by divergence time interval. When all OTU pairs that had one member with a larger maximum *SVL* than the other OTU are considered (i.e., full dataset), we can see that 75% of the pre-speciation (interpopulational) pairs exhibited geometric similarity (all ages) while the other 25% showed

geometric similarity (adults only) patterns, respectively (Figure 10A; Supplementary Tables 1-2). OTU pairs within the next older divergence time interval (i.e., 2-3 mya) also showed only geometric similarity (all ages) patterns. When all problematic OTU pairs (i.e., those in which it was not clear which OTU had the larger maximum body size) were excluded from the analysis (i.e., reduced dataset), the results largely mirrored those of the full dataset (Figure 10B; Supplementary Tables 1 and 3). These results suggest that geometric similarity preceded evolutionary allometry for ln*Tail* on ln*SVL* in pygopodid lizards as the model predicted.

Figure 11 shows the prevalence of scaling patterns for ln*Tail* on ln$\overline{BW}$ relationships by divergence time interval. When scaling patterns for the full dataset are first considered, we can see that 100% of the interpopulational pairs exhibited the geometric similarity (all ages) pattern (Figure 11A; Supplementary Tables 1 and 4). Moreover, during the 2-3 mya interval 2/3 of the OTU pairs also exhibited geometric similarity (all ages) while 1/3 showed evolutionary allometry overlap (slopes equal). However, closer scrutiny of these results reveals that the two geometric similarity pairs (*Delma butleri*/*D. haroldi* and *D. pax*/*D. desmosa*) arose approximately 2 mya while the evolutionary allometry overlap pair (*Aprasia pseudopulchella*/*A. parapulchella*) underwent speciation earlier at ~3 mya (Supplementary Table 4). Thus, according to these results geometric similarity patterns exclusively prevailed from the outset of trait divergence until about 2 mya. When the reduced dataset is examined, we can see that the results largely reflected the full dataset results with respect to the prevalence of geometric similarity-type patterns (Figure 11B; Supplementary Tables 1 and 5). Together, these findings suggest that tail length initially changed with average body width via geometric scaling and not by evolutionary allometric scaling.

Figure 12 shows the prevalence of scaling patterns for ln$\overline{BW}$ on lnSVL relationships by divergence time interval. When scaling patterns for the full dataset are considered, we can see that 50% of the interpopulational pairs exhibited geometric similarity (all ages) while the other 50% showed geometric similarity (adults only) patterns, respectively (Figure 12A; Supplementary Tables 1 and 6). Moreover, during the 2-3 mya interval 2/3 of the OTU pairs also exhibited geometric similarity (all ages) while 1/3 showed evolutionary allometry via transposition (all ages). However, divergence time estimates suggest that the two geometric similarity pairs (*Delma butleri*/*D. haroldi* and *D. pax*/*D. desmosa*) arose ~2 mya while the evolutionary allometry transposition pair (*Aprasia pseudopulchella*/*A. parapulchella*) underwent speciation earlier at ~3 mya (Supplementary Table 6). Thus, once again we see that only geometric similarity-type patterns are apparent for OTUs with pre-speciation to 2 mya divergence times. When the reduced dataset is examined, we can see that the results closely resembled the full dataset results except that all seven OTU pairs in the 2-3 mya time interval showed geometric similarity patterns (Figure 12B; Supplementary Tables 1 and 7). These findings show that during initial trait divergence ln$\overline{BW}$ on lnSVL relationships exhibited geometric similarity rather than evolutionary allometry as predicted by the model.

Prediction 2: Geometric similarity is a transient phase of trait divergence

For all three locomotor-relevant traits, we can see that the prevalence of geometric similarity (in all forms) largely declines as divergence times increase, whereas the prevalence of evolutionary allometry-type patterns increases as divergence times increase (Figures 10-12). These observations are consistent with the idea that geometric similarity is a temporary phase of key

trait divergence rather than a stable evolutionary end point. Moreover, if we assume that all interpopulational OTU pairs defined in this study represent conspecific populations rather than closely related species, then we can see that pygopodid lizards exhibited some form of geometric similarity for all three locomotor-relevant traits just before and after the time of speciation (Figs 10-12), thereby adding further support to this prediction.

Prediction 3: all allometric traits undergo geometric scaling with body size changes

If we examine the ln*Tail* on ln*SVL*, ln*Tail* on ln$\overline{BW}$, and ln$\overline{BW}$ on ln*SVL* scaling relationships for 36 OTU pairs that have divergence time estimates, we can see that all four OTU pairs with pre-speciation-level divergences and two of the three pairs with 2-3 mya divergence times only showed geometric similarity patterns (Figure 13A; Supplementary Tables 1 and 8). Closer inspection of these results reveals that the two OTU pairs with ~2 mya divergence times (*Delma butleri*/*D. haroldi* and *D. pax*/*D. desmosa*) only showed geometric similarity patterns while a third OTU pair that had a ~3 mya divergence time (*Aprasia pseudopulchella*/*A. parapulchella*) exhibited a mixture of geometric similarity and evolutionary allometry patterns (Supplementary Table 8). Therefore, all six OTU pairs with divergence times ranging from pre-speciation to ~2 mya only exhibited geometric similarity patterns, which is consistent with the model's prediction. However, another OTU pair, *L. burtonis* (wet biome vs. *L. jicari*, which also only showed geometric similarity patterns, departed from this pattern owing to its estimated divergence time of 16 mya (Figure 13A; Supplementary Table 8). Seen another way, 28/30 OTU pairs with divergence times greater than ~2 mya exhibited either a mixture of geometric similarity and EA patterns, or EA-only scaling patterns. When we examine the reduced data set,

we can see that all OTU pairs in the pre-speciation and 2-3 mya divergence time intervals only showed geometric similarity patterns (Figure 13B; Supplementary Table 9). Accordingly, the results displayed in Figure 13 mainly show geometric similarity patterns during the initial stage of trait divergence thereby largely in agreement with this prediction.

Geography of trait scaling patterns

In both the full and reduced datasets, the seven OTU pairs with the most recent divergence times (i.e., pre-speciation to ~3 mya) exhibited non-sympatric distribution patterns (Supplementary Tables 8-10). Of the 21 scaling patterns elucidated from these OTU pairs, 19 showed some form of geometric similarity. Within this set, all four pre-speciation OTU pairs as well as the two species-level OTU pairs with the shallowest estimated divergence times (~2 mya) in the group (i.e., *Delma butleri*/*D. haroldi* and *D. pax*/*D. desmosa*) exhibited parapatric or allopatric populations and only displayed geometric similarity for the three locomotor traits (Supplementary Tables 8-10). These results suggest that initial trait divergence is characterized by OTUs with non-sympatric distributions, and which underwent geometric scaling for all three traits. The *A. pseudopulchlla*/*A. parapulchella* pair, which has a ~3 mya divergence time and an allopatric distribution, exhibited a mixture of geometric similarity and evolutionary allometry patterns. In the ~6-7 mya divergence time category, one OTU pair in the *D. tincta* group had a sympatric distribution while one pair in the *D. impar* group had an allopatric distribution. The former pair displayed a mixture of geometric similarity and evolutionary allometry patterns for the three traits, while the latter showed only evolutionary allometry patterns. For the divergence time spanning the 8 to 11 mya range, only one pair (*D. nasuta*/*D. haroldi*) showed a sympatric

distribution while the other pairs exhibited parapatric and allopatric patterns. Lastly, in the 12 to 16 mya range, we can see that there were two pairs showing sympatry (*D. nasuta*/*D. butleri* and *L. burtonis* [wet biome]/*L. jicari*), one that exhibited a parapatric distribution, and two that had allopatric distributions.

Discussion

Ontogenetic allometry of tail length and body width in pygopodid lizards

All three locomotor-relevant traits in pygopodid lizards showed strong allometric trends during post-natal development. Tail length scaled in a positive allometric manner for nearly all OTUs regardless of whether lnSVL or ln$\overline{BW}$ was used as the body size measurement. In contrast, ln$\overline{BW}$ on lnSVL showed negative allometry across all OTUs. The slopes for the few OTUs that did not follow these trends may have been poorly estimated due to low sample size and samples that were biased towards one size-age class. For example, slopes for *A. litorea*, *A. rostrata*, and *D. hebesa* may have bucked the positive allometry trend in ln$Tail$ on lnSVL regressions owing to their small sample sizes. In other cases, some samples (e.g., *A. parapulchella* and *A. pseudopulchella*) lacked juveniles, which may have led to biased slope estimates.

Geometric scaling precedes evolutionary allometry

Pairwise comparisons of allometric trajectories for the three locomotor-relevant traits in pygopodid lizards revealed substantial variation in their scaling patterns. Of the 112 comparisons, there were 42 instances of geometric similarity (all forms), 26 cases of evolutionary allometry via overlap (all forms), and 44 examples of evolutionary allometry via

transpositions (all forms). Moreover, all three major scaling patterns could be found in most species groups in this study, which suggests that there was much lability in the evolution of ontogenetic trajectories in recent evolutionary time. When we examined the prevalence of each type of scaling pattern by divergence time interval, we could see that all OTU pairs with the most recent divergence times (i.e., pre-speciation and ~2 mya level divergences) only exhibited geometric similarity patterns. This observation supports Gould's (1971) rule that when two closely related populations or species differ in body size, and a trait of interest scales in an ontogenetic allometric manner, we expect the two OTUs to be geometrically similar to each other. In contrast, we only observed instances of evolutionary allometry for OTU pairs that exhibited older divergence times.

Did trait divergence begin before or after speciation? If we assume that each "pre-speciation" OTU pair represents a pair of conspecific populations that have not yet become genetically isolated from each other—that is, they have not yet become different species, then we can see that trait divergence via geometric scaling began before speciation in pygopodid lizards, as the model predicted. Moreover, geometric scaling apparently continues just past the point of speciation. The data for pygopodid lizards suggested that this initial period of divergence—characterized by geometric similarity—was estimated to last at least 2-3 million years since the populations began to diverge.

Geometric similarity is a transient but long lasting phase in trait divergence

The pygopodid data showed that initial trait divergence started with a geometric similarity phase as the model predicted. But what happens from there—is geometric similarity a stable evolutionary stage or does the trait undergo further modifications? Again, the pygopodid data

supported the model, as we saw that the prevalence of geometric similarity—in all three traits—attained their highest levels at the beginning of the divergence process before undergoing abrupt declines as divergence times increased, along with concomitant increases in the prevalence of various forms of evolutionary allometry (i.e., overlaps and transpositions of ontogenetic trajectories).

Although the pygopodid data showed that geometric similarity is a temporary phase of trait divergence, the duration of this phase—lasting at least several million years—is still a long evolutionary timespan for organisms to cope with their environments using presumably "biomechanically inferior" trait versions owing to geometric scaling. This suggests that allometric traits in populations that underwent geometric scaling still retained enough of their original function to permit those organisms to have normal lives. Still, however, the model predicts that the geometric similarity phase will eventually transition into an evolutionary allometry phase as directional natural selection (e.g., intraspecific competition or predation) hones the shapes of these traits in the incremental manner envisioned by Darwin. It seems, therefore, that trait divergence in pygopodids was an evolutionarily slow and gradualistic process, likely attributable to the waiting times for new advantageous mutations to arise, though occasional introgressive hybridization between closely related species could have injected new genetic variation (Grant and Grant 1994, 2024) and thus increased the rate of trait evolution during the re-optimization process.

Curiously, however, we also observed consistent upticks in the prevalence of geometrically similar OTUs in the 12-16 mya divergence time category among analyses, which are intriguing exceptions to the general pattern. One pair, *Lialis burtonis* (wet biome) and *L. jicari*, which had the oldest divergence time of ~16 mya, also exhibited more drastic

610 morphological divergence than was observed for younger OTU pairs that displayed geometric
611 similarity. Specifically, the trunks of *L. jicari* were tapered from mid-body towards the neck in a
612 more extreme fashion than was observed in any specimens of *L. burtonis*, while the heads and
613 snouts of the former species have become far narrower and elongated than was observed in the
614 latter species. These head and body shape differences between the two species suggest that
615 natural selection re-worked these bodily features—possibly owing to having different ecologies.
616 When traits undergo such reorganizations of their proportions, geometric similarity no longer
617 exists (Gould 1971). Thus, the relatively old divergence times between these species coupled
618 with their highly divergent morphologies suggest that these two species showed geometric
619 similarity *via evolutionary convergence* rather than geometric similarity *via initial trait*
620 *divergence*. Moreover, given that selection pressures may have caused their trajectories to escape
621 from the ancestral trajectories, it is questionable to even consider this a case of geometric
622 similarity. Thus, if we assume that these species do not represent cases of geometric similarity
623 via initial trait divergence, then only the most recently diverged populations and species of
624 pygopodids exhibited true geometric similarity for all examined locomotor traits.
625

626 All allometric traits undergo geometric scaling with changes in body size

627 Another prediction of the model holds that all traits showing ontogenetic allometry undergo
628 geometric scaling when there is a change in body size. Of the 36 OTU pairs with estimated
629 allometric relationships for all three traits, the six with the youngest divergence times (i.e., four
630 pre-speciation plus two 2 mya level divergences) exclusively exhibited geometric similarity,
631 which is consistent with the model prediction. However, as mentioned above, the *L. burtonis*

(wet biome population) and *L. jicari* pair stood out as an exception to this pattern owing to evolutionary convergence.

A test of Szarski's trait divergence hypothesis

The pygopodid trait data provided empirical support for the three main predictions of the GSF model, which are primarily concerned about how traits evolve during initial divergence, but what about trait divergence beyond the geometric similarity stage? As we observed earlier, Szarski (1964) hypothesized that a trait exhibiting negative ontogenetic allometry should undergo positive evolutionary allometry following the geometric similarity stage during a re-optimization phase of trait evolution. In contrast, the GSF model predicts that a trait showing negative allometry will instead undergo negative evolutionary allometry during the hypothetical re-optimization phase (see Phases 3 and 4 in Figure 2C-D). We can perform a test of Szarski's prediction by examining the relative frequencies of positive and negative evolutionary allometry scaling patterns for a negative allometric trait in the pygopodid data (i.e., $\ln\overline{BW}$ vs. $\ln SVL$) plots in Figures 4-9. If we remove from our consideration the plots showing the most recently diverged OTU pairs, which displayed geometric similarity patterns for all three locomotor traits, then we can sum the totals of plots showing patterns consistent with positive or negative evolutionary allometry. When we do this, we see that of 31 OTU pairs, 28 of them showed negative evolutionary allometry patterns, while only three showed positive evolutionary allometry patterns. These results largely support step 2 in the GSF model and contradict step 2 in Szarski's hypothesis. Thus, the pygopodid data provide support for both steps in the GSF model.

Choice of body size reference revisited

Selection of a body size reference represents a critically important step in allometry studies (Gould 1974). Choice of body size reference especially matters in this study because we needed to know which OTU in each pair exhibited the larger maximum body size to correctly ascertain their scaling pattern. This study followed tradition in lizard ecomorphology studies by using *SVL* as the measure of body size, but was this measure the most appropriate size reference to use? For most pygopodid OTU pairs this was not a problem because one OTU in those pairs had both the longer maximum *SVL* and larger maximum $\overline{BW}$. However, for most of the other pairs, one OTU had the longer maximum *SVL* while the other had the larger maximum $\overline{BW}$, making it less clear which OTU was larger. Thus, which has the larger body size in these odd couples—the long- and slender-bodied OTU or the short- and stout-bodied OTU?

It turns out that *SVL* is the appropriate body size reference in this study for several reasons. First, there were inconsequential differences between the results obtained from the full and reduced datasets when tested against the three predictions of the model. Second, the backbone of support for the first and second predictions of the model came from the trait scaling patterns of the six most-recently diverged (i.e., ≤ 2 mya) OTU pairs, each of which contained one OTU that was larger than the other OTU in both measures of maximum body size. Third, if $\overline{BW}$ were used as the size reference instead of *SVL*, then the only difference that would result is that the number of cases of geometric similarity would increase somewhat while the number of cases of evolutionary allometry via transposition would decrease. Even allowing this, the data would still uphold the model's predictions. But this is a moot point when it is realized that most of these "new" cases of geometric similarity would not be valid for the following reason. Of the 14 OTU pairs that have one member with the longest maximum *SVL* and the other member the largest

maximum $\overline{BW}$, four of them show evolutionary allometry via overlap patterns for the ln$\overline{BW}$ on ln*SVL* regressions (see Supplementary Table 8). This subset is not a concern for us because the scaling patterns do not change depending on which body size reference is used in these cases. However, it does matter for the remaining ten pairs because interpretations of transposition patterns crucially depend on which size reference is used. Indeed, when *SVL* was used as the size measure, all ten of the problematic pairs exhibited evolutionary allometry via transposition for the ln$\overline{BW}$ on ln*SVL* regressions. If instead, $\overline{BW}$ were used as the size measure, then these transpositions would reflect geometric similarity and thus conflict with Gould's (1971) rule for negative allometric traits; that is, a population that *increases* in *SVL* is expected to also *increase* in $\overline{BW}$ to maintain geometric similarity or, conversely, a population that *decreases* in *SVL* is predicted to also *decrease* in $\overline{BW}$ to maintain geometric similarity (Figure 1B). If this is correct, then it would be unlikely for one OTU to have a longer maximum *SVL* while the other OTU has a larger maximum $\overline{BW}$. Lastly, if *SVL* is used as the body size reference, then the GSF model actually accounts for these ten unusual OTU pairs. For instance, in a scenario whereby the population undergoes a body size increase, then *SVL* and $\overline{BW}$ for that population will initially *increase* during a geometric similarity phase, but then during the subsequent negative evolutionary allometry phase $\overline{BW}$ is expected to *decrease* in size (Figure 2C). Alternatively, if the population undergoes a body size *decrease*, then *SVL* and $\overline{BW}$ for that population will initially *decrease* during the geometric similarity phase, but then during the later negative evolutionary allometry phase $\overline{BW}$ is expected to *increase* in size (Figure 2D).

The GSF model provides new insights into beak evolution in Darwin's finches

As mentioned earlier, observations of tail-scaling data for pygopodid lizards and beak-scaling data for Galápagos ground finches inspired the GSF model. Although Boag's statistical analyses may have suffered from low sample sizes, we can still analyze the plotted regressions shown in Figure 3 of that paper. For this analysis, we will focus on the scaling relationships between three bill traits—bill length, bill depth, and bill width—on body weight because most research on Darwin's finches focused on their beaks (Lack 1947; Grant 1986; Weiner 1995; Grant and Grant 2008); and because all three bill traits showed strong positive allometry (Boag 1984). From the scaling patterns of 30 pairwise comparisons for these traits, which are shown in Figure 3 of Boag (1984), we can see that 22/30 pairs showed patterns consistent with evolutionary allometry while 8/30 pairs exhibited geometric similarity patterns (Table 12). As was noticed by the present author, the two *G. fortis* populations displayed geometric similarity patterns for all three traits in Figure 3 of Boag's paper, which of course are consistent with the first and third predictions of the model. Thus, what requires an explanation are the other five cases of apparent geometric similarity, all of which were at the interspecific level.

Notice that four of the five species pairs in Table 12 that showed geometric similarity included *G. scandens*, the cactus finch. This observation fits the larger pattern in Boag's data, which showed that 12 out of the 20 statistically significant transpositions involved the cactus finch, suggesting that this species is the most divergent in the group. Indeed, the morphological distinctiveness of the cactus finch is demonstrated by its specialized beak morphology, its adaptation to a cactus-based diet rather than the granivorous diets of other ground finches, and its deep phylogenetic divergence compared to other species of ground finches in Boag's study (Grant 1986; Grant and Grant 2008). Thus, like the pygopodid *L. jicari*, the highly divergent cactus finch beaks may represent a case of geometric similarity via convergence (i.e., allometric

escape), rather than geometric similarity via initial trait divergence. Further empirical support for this idea comes from a gene expression study, which showed that the gene that influences beak length is expressed at higher levels in the tips of cactus finch beaks—giving rise to their long and pointed beaks—compared to other ground finches at the same stage of development (Abzhanov et al. 2006; Grant and Grant 2008). Therefore, if we accept that all observations of geometric similarity involving cactus finches in Table 12 represent false cases of geometric similarity *via initial trait divergence*, then the pair of *G. fortis* populations and the *G. magnirostris*/*G. fortis* pair represent the only manifestations of geometric similarity via initial divergence involving the three bill traits. If this is correct, then the GSF model can provide a more complete picture of how the beaks of the storied Darwin's finches evolved. A more rigorous evaluation of this model using raw trait data on Darwin's finches, especially if additional population-level OTUs could be included in analyses, may be instructive.

Does ontogenetic scaling occur in nature?

Several recent comparative allometry studies of squamate reptiles concluded that ontogenetic scaling was the primary mechanism of trait divergence at both recent and deep timescales (Esquerré et al. 2017; Gray et al. 2019; Pavón-Vázquez et al. 2022). At first glance, these reported cases of ontogenetic scaling pose difficulties with the GSF model. However, we may be able to reconcile putative cases of ontogenetic scaling with the model.

According to Gould's (1971) thesis, traits that show "strong" allometry must undergo geometric scaling with changes in body size to avoid adverse fitness consequences of evolving maladaptive trait proportions. A corollary to this is that traits showing relatively "weak" allometry may be permitted to extrapolate up or down an ontogenetic trajectory to new body

sizes. If this is the case, then we can infer that ontogenetic scaling can occur but only when traits show relatively weak allometry. However, there are at least two difficulties with the ontogenetic scaling hypothesis. First, Lande (1985) asserted, based on quantitative genetics theory, that ontogenetic scaling cannot occur when body size is the target of selection. Another reason why ontogenetic scaling seems unlikely to occur is that it would require a developmental "switch" that determines whether ontogeny is constrained to follow a strictly ontogenetic scaling process or a geometric scaling process when a population undergoes an evolutionary shift in body size. If this is correct, then how strong does trait allometry need to be for such a mechanism to initiate the latter process? Although such a developmental switch may exist, there is a simpler explanation for observations of partially overlapping ontogenetic trajectories that have been interpreted as cases of ontogenetic scaling.

If we assume that true ontogenetic scaling does not occur, then how else can we explain partially overlapping allometric trajectories? Consider a scenario in which the maximum body size attained by one population is ~8% larger than another conspecific population. The 8% difference is chosen here because it corresponds to the minimum amount of body size difference observed between pygopodid populations that exhibited statistically supported geometric similarity patterns. If we examine a series of plots showing the ontogenetic trajectories for two populations on log-log plots, which only vary in the strength of ontogenetic allometry, then we can see that a geometric similarity pattern is nearly indistinguishable from an ontogenetic scaling pattern when the allometry is relatively weak—in this case defined as $\alpha = 1.1$ for a population's trajectory (Figure 14). This suggests that it may be particularly challenging to statistically-detect transpositions for traits that show such weak ontogenetic allometry unless large sample sizes are used and the full spectrum of post-natal size-age classes are well represented in samples. On the

other hand, notice that the spacing between the trajectories increases as the strength of the allometry increases, thereby making it easier (visually and statistically) to detect transpositions in the data (Figure 14). In the case of pygopodids, the average α across all OTUs for the two tail length on body size relationships ranged from 1.3 to 1.4 thereby suggesting that tail length is strongly allometric according to Figure 14.

If the GSF model is correct, then another implication of the scenarios illustrated in Figure 14 is that the amount of trait re-optimization via directional natural selection following the geometric similarity phase would be less than that required for a strongly allometric trait, all else equal. This might be why ontogenetic scaling was found to be the dominant scaling relationship in the above-cited squamate studies, especially since none of those studies included intraspecific samples. Thus, the apparent prevalence of ontogenetic scaling in those studies may reflect low sample sizes per species and/or advanced trait divergence stages rather than initial trait divergences. Future studies should examine trait divergences between conspecific populations in these groups, with the largest permissible samples sizes, in an attempt to determine if divergence began with ontogenetic scaling or geometric similarity. There may be negligible difference in the function of a trait that initially diverged via ontogenetic scaling compared to a trait that underwent geometric scaling when the trait is weakly allometric. However, the point here is to suggest that the GSF model may still explain the initial divergence of weakly allometric traits even when ontogenetic scaling patterns are observed in data.

Implications

Adaptive peak shifts through geometric scaling of viability traits

Locomotory adaptations are but one of several types of "viability traits" that enable organisms to exploit trophic and habitat niches located on an adaptive landscape (Bonduriansky 2011). Thus, how did pygopodid species undertake peak shifts that allowed them to occupy different habitat niches? If the adaptive landscape for habitat niches is mainly defined by body size on the X axis and a locomotory-related trait (e.g., tail length or body width) on the Y axis (see Figure 10.4 in Grant and Grant 2008), then there are three main ways for peak (or niche) shifts to occur on this fitness landscape. First, genetic drift can move the mean population phenotype from one peak to another unoccupied peak (Wright 1931, 1932), though this mode of peak shift may only occur when adaptive valleys are shallow and population sizes are small (Schluter 2000). Divergent natural selection on Y caused by spatial variation in environments can also cause peak shifts as studies have shown (Schluter 2000). A third possible mechanism of peak shift is "correlated response," which may occur when directional selection on X drags Y across a fitness valley and onto a new peak (Price et al. 1993). After a review of empirical studies, Schluter (2000) concluded that the evidence largely favored divergent natural selection on Y as being the predominant mode of peak shift.

Peak shifts in habitat use by pygopodid lizards that were driven by genetic drift is an unsatisfactory hypothesis because most species of pygopodids exhibited expansive geographical distributions on the Australian continent with ranges that often encompassed entire ecosystems or biomes (see Ehmann 1992). This leaves us with three selection-based hypotheses to explain habitat peak shifts in pygopodids: direct natural selection on Y (locomotory traits) may have caused correlated changes in X (body size), direct selection on X induced correlated responses in Y, and a combination of these two mechanisms (Gould 1966; 1974; Lande 1979; 1985; Price et al. 1993; Schluter 2000). There is evidence to suggest that some form of selection caused trait

divergence in these lizards. First, correlations between the distributions of the two pygopodid ecotypes along environmental gradients are consistent with the idea that spatially divergent natural selection drove morphological divergence between desert and forest populations of pygopodids (Schluter 2000). And second, the repeated independent evolution of these ecotypes constitutes robust evidence that divergent natural selection caused trait divergence (Gould 1966), though this does not pinpoint the target(s) of selection.

Gould (1971) argued that geometric scaling is a required condition for body size change when traits are strongly allometric, while at the same time the author argued that geometric similarity creates a new problem because it leads to the evolution of biomechanically inferior traits in the population or species that underwent the size change. Thus, at first glance, it seems unlikely that natural selection would select for biomechanically inferior versions of Y, which could then bring about a peak shift. An argument along these lines could be made for pygopodid tails, given that this is an important viability trait, especially in regard to predator evasion (Bauer 1986; Greer 1989; Ehmann 1992; Bamford 1998; Jennings 2002). However, for other organisms such as Darwin's finches, natural selection may still favor a biomechanically inferior version of a beak for a given body size if a smaller or larger version of that trait, in absolute terms, translates to improved fitness. In this case, selection would act on both beak and body size because of the high correlation between the two traits (Grant 1986). This is plausible given that different islands in the Galápagos archipelago have different adaptive landscapes for seed sizes and hardness (Schluter 2000). Thus, a population that colonizes an island with larger and harder seeds may evolve larger body and beak sizes even though the beak shape is not the optimal shape for that body size according to biomechanical analysis. If this is correct, then the absolute size of the beak may be good enough in the short-term to allow a population to gain a foothold in a new

niche (see other examples in Gould 1966 and Sweet 1980), while over subsequent evolutionary time directional selection (via intra- and possibly interspecific competition) can re-optimize the beak shape according to the GSF model. This may help explain why some pygopodid populations and species have persisted for millions of years despite having locomotor traits of presumably sub optimal shapes owing to geometric scaling at the outset of trait divergence.

Given the many advantages of having larger or smaller body sizes (e.g., Rensch 1948; Szarski 1964; Gould 1966, Lande 1979, 1985; Hanken and Wake 1993), it is also possible that natural selection acted only on body size of pygopodids for reasons other than exploiting new habitat niches. Such body size change, in turn, could have induced changes in the sizes (but not shapes) of the locomotor traits as correlated consequences. Although these locomotor traits may have suffered from biomechanical deficits to some degree due to geometric scaling, simply attaining new sizes—like the sizes of finch beaks just discussed—may have allowed the lizards to retain enough function to allow a population to exploit a new habitat niche.

If natural selection targeted Y and X together or only X in pygopodids, then this opens the possibility that peak shifts were accomplished via correlated response to selection acting on X. Simulation-based results in Price et al. (1993) suggested that peak shifts can readily occur via correlated response when either natural selection on X is strong or when the fitness valley is shallow. The finding that pygopodids can survive and reproduce with presumably suboptimal locomotor traits for millions of years suggests that stabilizing selection on Y was not particularly strong, which if true means that Y may have been dragged across shallow fitness valleys to new peaks by moderate to strong selection on X. This is important because it could mean that peak shifts via correlated response were a general feature of ecological diversification in pygopodid lizards.

According to current theory, it is thought that closely related species must first attain some amount of trait divergence (or "initial differences") while they are in allopatry so that ecological character displacement can later cause further adaptive divergence between the two species once they are in sympatry, thereby maintaining their coexistence (Lack 1947; Schluter 2000). The results in this study suggest that geometric scaling may be a general mechanism that produces these initial differences, but are these differences sufficient to facilitate a peak shift? The Delma tincta group may be a good model for understanding the evolution of initial trait divergences in adaptive radiation because this group contains pairs of species that exhibit allopatric and sympatric distributions. Similar to other recently diverged populations and sister species (i.e., those that diverged < 2 mya), the tincta group pair *D. desmosa* and *D. pax* displayed an allopatric distribution and showed geometric similarity patterns for all three locomotor traits. In contrast, while group members *D. branchia* and *D. pax* also display geometric similarity for the three locomotor traits (Appendix 3), theses two species are broadly sympatric across the Pilbara region of Western Australia and have even been found at the same localities (Storr et al. 1990; Maryan et al. 2007; Pepper et al. 2025). The observation that these two species co-occur together strongly implies that they occupy different niches (Grinnell 1917; MacArthur 1958), though little is known about their ecologies (Maryan et al. 2007; Pepper et al. 2025). If body size differences determined the niches these lizards occupy, then initial trait divergence via geometric scaling may have been sufficient to facilitate their coexistence, implying a peak shift must have happened early on in the trait divergence process. Thus, ecological character displacement (Wilson and Brown 1956) need not be invoked to explain the coexistence of these species, unless its main function was to finish the trait divergence process (Schluter 2000, p. 117).

Adaptive peak shifts through geometric scaling of sexually selected traits

Many studies have attempted to link sexual selection to speciation and ecological diversification (e.g., Lande 1981; Lande and Kirkpatrick 1988; Schluter 2000; Coyne and Orr 2004; Losos 2009; Bonduriansky 2011). Because secondary sexual traits often exhibit static allometry (Bonduriansky and Day 2003; Bonduriansky 2007; Eberhard et al. 2018; Stroud et al. 2023), they are also expected to diverge in the manner depicted by the GSF model. This implies that changes in body size—regardless of the cause—may induce correlated responses in viability and sexually selected traits, or vice-versa. Like viability traits, it is also possible that the *absolute* size changes of sexually selected traits brought about by geometric scaling may translate to phenotypes having improved fitness on adaptive landscapes. For example, Stroud et al. (2023) reported that the dewlaps of *Anolis* lizards tend to exhibit positive static allometry. These authors also suggested that the underlying reason for this may be explained by the dewlap's size acting to convey the size of the lizard to reproductive females and rivals. Thus, in the context of geometric similarity, conspecific adult males with larger body sizes are expected to have smaller dewlaps than allometry would predict but those same dewlaps should nonetheless show *larger absolute size differences* and thus may still give those males competitive advantages. Such advantages may play a role in speciation while correlated changes in one or more viability traits may drive peak shifts. A similar scenario could play out with genital characters in Poeciliid fishes, which show negative static allometry (Bonduriansky 2007). The interplay between body size and organs important to sexual selection and viability may also explain the diversification of birds of paradise given the dramatic variation in their body sizes (Frith and Beehler 1998).

The extinct Irish Elk (*Megaloceros giganteus*) has long attracted interest amongst evolutionary biologists because of its large body size and enormous antlers. Gould (1974) found

that the antlers of this species exhibited strong positive static allometry. Moreover, despite Gould's (1971) earlier concerns that ontogenetic scaling can lead to the evolution of maladaptive trait proportions, Gould suggested that the Irish Elk had undergone this mode of trait evolution, driven by selection on both body and antler sizes. However, Tsuboi et al. (2025) rejected Gould's hypothesis because they found that ontogenetic scaling could not account for relative antler size in this species, which was larger than predicted by ontogenetic scaling. The GSF model can account for Tsuboi et al.'s findings: when this species initially underwent body size increase, antler size would have been smaller than static allometry would have predicted (see phase 1 in Figure 2A). But subsequent directional selection (e.g., due to intersexual selection; Gould 1974) could have caused an increase in the size of the antlers until they became transposed above the intraspecific allometric line (see phase 4 in Figure 2A).

"Niche scaling": a possible mechanism for peak shifts via geometric scaling

If the GSF model is correct, then initial divergence of allometric traits follows a predictable evolutionary pathway by first undergoing geometric scaling, a process that can be driven by natural or sexual selection. The results here suggested that closely related (congeneric) species can come into sympatry even while viability traits were still in geometric similarity. This observation is significant because it raises the possibility that the amount of divergence that previously occurred when both species had allopatric or parapatric distributions was adequate to permit their later coexistence in the same community. In other words, it suggests that the fitness valleys in the adaptive landscape were shallow enough to easily facilitate peak shifts via correlated responses to natural selection on body size alone, or on body size and trait size together (see Price et al. 1993). Given the ubiquity of population-level body size evolution in

nature, geometric scaling may be a common mechanism of peak shifts and therefore play a major role in macroevolution as was first suggested by Gould (1971). However, adaptive radiation theory (Simpson 1944; Lack 1947; Simpson 1953; Grant 1986; Schluter 2000; Grant and Grant 2008, 2024; Losos 2009; Gillespie et al. 2020) has apparently overlooked geometric scaling as a mechanism of initial trait divergence and peak shifts during the ecological diversification process. Given the potential importance of this mechanism to macroevolution, we can propose to name it "niche scaling," in reference to the role that geometric scaling may play in peak shifts.

Conclusions

The model we presented here, called the geometric-similarity-first model (or GSF model), aims to explain the initial divergence and subsequent evolution of traits in species. It is a general model that applies to all allometric traits and thus includes many traits important to viability (e.g., mouthparts, locomotory apparatus, etc.) and sexual selection (e.g., weapons, signaling traits, etc.). In the model's first step, the trait undergoes geometric scaling with a population-level decrease or increase in body size. In the next step, traits that exhibit ontogenetic (or static) allometry are expected to undergo a "re-optimizing" step via one of two alternative pathways: 1) if the trait displays positive allometry, then it is expected to undergo positive evolutionary allometric scaling via directional natural selection; or 2) if the trait shows negative allometry, then it is predicted to undergo negative evolutionary allometric scaling via directional natural selection. This model contains similarities to a hypothesis advanced by Szarski (1964) except that Szarski's hypothesis predicted that re-optimization of a negative allometric trait in step 2 would occur via positive evolutionary allometric scaling.

The utility of the GSF model lies in its ability to elucidate the stages of trait divergence through pairwise comparisons of allometric growth trajectories for populations and species within recent time frames—a somewhat analogous approach to the classical cytological method of examining stained chromosomes in different cells under a microscope to understand the dynamic phases of cell division. Although this methodology is expected to perform well in identifying scaling pattern(s) that characterize initial divergence for pairs of populations or pairs of closely related species (i.e., populations just before and after speciation), it may inconsistently identify the correct scaling patterns for pairs of more divergent species owing to swings in body and trait sizes in one or both of the lineages over longer evolutionary time spans. Nonetheless, testing of the three main predictions of the model—geometric similarity precedes evolutionary allometry, geometric similarity is a temporary stage of trait divergence, and all allometric traits exhibit geometric similarity during initial body size divergence—using empirical data may not be adversely impacted by this problem because the predictions mostly pertain to initial trait divergence and thus scaling patterns caused by evolutionary convergence or allometric escape are expected to be absent from results for comparisons involving conspecific populations or closely related (congeneric) species. A morphological data set for three locomotor-relevant traits in Australian pygopodid lizards supported all three predictions of the GSF model. Moreover, scaling patterns for more highly divergent species pairs (i.e., divergences > 3 mya) were largely consistent with the second step in the model and therefore contradicted Szarski's hypothesis. The GSF model may clarify our understanding of trait divergence in other species. For instance, the model provides novel insights on beak divergence in Darwin's finches and antler evolution in the Irish Elk.

This study produced two other findings of possible importance to macroevolution. First, the hypothesized initial geometric similarity phase in pygopodid lizards lasted on the order of millions of years, which suggests that organisms can survive and reproduce over long evolutionary time intervals despite being equipped with presumably biomechanically deficient traits caused by geometric scaling. Perhaps this somewhat evolutionarily stable phase was sustainable because fitness losses due to suboptimal trait shapes were exceeded by fitness gains associated with new body sizes and *absolute* sizes of viability traits, trait alterations that may have enabled populations and species to exploit new ecological niches. The second key finding was that closely related pygopodid lizard species were found to coexist together even though they exhibited geometric similarity in viability traits—implying that one of the species had some biomechanically deficient traits. This latter finding is consistent with current thinking that interspecific competition between co-occurring closely related species (i.e., character displacement) acts mainly to finish the trait divergence process thereby facilitating species coexistence (Schluter 2000).

In the adaptive landscape context, these findings suggest that fitness valleys in the adaptive landscape for habitats exploited by pygopodid lizards were shallow enough to easily facilitate peak shifts via correlated responses to natural selection on body size alone, or body size and trait size together (see Price et al. 1993). Another implication of these results is that they suggest a novel mechanism, geometric scaling, through which sexual selection can drive ecological diversification, thus supporting Bonduriansky's (2011) hypothesis. It is hypothesized that natural selection can drive geometric scaling of traits important for viability and/or reproduction and thus act as a mechanism for peak shifts via correlated response on an adaptive landscape, a process here named "niche scaling." Given the universality of body size evolution in

species, and the predictable scaling consequences of these events according to the GSF model, niche scaling could be an important mechanism in adaptive radiation.

Materials and Methods

Study group

The geometric similarity-first model was tested using morphological data relevant to the locomotor abilities of lizards in the family Pygopodidae, a group that contains at least 48 extant species of limb-reduced and elongate lizards that are endemic to Australia and New Guinea (Kluge 1974, 1976; Cogger 1992; Ehmann 1992; Shea 1993; Oliver et al. 2010; Jennings 2002; Jennings et al. 2003; Brennan et al. 2016; Skipwith et al. 2019; Jennings 2021; Mahony et al. 2022). This group is ideal for testing the model for many reasons. First, as a result of the many phylogenetic and phylogenomic studies of this group, all species groups are well-defined, the interspecific relationships within these groups are largely resolved, and divergence times have been estimated for most species (Kluge 1976; Jennings et al. 2003; Brennan et al. 2016; Brennan and Oliver 2017; Skipwith et al. 2019; Jennings 2021). Moreover, this group can represent a natural experiment in this study because each species group can be thought of as an independent replicate of the early trait divergence process. Pygopodids also offer an opportunity to examine trait divergences both in lineages that exhibit the classic characteristics of adaptive radiation (Grant 1986; Schluter 2000; Grant and Grant 2008; Losos 2009) and in lineages that show the hallmarks of so-called non-adaptive radiation (Gittenberger 1991). For instance, the genus *Delma*, which accounts for half the group's species richness shows remarkable variation in relative tail lengths (i.e., 244-450% of their body lengths) and vertical habitat use (i.e., sub-surface, ground, grass, shrubs), which may help explain why sympatry among congeners is

commonly observed (Kluge 1974; Storr et al. 1990; Cogger 1992; Ehmann 1992; Jennings et al. 2002, 2003; Pianka 2010; Jennings unpublished data). Although the genus *Lialis* only includes two species, both show considerable morphological divergence and are broadly sympatric with each other. Kluge (1974) obtained preliminary evidence suggesting that these two species may represent a case of character displacement. In contrast, the genus *Aprasia*, which contains at least 15 species, shows relative morphological uniformity, especially in their relative tail lengths (i.e., 65-92% of their body lengths) and habitat use (all are fossorial in habit), and all only show parapatric or allopatric distributions (Storr et al. 1990; Jennings et al. 2003; Maryan et al. 2013a, b; Maryan et al. 2015a). These features of *Aprasia* biology are remarkably similar to *Batrachoseps* salamanders, a well-studied group that underwent a non-adaptive radiation (Wake 2006).

Trait data

Morphometric data were initially collected from 743 ethanol-preserved specimens as part of a doctoral dissertation (Jennings 2002). The sampling goal at the time was to obtain data from specimens spanning the post-natal growth range for as many species in the group as possible. These specimens were made available by the Australian Museum (AM), Museum and Art Gallery Northern Territory (MAGNT), Museums Victoria (MV), Queensland Museum (QM), South Australian Museum (SAM), Western Australian Museum (WAM), W. Bryan Jennings personal collection (WBJ), and Eric R. Pianka personal collection (ERP). Later, between September 2022 to September 2023, additional morphological data were obtained from specimens in the AM, MAGNT, MV, QM, SAM, and Museum of Comparative Zoology Harvard

University (MCZ). The main goal of this second round of sampling was to obtain data for different populations/subspecies and closely related species, which were not adequately sampled earlier. In total, this study is based on data from 1,756 specimens representing 31 of 47 known pygopodid species. Note that some data from the dissertation were not used in this study because some species were highly divergent from other pygopodids and thus it is unlikely much could be learned about their initial trait divergence histories. These included *Pygopus* (*Paradelma*) *orientalis* and *Ophidiocephalus taeniatus*. The subspecies pair *Delma concinna concinna* and *D. c. major* and closely related sister species *Pletholax gracilis* and *P. edelensis* also were not included due to insufficient sample sizes for one member of each pair.

Five linear measurements to the nearest millimeter (mm) using dial calipers were recorded from each specimen: snout-vent length (*SVL*), tail length (*Tail*), body width at the ear (*BW1*), body width in the middle of the trunk (*BW2*), and body width at the vent (*BW3*). Tails were only measured if they were original (i.e., non-regenerated) tails. These measurements were selected because pygopodids are effectively limbless, and therefore their size and shapes of their trunks and tails completely determine their locomotor modes and abilities. All morphometric data used in this study can be obtained from Jennings (2025).

Analyses

Definition of OTUs

The operational taxonomic units (OTUs) used in this study mostly corresponded to the species shown in the phylogeny of Jennings (2021). However, multiple population-level OTUs for some species were herein identified using the following criteria: (1) if a species was comprised of

multiple geographically disjunct populations or sub-species, then each one was defined as an OTU; and (2) if a species had a widespread distribution that spanned multiple biomes, then the sub-population for each biome was defined as a separate OTU because these biome boundaries commonly mark the geographical division between closely-related species. Although the definition of OTUs under criterion (2) was subjective—because it is not yet known if biome-defined sub-populations are genetically connected to other sub-populations, preliminary observations of specimens suggested that the intraspecific ontogenetic trajectories varied across biomes, possibly in response to different rainfall regimes. Accordingly, some species consisted of a population in a "wet biome" (tropical regions) and a "dry biome" (deserts and Mediterranean heaths).

Testing the null hypothesis of isometry

Before the GSF model can be tested it is necessary to first establish that the traits of interest exhibit ontogenetic or static allometry. Accordingly, post-natal ontogenetic or static growth trajectories must be estimated for all OTUs so that their slopes can be statistically tested to determine if they deviate from the null hypothesis of isometry (i.e., show positive or negative ontogenetic allometry).

Growth trajectories represented by the bivariate scaling relationship between a trait of interest and body size can be estimated using a linearized version of Huxley's (1932) allometric equation:

$$\ln Y = \ln \alpha + b(\ln X) \quad (1)$$

in which ln$Y$ is the natural log-transformed trait variable (Y), ln$X$ is the natural log-transformed body size variable (X), α is the slope, and b is the Y-intercept. Following previous studies (e.g., Pounds et al., 1983; Garland, 1985), intraspecific samples of preserved lizards spanning the post-natal body-size spectrum were used in lieu of actual growth data. These "cross-sectional" data (Cock, 1966) were then used to generate an "ontogenetic" growth curve for each OTU. Although these data cannot be interpreted as individual growth trajectories, they may provide reasonable estimates of average ontogenetic growth within a population (Cock, 1966; Garland, 1985). The line-fitting method of reduced major axis (RMA) has often been employed for estimating allometric slopes owing to concerns that ordinary least squares (OLR) regression may underestimate the true slopes when measurement error exists in the data (e.g., Harvey and Pagel, 1991). However, others have recommended the use of OLR over RMA because the former is expected to perform well enough in most studies while the latter has drawbacks that make it unsuitable for allometry studies (Seim and Sæther 1983; Kelly and Price 2004; Hansen and Bartoszek 2012; Pélabon et al. 2014; Voje et al. 2014; Kilmer and Rodríguez 2017). Accordingly, ontogenetic allometric slopes were estimated via OLR using the *R* package *SMATR* (Warton and Weber, 2002; Warton et al. 2006; Taskinen and Warton 2011) implemented in the *R* statistical package (version 4.3.0., *R* Development Core Team, 2023).

In this study, the shapes of three traits were examined in pygopodid lizards. The first of these was the relationship ln*Tail* regressed on ln*SVL*, which describes post-natal ontogenetic changes in relative tail length using *SVL* as the measure of body size. The second relationship was ln*Tail* on ln$\overline{BW}$, which characterizes relative tail length using $\overline{BW}$, the average body width ($BW1 + BW2 + BW3$)/3 as the body size reference. The third scaling relationship examined for each OTU was ln$\overline{BW}$ on ln*SVL*, which is a measure of body girth relative to *SVL*.

One advantage to estimating linearized ontogenetic growth trajectories is that a test for isometry can be readily performed in which α is compared to a null isometric value (Sweet, 1980; Pounds et al., 1983; Garland, 1985). When *Y* and *X* are the same dimensional units, an ontogenetic allometric regression with a slope of 1.0 indicates isometry, $\alpha > 1.0$ signifies positive ontogenetic allometry, and $\alpha < 1.0$ means negative ontogenetic allometry (Pounds et al. 1983; Garland 1985). Given that the trait and body size variables in this study were one-dimensional measurements, a slope of 1.0 was used as the null hypothesis for isometry. Isometry tests were conducted using the *R* package *SMATR* and slopes were considered to be allometric if $p < 0.05$.

Pairwise comparisons of post-natal ontogenetic allometric trajectories

To characterize each scaling pattern in analyses of pairwise trajectories, we must know or assume which OTU in a pair has the larger maximum body size (Gould 1971). Snout-vent length (*SVL*) has long been the standard body size reference or lizards and snakes, especially in studies based on museum specimens (e.g., Pavón et al. 2022). However, an unforeseen complication arose during the analyses of maximum body size in pygopodid OTUs. Although maximum *SVL* proved to be a useful metric for identifying the "larger-sized" OTU in most OTU pairs, in other pairs the OTU with the smaller maximum *SVL* had a larger maximum $\overline{BW}$ than the OTU having the larger maximum *SVL*. This presented a dilemma—should we consider the longer- and slenderer-bodied OTU as the one with the larger maximum body size or should we consider the shorter- and stouter-bodied OTU to be the one with the larger size?

Given the uncertainty as to which measure of body size may be more appropriate to use in this study, two versions of each dataset were constructed for testing the model's predictions.

The "full datasets" each contained all OTU pairs that had one OTU with a larger maximum *SVL* compared to the other OTU in each comparison, while the "reduced datasets" each contained all OTU pairs that had one OTU with a larger maximum *SVL* and $\overline{BW}$ compared to the other OTU in the comparison—thus it was clear which OTU was larger in the latter datasets. Although this approach could introduce a bias into the findings, it offered a way to check the sensitivity of results to the use of different metrics for maximum body size in these lizards.

To test the predictions of the model it was necessary to first perform pairwise comparisons of ontogenetic trajectories for the ln*Tail* on ln*SVL*, ln*Tail* on ln$\overline{BW}$, and ln$\overline{BW}$ on ln*SVL* regressions and then identify the resulting spatial patterns. Because a major focus of this study was to ascertain the details of initial trait divergence, pairwise comparisons were limited to conspecific populations and species belonging to the same species group. Thus, pairwise comparisons of ontogenetic trajectories were performed between OTUs within the *Aprasia reprens* species group, southeastern Australia *Aprasia* species group, *Delma australis* species group, *Delma fraseri* species group, *Delma impar* species group, *Delma nasuta* species group, *Delma tincta* species group, *Lialis* species group, and *Pygopus nigriceps* species group (see Jennings 2021 for more details about these groups). Additionally, pairwise comparisons were made between two populations of *P. lepidopodus*.

To determine whether a pair of trajectories partially overlapped with each other (i.e., exhibited ontogenetic scaling) or were transposed from each other (i.e., showed geometric similarity or evolutionary allometry via transposition) it was necessary to test the null hypotheses equal slopes and equal elevations using statistical methods. The test for common elevations is only meaningful if the test for common slopes indicates that the slopes are the same in a statistical sense. The *R* package *SMATR* was used to conduct common slopes and common

elevations (when appropriate) tests for each pair of OTUs. If the results indicated that a pair of slopes were equal, then a common elevations test based on the Wald's statistic (analogous to analysis of covariance) was performed. Null hypotheses of equal slopes and equal elevations were rejected if p was less than 0.05.

Although the aforementioned statistical procedures can objectively discriminate between ontogenetic scaling and transpositions that reflect geometric similarity or evolutionary allometry, intermediate patterns between these extremes may exist. If the GSF model is correct, then we could expect to see many such intermediates, which would make it more challenging to unambiguously identify scaling patterns. This may mean that it is not possible to eliminate all subjectivity from these analyses. Nonetheless, when statistical results cannot be used to objectively characterize a particular scaling pattern, we can at least use those results to guide the descriptions of patterns. In this study, eight different scaling patterns were defined. The first three scaling patterns were straightforward to identify using the above statistical procedures while scaling patterns 4-8 were characterized partly on the basis of the statistical results and partly by visual analysis of bivariate scatterplots with the superimposed regression lines (trajectories). The eight scaling patterns were: 1) *geometric similarity (all ages)* = statistical results indicated equal slopes and unequal elevations while visual analysis revealed that the two trajectories matched Figure 1A or 1B; 2) *evolutionary allometry overlap (equal slopes)* = statistical results indicated equal slopes and equal elevations while visual analysis revealed partially overlapping trajectories that matched Figure 1C or 1D—notice that this "overlap" pattern was not defined as ontogenetic scaling because the GSF model suggests that trajectories may partially overlap each other in coincidental fashion and thus cannot represent true ontogenetic scaling (see Phase 3 in Figure 2); 3) *evolutionary allometry transposition (all ages)* = statistical results indicated equal slopes and

unequal elevations while visual analysis revealed that the two trajectories matched Figure 1E or 1F; 4) *geometric similarity (adults only*) = statistical analysis indicated unequal slopes while visual analysis revealed that the trajectories displayed a V-shaped pattern in which they overlapped for the juvenile classes while the adult classes diverged from each other in a transposition-like pattern that was consistent with Figure 1A or 1B; 5) *geometric similarity (juveniles only)* = statistical analysis indicated unequal slopes while visual analysis revealed that the trajectories displayed a V-shaped pattern in which they overlapped for the adult classes while the juvenile classes diverged from each other in a transposition-like pattern that was consistent with Figure 1A or 1B; 6) *evolutionary allometry overlap (unequal slopes)* = statistical results indicated unequal slopes while visual analysis revealed partially overlapping trajectories that formed a flattened X-shaped pattern—note that this pattern is not compatible with ontogenetic scaling; 7) *evolutionary allometry transposition (adults only)* = statistical analysis indicated unequal slopes while visual analysis revealed that the trajectories displayed a V-shaped pattern in which they overlapped for the juvenile classes while the adult classes diverged from each other in a transposition-like pattern that was consistent with Figure 1E or 1F; and 8) *evolutionary allometry transposition (juveniles only)* = statistical analysis indicated unequal slopes while visual analysis revealed that the trajectories displayed a V-shaped pattern in which they overlapped for the adult classes while the juvenile classes diverged from each other in a transposition-like pattern that was consistent with Figure 1E or 1F.

Acknowledgements

Work on this project began during the present author's Ph.D. dissertation research but was only recently finished thanks to tremendous assistance from many institutions and individuals. Critical assistance was provided by the Department of Integrative Biology at the University of Texas at Austin, Museum of Comparative Zoology at Harvard University, and the Department of Evolution, Ecology & Organismal Biology at the University of California, Riverside. Access to specimens was provided by Andrew Amey and Patrick Couper (Queensland Museum), Paul Horner, Sue Horner, and Danielle Edwards (Museum and Art Gallery of the Northern Territory), Jane Melville and Katie Date (Museums Victoria), Ross Sadlier, Allen Greer, Dane Trembath, and Jodi Rowley (Australian Museum), Mark Hutchinson (South Australian Museum), Laurie Smith, Paul Doughty, and Kailah Thorn (Western Australian Museum), Jose Rosado, James Hanken, Stevie Kennedy-Golds, and Joe Martinez (Museum of Comparative Zoology, Harvard University [MCZ]). Funding for travel to museums in 1999 was provided by a Continuing Graduate Student Fellowship from the University of Texas at Austin while funding for trips between 2022 and 2023 to the MCZ and museums in Australia were provided by an Ernst Mayr Travel Grant from Harvard University and a Science, Discovery & Breakthrough Grant from Geeks without Frontiers. The present author is also grateful for the assistance he received from his doctoral advisor, Eric R. Pianka, and dissertation committee members Robert Dudley, David Cannatella, Carl Gans, Theodore Garland, Jr., and David Hillis. Samuel Sweet, Scott Edwards, Michael and Margaret Potter, and Vivian Menezes Leandro provided much assistance and encouragement over the years, without which this study could not have been completed.

Data availability

The original data can be downloaded from the Figshare data repository under doi: 10.6084/m9.figshare.30479747. Additional metadata used in analyses are included in the manuscript and supporting files.

References

Abzhanov, A., Kuo, W. P., Hartmann, C., Grant, B. R., Grant, P. R. and Tabin, C. J. 2006. The calmodulin pathway and evolution of elongated beak morphology in Darwin's finches. *Nature*, 442:563-567.

Bamford, M. J. 1998. Field observations of the semi-arboreal pygopodids *Aclys concinna* (Kluge 1974) and *Pletholax gracilis* (Cope 1864). *Herpetofauna* 28:2–4.

Bauer, A. M. 1986. Saltation in the Pygopodid lizard, *Delma tincta*. *Journal of Herpetology* 20:462–463.

Boag, P. T. 1984. Growth and allometry of external morphology in Darwin's finches (*Geospiza*) on Isla Daphne Major, Galapagos. *Journal of Zoology* 204:413–441.

Bonduriansky, R. and Day, T. 2003. The evolution of static allometry in sexually selected traits. *Evolution*, 57:2450-2458.

Bonduriansky, R., 2007. Sexual selection and allometry: a critical reappraisal of the evidence and ideas. *Evolution*, 61:838-849.

Bonduriansky, R. 2011. Sexual selection and conflict as engines of ecological diversification. *The American Naturalist*, 178:729-745.

Brennan, I.G., and Oliver, P.M. 2017. Mass turnover and recovery dynamics of a diverse Australian continental radiation. *Evolution* 71:1352–1365

Brennan, I. G., A. M. Bauer, and T. R. Jackman. 2016. Mitochondrial introgression via ancient

hybridization, and systematics of the Australian endemic pygopodid gecko genus *Delm*a. *Molecular Phylogenetics and Evolution* 94:577–590.

Cock, A. G. 1966. Genetical aspects of metrical growth and form in animals. *Q. Rev. Biol.* 41:131-190.

Cogger, H. G. 1992. *Reptiles & Amphibians of Australia*. Comstock/Cornell, Ithaca, N.Y.

Coyne, J. A., and H. A. Orr. 2004. *Speciation*. Sinauer Associates, Sunderland.

Darwin, C. R. 1859. *On the Origin of Species by Means of Natural Selection, or the Preservation of Favoured Races in the Struggle for Life*. John Murray, London.

Eberhard, W. G., Rodríguez, R. L., Huber, B. A., Speck, B., Miller, H., Buzatto, B. A. and Machado, G. 2018. Sexual selection and static allometry: the importance of function. *The Quarterly Review of Biology*, 93:207-250.

Ehmann, H. (ed). 1992. *Encyclopedia of Australian Animals: Reptiles*. Angus & Robertson, Pymble, N.S.W.

Esquerré, D., E. Sherratt, and J. S. Keogh. 2017. Evolution of extreme ontogenetic allometric diversity and heterochrony in pythons, a clade of giant and dwarf snakes. *Evolutio*n 71:2829–2844.

Frith, C. B., and B. M. Beehler. 1998. *The Birds of Paradise*. Oxford University Press, New York.

Garland, T., Jr. 1985. Ontogenetic and individual variation in size, shape and speed in the Australian agamid lizard *Amphibolurus nuchalis*. *J. Zool. (Lond.)* 207:425-439.

Gillespie, R. G., G. M. Bennett, L. De Meester, J. L. Feder, R. C. Fleischer, L. J. Harmon, A. P. Hendry, M. L. Knope, J. Mallet, C. Martin, C. E. Parent, A. H. Patton, K. S. Pfennig, D. Rubinoff, D. Schluter, O. Seehausen, K. L. Shaw, E. Stacy, M. Stervander, J. T. Stroud, C.

Wagner, and G. O. U. Wogan. 2020. Comparing adaptive radiations across space, time, and taxa. *Journal of Heredity* 111:1–20.

Gittenberger, E. 1991. What about non-adaptive radiation?. *Biological Journal of the Linnean Society*, 43:263-272.

Gould, S. J. 1966. Allometry and size in ontogeny and phylogeny. *Biol. Rev.* 41:587–640.

Gould, S. J. 1971. Geometric similarity in allometric growth: a contribution to the problem of scaling in the evolution of size. *The American Naturalist* 105.

Gould, S. J. 1974. The origin and function of "bizarre" structures: antler size and skull size in the "Irish Elk," *Megaloceros giganteus*. *Evolution* 28:191.

Grant, P. R. 1986. *Ecology and Evolution of Darwin's Finches*. Princeton University Press, Princeton, N.J.

Grant, P. R. and Grant, B. R., 1994. Phenotypic and genetic effects of hybridization in Darwin's finches. *Evolution*, 48:297-316.

Grant, P. R., and B. R. Grant. 2008. *How and Why Species Multiply: The Radiation of Darwin's Finches*. Princeton University Press, Princeton.

Grant, P. R., and Grant, B. R. 2024. From microcosm to macrocosm: adaptive radiation of Darwin's finches. *Evolutionary Journal of the Linnean Society*, 3(1), p.kzae006.

Gray, J. A., E. Sherratt, M. N. Hutchinson, and M. E. H. Jones. 2019. Changes in ontogenetic patterns facilitate diversification in skull shape of Australian agamid lizards. *BMC Evol Biol* 19:7.

Greer, A. E. 1989. *Biology and Evolution of Australian Lizards*. Surrey Beatty & Sons, Chipping Norton, NSW.

Grinnell, J. 1917. The niche-relationships of the California Thrasher. *The Auk*, 34:427-433.

Hanken, J., and Wake, D.B. 1993. Miniaturization of body size: organismal consequences and evolutionary significance. *Annual Review of Ecology and Systematics*, 24:501-519.

Hansen, T. F., and Bartoszek, K. 2012. Interpreting the evolutionary regression: The interplay between observational and biological errors in phylogenetic comparative studies. *Systematic Biology*, 61:413–425.

Harvey, P. H., and M. D. Pagel. 1991. *The comparative method in evolutionary biology*. Oxford University Press, New York.

Huxley, J. S. 1932. *Problems of relative growth*. Methuen, London.

James, B.H., Donnellan, S.C., Hutchinson, M.N. 2001. Taxonomic revision of the Australian lizard *Pygopus nigriceps* (Squamata: Gekkonoidea). *Records of the South Australian Museum* 34(1):37–52.

Jennings, W. B. 2002. Phylogeny, ecology, and the nature of cladogenesis in Australian pygopodid lizards. Ph.D. Dissertation, University of Texas at Austin.

Jennings, W. B. 2021. Evolutionary relationships among the snakelike pygopodid lizards: a review of phylogenetic studies of an enigmatic Australian adaptive radiation. *PeerJ* 9:e11502.

Jennings, W. B. 2025. Data for “A scaling theory of trait evolution.” Figshare. (doi: 10.6084/m9.figshare.30479747).

Jennings, W. B., E. R. Pianka, and S. Donnellan. 2003. Systematics of the lizard family Pygopodidae with implications for the diversification of Australian temperate biotas. *Systematic Biology* 52:757–780.

Kealley, L., Doughty, P., Edwards, D., Brennan, I.G. 2020. Taxonomic assessment of two

pygopodoid gecko subspecies from Western Australia. *Israel Journal of Ecology and Evolution*, 66:126–141.

Kelly, C., and Price, T. D. 2004. Comparative methods based on species mean values. *Mathematical Biosciences*, 187:135–154.

Kilmer, J.T. and Rodríguez, R.L., 2017. Ordinary least squares regression is indicated for studies of allometry. *Journal of Evolutionary Biology*, 30(1), pp.4-12.

Klingenberg, C. P. 1998. Heterochrony and allometry: the analysis of evolutionary change in ontogeny. *Biol. Rev.* 73:79–123.

Kluge, A. G. 1974. A taxonomic revision of the lizard family Pygopodidae. *Miscellaneous Publications Museum of Zoology*, University of Michigan, No 147 221.

Kluge, A. G. 1976. Phylogenetic relationships in the lizard family Pygopodidae: an evaluation of theory, methods, and data. *Miscellaneous Publications Museum of Zoology*, University of Michigan, No 152 72.

Kurtén, B. 1954. Observations on allometry in mammalian dentitions; its interpretation and evolutionary significance. *Acta Zoologica Fennica* 1–13.

Kurtén, B. 1955. Contribution to the history of a mutation during 1,000,000 years. *Evolution* 9:107–118.

Lack, D., 1947. *Darwin's finches*. Cambridge University Press.

Lande, R. 1979. Quantitative genetic analysis of multivariate evolution, applied to brain: body size allometry. *Evolution*, 33:402-416.

Lande, R. 1981. Models of speciation by sexual selection on polygenic traits. *Proceedings of the National Academy of Sciences*, 78:3721-3725.

Lande, R. 1985. Genetic and evolutionary aspects of allometry. In *Size and Scaling in Primate*

Biology (pp. 21-32). Boston, MA: Springer US.

Lande, R. and Kirkpatrick, M. 1988. Ecological speciation by sexual selection. *Journal of Theoretical Biology*, 133:85-98.

Losos, J. B. 2009. *Lizards in an Evolutionary Tree: the Ecology of Adaptive Radiation in Anoles*. University of California Press, Berkeley.

MacArthur, R. H. 1958. Population ecology of some warblers of northeastern coniferous forests. *Ecology*, 39:599-619.

Mahony, S. V., T. Cutajar, and J. J. L. Rowley. 2022. A new species of *Delm*a Gray 1831 (Squamata: Pygopodidae) from the Hunter Valley and Liverpool Plains of New South Wales. *Zootaxa* 5162:541–556.

Maryan, B., Aplin, K.P., Adams, M. 2007. Two new species of the *Delma tincta* group (Squamata: Pygopodidae) from northwestern Australia. *Records of the Western Australian Museum* 23(3):273–305.

Maryan, B., Bush, B.G., Adams, M. 2013a. Morphological and molecular assessment of *Aprasia fusca* and *A. rostrata* (Squamata: Pygopodidae), with a description of a new species from the Lake MacLeod region, Western Australia. *Records of the Western Australian Museum* 28:144–163.

Maryan, B., R. A. How, and M. Adams. 2013b. A new species of the *Aprasia repens* species-group (Squamata: Pygopodidae) from Western Australia. *Rec West Aust Mus* 28:30.

Maryan, B., Adams, M., Aplin, K.P. 2015a. Taxonomic resolution of the *Aprasia repens* species-group (Squamata: Pygopodidae) from the Geraldton Sandplains: a description of a new species and additional mainland records of *A. clairae*. *Records of the Western Australian Museum* 30(1):12–32.

Maryan, B., Brennan, I.G., Adams, M., Aplin, K.P. 2015b. Molecular and morphological assessment of *Delma australis* Kluge (Squamata: Pygopodidae), with a description of a new species from the biodiversity 'hotspot' of southwestern Western Australia. *Zootaxa* 3946(3):301–330.

Meunier, K. 1959a. Die Allometrie des Vogelflügels. *Z. wiss. Zool*. 161:444-482.

Meunier, K. 1959b. Die Grössenabhängigkeit der Körperform bei Vögeln. *Z. wiss. Zool*. 162: 328-355.

Oliver, P.M., Couper, P., Amey, A. 2010. A new species of *Pygopus* (Pygopodidae; Gekkota; Squamata) from north-eastern Queensland. *Zootaxa* 2578(1):47–61

Pavón-Vázquez, C. J., D. Esquerré, and J. S. Keogh. 2022. Ontogenetic drivers of morphological evolution in monitor lizards and allies (Squamata: Paleoanguimorpha), a clade with extreme body size disparity. *BMC Ecol Evo* 22:15.

Pélabon, C., Firmat, C., Bolstad, G. H., Voje, K. L., Houle, D., Cassara, J., Le Rouzic, A., and Hansen, T. F. 2014. Evolution of morphological allometry. *Annals of the New York Academy of Sciences*, 1320:58–75.

Pepper, M., Doughty, P., Fletcher, J., and Keogh, J. S. 2025. Molecular and morphological assessment of the widely distributed legless gecko *Delma tincta* Kluge (Squamata: Pygopodidae), including a taxonomic revision. *Records of the Western Australian Museum*, 40: 001-046.

Pianka, E.R. 2010. Notes on the ecology of four species of pygopodid lizards in the Great Victoria Desert. *The Western Australian Naturalist*, 27:175-81.

Pounds, J. A., J. F. Jackson, and S. H. Shively. 1983. Allometric growth of the hind limbs of some terrestrial iguanid lizards. *Am. Midl. Nat*. 110:201-207.

Price, T., Turelli, M., and Slatkin, M. 1993. Peak shifts produced by correlated response to selection. *Evolution*, 47(1):280-290.

R Development Core Team. 2023. R: A Language and Environment for Statistical Computing. Available at: https://cran.r-project.org/.

Rensch, B. 1948. Histological changes correlated with evolutionary changes of body size. *Evolutio*n, 2: 218-230.

Schluter, D. 2000. *The Ecology of Adaptive Radiation*. Oxford University Press, New York.

Seim, E., and Sæther, B. E. 1983. On rethinking allometry: Which regression model to use? *Journal of Theoretical Biology*, 104:161–168.

Shea, G. M. 1991. Revisionary notes on the genus *Delma* (Squamata: Pygopodidae) in South Australia and the Northern Territory. *Records of the South Australian Museum*, 25:71-90.

Shea, G. M. 1993. 28. *Family Pygopodidae*. Pp. 234–239 in Fauna of Australia Volume 2A Amphibia & Reptilia. Australian Government Publishing Process, Canberra.

Simpson, G. G. 1944. *Tempo and mode in evolution*. Columbia University Press, New York.

Simpson, G. G. 1953. *The major features of evolution*. Columbia University Press, New York.

Skipwith, P. L., K. Bi, and P. M. Oliver. 2019. Relicts and radiations: Phylogenomics of an Australasian lizard clade with east Gondwanan origins (Gekkota: Diplodactyloidea). *Molecular Phylogenetics and Evolution* 140:106589.

Storr, G. M. 1978. Taxonomic notes on the reptiles of the Shark Bay region, Western Ausralia. *Rec. West. Aust. Mus*. 6(3):303-318.

Storr, G. M. 1987. Three new legless lizards (Pygopodidae) from Western Australia. *Rec. West. Aust. Mus*. 13(3):345-355.

Storr, G. M., L. A. Smith, and R. E. Johnstone. 1990. *Lizards of Western Australia III: Geckos*

and Pygopods. Western Australian Museum, Perth.

Stroud, J. T., and J. B. Losos. 2020. Bridging the process-pattern divide to understand the origins and early stages of adaptive radiation: a review of approaches with insights from studies of Anolis lizards. *Journal of Heredity* 111:33–42.

Stroud, J. T., A. Petherick, B. Krasnoff, K. Walker, J. J. Suh, and J. B. Losos. 2023. Signal size allometry in Anolis lizard dewlaps. *Biol. Lett*. 19:20230160.

Sweet, S. S. 1980. Allometric Inference in morphology. *Am Zool* 20:643–652.

Szarski, H., 1964. The structure of respiratory organs in relation to body size in amphibia. *Evolution*, 18:118-126.

Taskinen S. and Warton D. I. 2011. Robust estimation and inference for bivariate line-fitting in allometry. *Biometrical Journal* 53:652-672.

Teissier, G. 1936. Croissance comparée des formes locales d 'une même espèce. *Mém. Mus. roy. d'hist. natur. Belg*. 3:627-634.

Tobias, J. A., Sheard, C., Pigot, A. L., Devenish, A. J., Yang, J., Sayol, F., Neate-Clegg, M. H., Alioravainen, N., Weeks, T. L., Barber, R. A. and Walkden, P. A. 2022. AVONET: morphological, ecological and geographical data for all birds. *Ecology Letters*, 25(3):581-597.

Tonini, J. F. R., Provete, D. B., Maciel, N. M., Morais, A. R., Goutte, S., Toledo, L. F. and Pyron, R. A. 2020. Allometric escape from acoustic constraints is rare for frog calls. *Ecology and Evolution*, 10(8):3686-3695.

Tsuboi, M., Kopperud, B. T., Matschiner, M., Grabowski, M., Syrowatka, C., Pélabon, C. and Hansen, T. F. 2024. Antler allometry, the Irish Elk and Gould revisited. *Evolutionary Biology*, 51:149-165.

Voje, K. L., Hansen, T. F., Egset, C. K., Bolstad, G. H., and Pélabon, C. 2014. Allometric constraints and the evolution of allometry. *Evolution*, 68, 865–885.

Wake, D. B. 2006. Problems with Species: Patterns and Processes of Species Formation in Salamanders 1. *Annals of the Missouri Botanical Garden*, 93:8-23.

Warton D. I. and Weber N. C. 2002. Common slope tests for bivariate structural relationships. *Biometrical Journal* 44, 161–174.

Warton D. I., Wright I. J., Falster D. S. and Westoby M. 2006. A review of bivariate line-fitting methods for allometry. *Biological Reviews* 81, 259–291.

Weiner, J. 1995. *The Beak of the Finch: A Story of Evolution in Our Time*. Vintage, London.

Wright, S. 1931. Evolution in Mendelian populations. *Genetics*, 16:97.

Wright, S. 1932. The roles of mutation, inbreeding, crossbreeding, and selection in evolution. *Proceedings of the 6th International Congress of Genetics*, 1:356-366.

Tables

Table 1. Maximum known body sizes for pygopodid lizards. The longest and second longest snout-vent length (*SVL*) records for each operational taxonomic unit (OTU) are presented along with their source. The largest known average body widths ($\overline{BW}$) together with their associated *SVL* measurements (i.e., $\overline{BW}$ and *SVL* for the same specimen) are also shown. Body width measurements were not taken from specimens that had distended abdomens due to food items or being gravid. All measurements are in millimeters (mm).

Species/Population Group	OTU	Maximum SVL (mm)	Maximum BW [SVL] (mm)	Source
Aprasia repens	*Aprasia clairae*	103[a], 97[b]	2.5 [87]	Maryan et al. 2015a[a], this study[b]
Aprasia repens	*Aprasia haroldi*	92, 92	2.6 [89]	this study
Aprasia repens	*Aprasia litorea*	105, 102	2.5 [105]	this study
Aprasia repens	*Aprasia repens*	126, 107	3.8 [126]	this study
Aprasia repens	*Aprasia rostrata*	126[a], 120[b]	2.7 [117]	Maryan et al. 2013a[a], this study[b]
Aprasia repens	*Aprasia smithi*	128[a], 127[b]	3.7 [127]	Storr et al. 1990[a], this study[b]
SE Australia Aprasia	*Aprasia inaurita*	136[a], 126[b]	3.7 [110]	Kluge 1974[a], this study[b]
SE Australia Aprasia	*Aprasia parapulchella*	148, 145	4.1 [115]	this study
SE Australia Aprasia	*Aprasia pseudopulchella*	151[a], 143.5[b]	3.8 [129]	this study[a], Kluge 1974[b]
SE Australia Aprasia	*Aprasia striolata*	131.8[a], 126[b]	4.3 [126]	Kluge 1974[a], this study[b]
Delma australis	*Delma australis*	89, 85	5.4 [72]	this study
Delma australis	*Delma hebesa*	82[a], 79[b]	5.4 [73]	this study[a], Maryan et al. 2015b[b]
Delma fraseri	*Delma fraseri*	131, 127	8.9 [131]	this study
Delma fraseri	*Delma petersoni*	131, 130	10.4 [130]	this study
Delma nasuta	*Delma butleri*	96, 94	7 [96]	this study
Delma nasuta	*Delma grayii*	121[a], 120.5[b]	7.2 [111]	Storr et al. 1990[a], Kluge 1974[b]
Delma nasuta	*Delma haroldi*	88, 80	6 [80]	this study
Delma nasuta	*Delma inornata*	135[a], 133[b]	7.9 [119]	Kluge 1974[a], Shea 1991[b]
Delma nasuta	*Delma nasuta*	112[a], 106[b]	7.6 [105]	Storr 1987[a], this study[b]
Delma tincta	*Delma borea*	98[a], 96[b]	7.1 [92]	Storr et al. 1990[a], this study[b]
Delma tincta	*Delma desmosa*	90[a,b], 88[b]	6 [88]	this study[a], Maryan et al. 2007[b]
Delma tincta	*Delma pax*	98[a], 95[b]	6.9 [85]	Maryan et al. 2007[a], this study[b]
Delma impar	*Delma impar*	108, 103	7.7 [108]	this study
Delma impar	*Delma molleri*	111[a], 111[b]	7.4 [107]	Kluge 1974[a], this study[b]
Delma impar	*Delma plebeia*	124, 123	7 [109]	this study
Lialis	*Lialis burtonis* (wet biome)	327, 309	17.1 [299]	this study
Lialis	*Lialis burtonis* (dry biome)	259, 249	12 [233]	this study
Lialis	*Lialis jicari*	323, 321	11.6 [308]	this study
Pygopus lepidopodus	*Pygopus lepidopodus* (wet biome	253, 245	15 [236]	this study
Pygopus lepidopodus	*Pygopus lepidopodus* (dry biome)	212, 211	12.5 [205]	this study
Pygopus nigriceps	*Pygopus nigriceps* (wet biome)	222, 217	11.4 [217]	this study
Pygopus nigriceps	*Pygopus nigriceps* (dry biome)	208, 204	9.2 [177]	this study
Pygopus nigriceps	*Pygopus schraderi* (wet biome)	201, 198	12.5 [180]	this study
Pygopus nigriceps	*Pygopus schraderi* (dry biome)	183, 176	10.1 [176]	this study
Pygopus nigriceps	*Pygopus steelescotti*	194, 188	9.9 [194]	this study

Table 2. Ontogenetic isometry tests for the ln*Tail* on ln*SVL* relationship in pygopodid lizards. Slopes are negatively or positively allometric when they are significantly smaller or larger, respectively, than the null value of 1.0 (isometry). n = subsample size for each OTU; slope = ordinary least squares regression slope; C.I. = confidence interval; and R^2 = coefficient of determination. *p*-values shaded in gray are statistically significant at the 0.05 level. Specimens having incomplete or regenerated tails were excluded from these analyses.

Species/Population Group	OTU	n	Slope	95% C.I.	R^2	*p*-value
Aprasia repens group	*Aprasia litorea*	8	1.24	(0.70-1.77)	0.84	0.3184
Aprasia repens group	*Aprasia repens*	37	1.21	(1.02-1.41)	0.82	0.0320
Aprasia repens group	*Aprasia rostrata*	10	1.56	(0.34-2.78)	0.52	0.3235
Southeastern Australia Aprasia group	*Aprasia inaurita*	26	1.06	(0.88-1.23)	0.86	0.5212
Southeastern Australia Aprasia group	*Aprasia parapulchella*	25	0.94	(0.75-1.14)	0.81	0.5480
Southeastern Australia Aprasia group	*Aprasia pseudopulchella*	25	1.02	(0.84-1.21)	0.85	0.7951
Southeastern Australia Aprasia group	*Aprasia striolata*	39	1.12	(1.00-1.24)	0.91	0.0516
Delma australis group	*Delma australis*	53	1.24	(1.11-1.36)	0.88	0.0005
Delma australis group	*Delma hebesa*	13	0.88	(0.57-1.19)	0.78	0.4181
Delma fraseri group	*Delma fraseri*	30	1.35	(1.26-1.44)	0.97	0.0000
Delma fraseri group	*Delma petersoni*	23	1.33	(1.13-1.54)	0.90	0.0026
Delma impar group	*Delma impar*	36	1.25	(1.09-1.41)	0.88	0.0026
Delma impar group	*Delma molleri*	26	1.37	(1.21-1.54)	0.93	0.0001
Delma impar group	*Delma plebeia*	29	1.36	(1.21-1.52)	0.93	0.0000
Delma nasuta group	*Delma butleri*	73	1.13	(1.02-1.25)	0.85	0.0259
Delma nasuta group	*Delma grayii*	27	1.40	(1.31-1.48)	0.98	0.0000
Delma nasuta group	*Delma haroldi*	37	1.32	(1.12-1.52)	0.84	0.0029
Delma nasuta group	*Delma inornata*	50	1.35	(1.22-1.49)	0.90	0.0000
Delma nasuta group	*Delma nasuta*	52	1.38	(1.23-1.54)	0.87	0.0000
Delma tincta group	*Delma borea*	34	1.34	(1.19-1.49)	0.92	0.0000
Delma tincta group	*Delma desmosa*	21	1.26	(1.07-1.46)	0.91	0.0110
Delma tincta group	*Delma pax*	49	1.30	(1.22-1.39)	0.95	0.0000
Lialis group	*Lialis burtonis* (wet biome)	71	1.13	(1.04-1.21)	0.92	0.0031
Lialis group	*Lialis burtonis* (dry biome)	130	1.21	(1.15-1.27)	0.93	0.0000
Lialis group	*Lialis jicari*	34	1.33	(1.27-1.39)	0.99	0.0000
Pygopus lepidopodus group	*Pygopus lepidopodus* (wet biome)	18	1.41	(1.28-1.54)	0.97	0.0000
Pygopus lepidopodus group	*Pygopus lepidopodus* (dry biome)	84	1.39	(1.32-1.46)	0.95	0.0000
Pygopus nigriceps group	*Pygopus nigriceps* (wet biome)	15	1.23	(1.06-1.39)	0.95	0.0113
Pygopus nigriceps group	*Pygopus nigriceps* (dry biome)	62	1.38	(1.30-1.46)	0.95	0.0000
Pygopus nigriceps group	*Pygopus schraderi* (wet biome)	31	1.48	(1.39-1.58)	0.97	0.0000
Pygopus nigriceps group	*Pygopus schraderi* (dry biome)	36	1.36	(1.25-1.47)	0.95	0.0000
Pygopus nigriceps group	*Pygopus steelescotti*	27	1.55	(1.35-1.74)	0.91	0.0000

Table 3. Ontogenetic isometry tests for the ln*Tail* on ln$\overline{BW}$ relationship in pygopodid lizards. Slopes are negatively or positively allometric when they are significantly smaller or larger, respectively, than the null value of 1.0 (isometry). n = subsample size for each OTU; slope = ordinary least squares regression slope; C.I. = confidence interval; and R^2 = coefficient of determination. *p*-values shaded in gray are statistically significant at the 0.05 level. Specimens having incomplete or regenerated tails were excluded from these analyses.

Species/Population Group	OTU	n	Slope	95% C.I.	R^2	*p*-value
Aprasia repens group	*Aprasia litorea*	8	1.87	(1.22-2.53)	0.89	0.0172
Aprasia repens group	*Aprasia repens*	37	1.38	(1.07-1.69)	0.70	0.0173
Aprasia repens group	*Aprasia rostrata*	10	1.43	(0.51-2.35)	0.62	0.3149
Southeastern Australia Aprasia group	*Aprasia inaurita*	26	1.76	(1.30-2.21)	0.73	0.0021
Southeastern Australia Aprasia group	*Aprasia parapulchella*	25	0.97	(0.61-1.33)	0.57	0.8636
Southeastern Australia Aprasia group	*Aprasia pseudopulchella*	25	1.00	(0.64-1.37)	0.58	0.9843
Southeastern Australia Aprasia group	*Aprasia striolata*	39	1.19	(0.94-1.44)	0.72	0.1342
Delma australis group	*Delma australis*	53	1.23	(1.09-1.36)	0.87	0.0015
Delma australis group	*Delma hebesa*	13	0.81	(0.50-1.13)	0.75	0.2155
Delma fraseri group	*Delma fraseri*	30	1.53	(1.33-1.74)	0.89	0.0000
Delma fraseri group	*Delma petersoni*	23	1.40	(1.18-1.63)	0.89	0.0012
Delma impar group	*Delma impar*	36	1.34	(1.06-1.62)	0.73	0.0200
Delma impar group	*Delma molleri*	26	1.57	(1.29-1.85)	0.85	0.0003
Delma impar group	*Delma plebeia*	29	1.86	(1.53-2.20)	0.83	0.0000
Delma nasuta group	*Delma butleri*	73	1.35	(1.22-3.30)	0.86	0.0000
Delma nasuta group	*Delma grayii*	27	1.41	(1.22-1.61)	0.90	0.0002
Delma nasuta group	*Delma haroldi*	37	1.48	(1.17-1.79)	0.73	0.0031
Delma nasuta group	*Delma inornata*	50	1.57	(1.35-1.78)	0.81	0.0000
Delma nasuta group	*Delma nasuta*	52	1.54	(1.33-1.74)	0.82	0.0000
Delma tincta group	*Delma borea*	34	1.61	(1.42-1.79)	0.91	0.0000
Delma tincta group	*Delma desmosa*	21	1.19	(0.96-1.41)	0.86	0.0996
Delma tincta group	*Delma pax*	49	1.31	(1.17-1.44)	0.89	0.0000
Lialis group	*Lialis burtonis* (wet biome)	72	1.21	(1.08-1.33)	0.84	0.0018
Lialis group	*Lialis burtonis* (dry biome)	130	1.37	(1.28-1.47)	0.86	0.0000
Lialis group	*Lialis jicari*	34	1.56	(1.35-1.76)	0.88	0.0000
Pygopus lepidopodus group	*Pygopus lepidopodus* (wet biome)	18	1.69	(1.55-1.83)	0.98	0.0000
Pygopus lepidopodus group	*Pygopus lepidopodus* (dry biome)	84	1.53	(1.42-1.65)	0.90	0.0000
Pygopus nigriceps group	*Pygopus nigriceps* (wet biome)	15	1.40	(1.18-1.62)	0.94	0.0017
Pygopus nigriceps group	*Pygopus nigriceps* (dry biome)	62	1.50	(1.35-1.65)	0.88	0.0000
Pygopus nigriceps group	*Pygopus schraderi* (wet biome)	31	1.53	(1.37-1.69)	0.93	0.0000
Pygopus nigriceps group	*Pygopus schraderi* (dry biome)	36	1.66	(1.50-1.82)	0.93	0.0000
Pygopus nigriceps group	*Pygopus steelescotti*	27	1.81	(1.57-2.50)	0.91	0.0000

Table 4. Ontogenetic isometry tests for the ln$\overline{BW}$ on lnSVL relationship in pygopodid lizards. Slopes are negatively or positively allometric when they are significantly smaller or larger, respectively, than the null value of 1.0 (isometry). n = subsample size for each OTU; slope = ordinary least squares regression slope; C.I. = confidence interval; and R^2 = coefficient of determination. *p*-values shaded in gray are statistically significant at the 0.05 level. Specimens having incomplete or regenerated tails were excluded from these analyses.

Species/Population Group	OTU	n	Slope	95% C.I.	R^2	*p*-value
Aprasia repens group	*Aprasia clairae*	8	0.45	(0.27-0.64)	0.86	0.0003
Aprasia repens group	*Aprasia haroldi*	14	0.47	(0.26-0.67)	0.67	0.0001
Aprasia repens group	*Aprasia litorea*	11	0.64	(0.50-0.78)	0.92	0.0002
Aprasia repens group	*Aprasia repens*	48	0.75	(0.63-0.88)	0.76	0.0002
Aprasia repens group	*Aprasia rostrata*	25	0.66	(0.42-0.89)	0.59	0.0061
Aprasia repens group	*Aprasia smithi*	18	0.65	(0.46-0.84)	0.76	0.0014
Southeastern Australia Aprasia group	*Aprasia inaurita*	34	0.52	(0.42-0.62)	0.77	0.0000
Southeastern Australia Aprasia group	*Aprasia parapulchella*	33	0.70	(0.49-0.90)	0.61	0.0050
Southeastern Australia Aprasia group	*Aprasia pseudopulchella*	31	0.71	(0.53-0.88)	0.71	0.0017
Southeastern Australia Aprasia group	*Aprasia striolata*	69	0.72	(0.59-0.86)	0.64	0.0000
Delma australis group	*Delma australis*	56	0.90	(0.79-1.01)	0.83	0.0662
Delma australis group	*Delma hebesa*	43	0.68	(0.50-0.87)	0.57	0.0012
Delma fraseri group	*Delma fraseri*	32	0.83	(0.76-0.91)	0.94	0.0001
Delma fraseri group	*Delma petersoni*	45	0.90	(0.80-1.00)	0.89	0.0530
Delma impar group	*Delma impar*	38	0.79	(0.67-0.92)	0.83	0.0016
Delma impar group	*Delma molleri*	29	0.82	(0.75-0.90)	0.95	0.0001
Delma impar group	*Delma plebeia*	30	0.62	(0.49-0.74)	0.79	0.0000
Delma nasuta group	*Delma butleri*	93	0.79	(0.72-0.85)	0.86	0.0000
Delma nasuta group	*Delma grayii*	29	0.88	(0.78-0.98)	0.92	0.0253
Delma nasuta group	*Delma haroldi*	74	0.80	(0.72-0.89)	0.85	0.0000
Delma nasuta group	*Delma inornata*	54	0.76	(0.67-0.85)	0.85	0.0000
Delma nasuta group	*Delma nasuta*	53	0.82	(0.73-0.91)	0.87	0.0002
Delma tincta group	*Delma borea*	38	0.86	(0.77-0.95)	0.91	0.0027
Delma tincta group	*Delma desmosa*	64	0.87	(0.76-0.99)	0.79	0.0299
Delma tincta group	*Delma pax*	53	0.90	(0.82-0.99)	0.90	0.0245
Lialis group	*Lialis burtonis* (wet biome)	136	0.86	(0.81-0.91)	0.91	0.0000
Lialis group	*Lialis burtonis* (dry biome)	142	0.78	(0.73-0.83)	0.88	0.0000
Lialis group	*Lialis jicari*	96	0.79	(0.72-0.85)	0.84	0.0000
Pygopus lepidopodus group	*Pygopus lepidopodus* (wet biome)	20	0.84	(0.74-0.93)	0.95	0.0018
Pygopus lepidopodus group	*Pygopus lepidopodus* (dry biome)	131	0.80	(0.76-0.85)	0.92	0.0000
Pygopus nigriceps group	*Pygopus nigriceps* (wet biome)	15	0.84	(0.70-0.98)	0.93	0.0256
Pygopus nigriceps group	*Pygopus nigriceps* (dry biome)	69	0.81	(0.73-0.90)	0.85	0.0000
Pygopus nigriceps group	*Pygopus schraderi* (wet biome)	35	0.90	(0.80-1.00)	0.91	0.0404
Pygopus nigriceps group	*Pygopus schraderi* (dry biome)	51	0.75	(0.69-0.82)	0.92	0.0000
Pygopus nigriceps group	*Pygopus steelescotti*	39	0.79	(0.70-0.87)	0.91	0.0000

Table 5. Scaling patterns for pairs of ontogenetic trajectories in the *Aprasia repens* group. All scaling patterns were obtained from Figure 3 by using maximum *SVL* as the measure of body size. GS = geometric similarity; EA = evolutionary allometry; X = one or both OTUs had insufficient data (i.e., missing or regenerated tails); * indicates that the left OTU has a larger maximum $\overline{BW}$ than the right OTU but both OTUs have the same maximum *SVL*; ** indicates that the right OTU has a larger maximum $\overline{BW}$ than the left OTU but the left OTU has a longer maximum *SVL* than the right OTU; *** indicates that the left OTU has a longer maximum *SVL* than the right OTU but both OTUs have the same maximum $\overline{BW}$. Scaling relationships for *A. repens* vs. *A. rostrata* pairs could not be determined because both OTUs had the same maximum *SVL*. See Materials and Methods for more details and Table 1 for maximum (max) *SVL* and $\overline{BW}$.

Larger Max SVL & BW	**Smaller Max SVL & BW**	**lnSVL vs. lnTail**	**lnBW vs. lnTail**	**lnSVL vs. lnBW**
Aprasia repens	*Aprasia litorea*	GS (all ages)	GS (all ages)	GS (all ages)
Aprasia rostrata	*Aprasia litorea*	EA overlap (slopes equal)	EA overlap (slopes equal)	GS (all ages)
*Aprasia repens**	*Aprasia rostrata*	ambiguous	ambiguous	ambiguous
Aprasia repens	*Aprasia clairae*	X	X	GS (adults)
Aprasia repens	*Aprasia haroldi*	X	X	GS (adults)
Aprasia rostrata	*Aprasia clairae*	X	X	EA overlap (slopes equal)
Aprasia rostrata	*Aprasia haroldi*	X	X	EA overlap (slopes equal)
Aprasia smithi	*Aprasia clairae*	X	X	GS (all ages)
Aprasia smithi	*Aprasia litorea*	X	X	GS (all ages)
Aprasia smithi	*Aprasia haroldi*	X	X	GS (all ages)
Aprasia smithi	*Aprasia rostrata*	X	X	GS (all ages)
Aprasia clairae	*Aprasia haroldi***	X	X	EA overlap (slopes equal)
Aprasia litorea	*Aprasia haroldi***	X	X	EA transposition (all ages)
Aprasia smithi	*Aprasia repens***	X	X	EA overlap (slopes equal)
*Aprasia litorea****	*Aprasia clairae*	X	X	EA transposition (all ages)

Table 6. Scaling patterns for pairs of ontogenetic trajectories in the southeastern Australia *Aprasia* group. All scaling patterns were obtained from Figure 4 by using maximum *SVL* as the measure of body size. GS = geometric similarity; EA = evolutionary allometry; ** indicates that the right OTU has a larger maximum $\overline{BW}$ than the left OTU but the left OTU has a longer maximum *SVL* than the right OTU. See Materials and Methods for more details and Table 1 for maximum (max) *SVL* and $\overline{BW}$.

Larger Max SVL & BW	**Smaller Max SVL & BW**	**lnSVL vs. lnTail**	**lnBW vs. lnTail**	**lnSVL vs. lnBW**
Aprasia parapulchella	*Aprasia inaurita*	EA transposition (all ages)	EA overlap (slopes not equal)	GS (all ages)
Aprasia pseudopulchella	*Aprasia inaurita*	EA overlap (slopes equal)	EA transposition (juveniles)	EA transposition (all ages)
Aprasia pseudopulchella	*Aprasia parapulchella***	GS (all ages)	EA overlap (slopes equal)	EA transposition (all ages)
Aprasia parapulchella	*Aprasia striolata***	EA transposition (all ages)	EA transposition (all ages)	EA transposition (all ages)
Aprasia pseudopulchella	*Aprasia striolata***	EA transposition (all ages)	EA transposition (all ages)	EA transposition (all ages)
Aprasia inaurita	*Aprasia striolata***	EA transposition (all ages)	EA transposition (adults)	EA transposition (adults)

Table 7. Scaling patterns for pairs of ontogenetic trajectories in the *Delma australis*, *D. fraseri*, and *D. impar* groups. All scaling patterns were obtained from Figure 5 by using maximum *SV*L as the measure of body size. GS = geometric similarity; EA = evolutionary allometry; * indicates that the left OTU has a larger maximum $\overline{BW}$ than the right OTU but both OTUs have the same maximum *SVL*; ** indicates that the right OTU has a larger maximum $\overline{BW}$ than the left OTU but the left OTU has a longer maximum *SVL* than the right OTU; *** indicates that the left OTU has a longer maximum *SVL* than the right OTU but both OTUs have the same maximum $\overline{BW}$. Scaling relationships for *D. petersoni* vs. *D. fraseri* pairs could not be determined because both OTUs had the same maximum *SVL*. See Materials and Methods for more details and Table 1 for maximum (max) *SVL* and $\overline{BW}$.

Larger Max SVL & BW	**Smaller Max SVL & BW**	**lnSVL vs. lnTail**	**lnBW vs. lnTail**	**lnSVL vs. lnBW**
*Delma australis****	*Delma hebesa*	EA overlap (slopes equal)	EA overlap (slopes not equal)	EA overlap (slopes not equal)
*Delma petersoni**	*Delma fraseri*	ambiguous	ambiguous	ambiguous
Delma molleri	*Delma impar***	EA transposition (all ages)	EA transposition (all ages)	EA overlap (slopes equal)
Delma plebeia	*Delma impar***	EA transposition (all ages)	EA transposition (adults)	EA overlap (slopes not equal)
Delma plebeia	*Delma molleri***	EA overlap (slopes equal)	EA overlap (slopes equal)	EA overlap (slopes not equal)

Table 8. Scaling patterns for pairs of ontogenetic trajectories in the *Delma nasuta* group. All scaling patterns were obtained from Figure 6 by using maximum *SVL* as the measure of body size. GS = geometric similarity; EA = evolutionary allometry; ** indicates that the right OTU has a larger maximum $\overline{BW}$ than the left OTU but the left OTU has a longer maximum *SV*L than the right OTU. See Materials and Methods for more details and Table 1 for maximum (max) *SV*L and $\overline{BW}$.

Larger Max SVL & BW	**Smaller Max SVL & BW**	**lnSVL vs. lnTail**	**lnBW vs. lnTail**	**lnSVL vs. lnBW**
Delma butleri	*Delma haroldi*	GS (all ages)	GS (all ages)	GS (all ages)
Delma grayii	*Delma butleri*	EA transposition (adults)	EA transposition (all ages)	EA transposition (all ages)
Delma grayii	*Delma haroldi*	EA overlap (slopes equal)	EA overlap (slopes equal)	EA overlap (slopes equal)
Delma inornata	*Delma butleri*	GS (juveniles)	EA overlap (slopes equal)	EA transposition (all ages)
Delma inornata	*Delma grayii*	GS (all ages)	GS (all ages)	EA transposition (all ages)
Delma inornata	*Delma haroldi*	GS (all ages)	GS (all ages)	EA transposition (all ages)
Delma inornata	*Delma nasuta*	GS (all ages)	GS (all ages)	EA transposition (all ages)
Delma nasuta	*Delma butleri*	EA transposition (adults)	EA transposition (all ages)	EA overlap (slopes equal)
Delma nasuta	*Delma haroldi*	GS (all ages)	GS (all ages)	EA overlap (slopes equal)
Delma grayii	*Delma nasuta***	EA transposition (all ages)	EA transposition (all ages)	EA overlap (slopes equal)

Table 9. Scaling patterns for pairs of ontogenetic trajectories in the *Delma tincta* group. All scaling patterns were obtained from Figure 7 by using maximum *SVL* as the measure of body size. GS = geometric similarity; EA = evolutionary allometry; * indicates that the left OTU has a larger maximum $\overline{BW}$ than the right OTU but both OTUs have the same maximum *SVL*. Scaling relationships for *D. borea* vs. *D. pax* pairs could not be determined because both OTUs had the same maximum *SVL*. See Materials and Methods for more details and Table 1 for maximum *SVL* and $\overline{BW}$.

Larger Max SVL & BW	**Smaller Max SVL & BW**	**lnSVL vs. lnTail**	**lnBW vs. lnTail**	**lnSVL vs. lnBW**
Delma borea	*Delma desmosa*	GS (all ages)	EA overlap (slopes not equal)	EA overlap (slopes equal)
*Delma borea**	*Delma pax*	ambiguous	ambiguous	ambiguous
Delma pax	*Delma desmosa*	GS (all ages)	GS (all ages)	GS (all ages)

Table 10. Scaling patterns for pairs of ontogenetic trajectories in the *Lialis* and *Pygopus lepidopodus* groups. All scaling patterns were obtained from Figure 8 by using maximum *SVL* as the measure of body size. GS = geometric similarity; EA = evolutionary allometry; ** indicates that the right OTU has a larger maximum $\overline{BW}$ than the left OTU but the left OTU has a longer maximum *SVL* than the right OTU. See Materials and Methods for more details and Table 1 for maximum *SVL* and $\overline{BW}$.

Larger Max SVL & BW	**Smaller Max SVL & BW**	**lnSVL vs. lnTail**	**lnBW vs. lnTail**	**lnSVL vs. lnBW**
Lialis burtonis (wet biome)	*Lialis burtonis* (dry biome)	GS (all ages)	GS (all ages)	GS (adults)
Lialis burtonis (wet biome)	*Lialis jicari*	GS (adults)	GS (adults)	GS (all ages)
Lialis jicari	*Lialis burtonis*** (dry biome)	EA transposition (adults)	EA transposition (all ages)	EA transposition (all ages)
Pygopus lepidopodus (wet biome)	*Pygopus lepidopodus* (dry biome)	GS (all ages)	GS (all ages)	GS (all ages)

Table 11. Scaling patterns for pairs of ontogenetic trajectories in the *Pygopus nigriceps* group. All scaling patterns were obtained from Figure 9 by using maximum *SVL* as the measure of body size. GS = geometric similarity; EA = evolutionary allometry; ** indicates that the right OTU has a larger maximum $\overline{BW}$ than the left OTU but the left OTU has a longer maximum *SV*L than the right OTU. See Materials and Methods for more details and Table 1 for maximum (max) *SVL* and $\overline{BW}$.

Larger Max SVL & BW	**Smaller Max SVL & BW**	**lnSVL vs. lnTail**	**lnBW vs. lnTail**	**lnSVL vs. lnBW**
Pygopus nigriceps (wet biome)	*Pygopus nigriceps* (dry biome)	GS (adults)	GS (all ages)	GS (all ages)
Pygopus nigriceps (wet biome)	*Pygopus schraderi* (dry biome)	GS (all ages)	EA transposition (all ages)	EA transposition (all ages)
Pygopus nigriceps (wet biome)	*Pygopus steelescotti*	EA overlap (slopes not equal)	EA transposition (juveniles)	EA transposition (all ages)
Pygopus schraderi (wet biome)	*Pygopus schraderi* (dry biome)	GS (all ages)	GS (all ages)	GS (adults)
Pygopus schraderi (wet biome)	*Pygopus steelescotti*	EA overlap (slopes equal)	GS (adults)	GS (all ages)
Pygopus nigriceps (wet biome)	*Pygopus schraderi*** (wet biome)	EA overlap (slopes not equal)	EA transposition (all ages)	EA transposition (all ages)
Pygopus nigriceps (dry biome)	*Pygopus schraderi*** (wet biome)	EA overlap (slopes equal)	EA transposition (all ages)	EA transposition (all ages)
Pygopus nigriceps (dry biome)	*Pygopus schraderi*** (dry biome)	GS (all ages)	EA transposition (all ages)	EA transposition (all ages)
Pygopus nigriceps (dry biome)	*Pygopus steelescotti***	EA overlap (slopes equal)	EA transposition (juveniles)	EA transposition (all ages)
Pygopus steelescotti	*Pygopus schraderi*** (dry biome)	GS (all ages)	EA overlap (slopes equal)	EA transposition (all ages)

Table 12. Scaling patterns for pairs of adult growth trajectories in four species of Darwin's finches belonging to the genus *Geospiza*. Scaling patterns were obtained from log-log plots of geometric mean regressions for logBLG on logWGT, logBDT on logWGT, and logBWD on logWGT relationships shown in Figure 3 of Boag (1984). Each scaling pattern was classified as here as reflecting either geometric similarity or evolutionary allometry based on the spatial arrangement of the trajectories. Note that nine of the comparisons involved pairs of species while one comparison involved two allopatric populations of *G. fortis*. OTU = operational taxonomic unit; BLG = bill length; BDT = bill depth; BWD = bill width; and WGT = body mass (see Boag 1984 for more details).

larger OTU/smaller OTU	**BLG on WGT**	**BDT on WGT**	**BWD on WGT**
G. magnirostris /*G. fortis* (Daphne Major Island)	geometric similarity	evolutionary allometry	evolutionary allometry
G. magnirostris /*G. fortis* (Santa Cruz Island)	evolutionary allometry	evolutionary allometry	evolutionary allometry
G. magnirostris /*G. scandens*	geometric similarity	evolutionary allometry	evolutionary allometry
G. magnirostris /*G. fuliginosa*	evolutionary allometry	evolutionary allometry	evolutionary allometry
G. fortis (Santa Cruz Island)/*G. fortis* (Daphne Major Island)	geometric similarity	geometric similarity	geometric similarity
G. fortis (Daphne Major Island)/*G. fuliginosa*	evolutionary allometry	evolutionary allometry	evolutionary allometry
G. scandens /*G. fortis* (Daphne Major Island)	evolutionary allometry	geometric similarity	geometric similarity
G. scandens /*G. fuliginosa*	evolutionary allometry	evolutionary allometry	evolutionary allometry
G. fortis (Santa Cruz Island)/*G. fuliginosa*	evolutionary allometry	evolutionary allometry	evolutionary allometry
G. fortis (Santa Cruz Island)/*G. scandens*	geometric similarity	evolutionary allometry	evolutionary allometry

Figure Captions

Figure 1. Body and trait size scaling patterns in pairwise comparisons of ontogenetic allometric regressions. Blue and green lines represent ontogenetic regressions or "trajectories" of log trait size against log body size for two conspecific populations or closely related species. (A) *Geometric similarity when the trait exhibits positive ontogenetic allometry*. This scaling pattern occurs when the slopes of both trajectories (α_1 and α_2) reflect positive ontogenetic allometry (i.e., $\alpha_1 > 1.0$ and $\alpha_2 > 1.0$, assuming an isometric slope of 1.0) and the trajectory of the smaller population (or species) is transposed above and to the left of the trajectory of the larger population (or species). The interspecific slope (α_i) is then expected to approximate a value of 1.0, indicating that both populations (or species) diverged in body and trait sizes but with no change in trait shape. (B) *Geometric similarity when the trait exhibits negative ontogenetic allometry*. This scaling pattern occurs when the slopes of both trajectories (α_1 and α_2) show negative ontogenetic allometry (i.e., $\alpha_1 < 1.0$ and $\alpha_2 < 1.0$, assuming an isometric slope of 1.0) and the trajectory of the larger population (or species) is transposed above and to the right of the trajectory of the smaller population (or species). The interspecific slope (α_i) is then expected to approximate a value of 1.0, indicating that both populations (or species) diverged in body and trait sizes but with no change in trait shape. (C) *Positive evolutionary allometry via ontogenetic scaling*. This scaling pattern occurs when the slopes of both trajectories (α_1 and α_2) reflect positive ontogenetic allometry (i.e., $\alpha_1 > 1.0$ and $\alpha_2 > 1.0$, assuming an isometric slope of 1.0) and the trajectories partially overlap each other. (D) *Negative evolutionary allometry via ontogenetic scaling*. This scaling pattern occurs when the slopes of both trajectories (α_1 and α_2) reflect negative ontogenetic allometry (i.e., $\alpha_1 < 1.0$ and $\alpha_2 < 1.0$, assuming an isometric slope of

1.0) and the trajectories partially overlap each other. (E) *Positive evolutionary allometry via transposition*. This scaling pattern occurs when the slopes of both trajectories (α_1 and α_2) display positive ontogenetic allometry (i.e., $\alpha_1 > 1.0$ and $\alpha_2 > 1.0$, assuming an isometric slope of 1.0) and the trajectory of the larger population (or species) is transposed above and to the right of the trajectory of the smaller population (or species). The interspecific slope (α_i) is greater than the slopes of the two trajectories (α_1 and α_2). (F) *Negative evolutionary allometry via transposition*. This scaling pattern occurs when the slopes of both trajectories (α_1 and α_2) show negative ontogenetic allometry (i.e., $\alpha_1 < 1.0$ and $\alpha_2 < 1.0$, assuming an isometric slope of 1.0) and the trajectory of the smaller population (or species) is transposed above and to the left of the trajectory of the larger population (or species). The interspecific slope (α_i) is less than the slopes of the two trajectories (α_1 and α_2). Dotted lines depict interpopulational or intespecific allometries between the largest adults in each population or species.

Figure 2. Geometric similarity-first model of trait divergence. Each graph shows one or two post-natal ontogenetic allometric trajectories plotted as log trait size on log body size. Dashed lines depict interpopulational or interspecific scaling relationships for the adult size classes. Because the direction of evolutionary body size change and the type of ontogenetic allometry exhibited by a trait could determine how a trait diverges, the model posits four different scenarios of trait divergence. In each scenario, the divergence process starts during a “Pre-population divergence” and ends in “Phase 1” when a large- or small-bodied ancestor (gray trajectory) splits into populations A (green trajectory) and B (yellow trajectory). The divergence process continues during Phases 2 to 4. **(A)** Scenario 1: body size increases in population B (relative to the

ancestor) and the trait shows positive ontogenetic allometry. **(B)** Scenario 2: body size decreases in population B and the trait shows positive ontogenetic allometry. **(C)** Scenario 3: body size increases in population B and the trait shows negative ontogenetic allometry. **(D)** Scenario 4: body size decreases population B and the trait exhibits negative ontogenetic allometry. Note that on each graph the yellow trajectory has the larger maximum body size compared to the corresponding green trajectory. Also, "population A" and "species A" trajectories always resemble their ancestral trajectory, whereas "population B" and "species B" trajectories always phenotypically diverge away from their ancestral trajectory. Intraspecific slopes (α_A, α_B) that are greater than one indicates positive ontogenetic allometry while slopes less than one show negative ontogenetic allometry (i.e., α_A or α_B = 1.0 indicates isometry). Interpopulational and interspecific slopes (α_i) equal to one signify geometric similarity, α_i values greater than one exhibit positive evolutionary allometry, and α_i values less than one display negative evolutionary allometry (α_i = 1 represents geometric similarity). Note that interpretations of these slopes change if the isometric and geometric similarity slopes assume other values. See text for explanations of each phase.

Figure 3. Pairwise comparisons of post-natal ontogenetic trajectories for the *Aprasia repens* species group. Plots A-I show bivariate scaling relationships ln*Tail* on ln*SVL*, ln*Tail* on ln$\overline{BW}$, and ln$\overline{BW}$ on ln*SVL* for the *A. repens*/*A. litorea*, *A. rostrata*/*A. litorea*, and *A. repens*/*A. rostrata* pairs. Plots J-U only show the ln$\overline{BW}$ on ln*SVL* relationship for other OTU pairs because one or both OTUs had insufficient tail length data (i.e., due to regenerated or incomplete tails on many specimens). In plots A-F and J-U, yellow OTUs exhibited longer maximum *SVL* compared to

corresponding green OTUs. In A-Q, yellow OTUs had a larger maximum $\overline{BW}$ than corresponding green OTUs. In G-I, both OTUs have the same maximum *SVL* but the yellow OTU (*) had a larger maximum $\overline{BW}$ than the green OTU. In R-T, green OTUs (**) had larger maximum $\overline{BW}$ compared to corresponding yellow OTUs. In plot U, the yellow OTU (***) had a longer maximum *SVL* than the green OTU but both OTUs had the same maximum $\overline{BW}$. Each dot represents an individual. Results of the equal slopes and equal *y*-intercepts tests are shown. *p*-values > 0.05 were statistically non-significant (n.s.). Equal intercepts tests were not applicable (n.a.) whenever equal slopes hypotheses were rejected.

Figure 4. Pairwise comparisons of post-natal ontogenetic trajectories for the southeastern Australia *Aprasia* species group. Plots A-R show bivariate scaling relationships ln*Tail* on ln*SVL*, ln*Tail* on ln$\overline{BW}$, and ln$\overline{BW}$ on ln*SVL* comparisons for each OTU pair. In all plots, yellow OTUs exhibited longer maximum *SVL* compared to corresponding green OTUs. In A-F, yellow OTUs had larger maximum $\overline{BW}$ compared to corresponding green OTUs, whereas in G-R green OTUs (**) had larger maximum $\overline{BW}$ than corresponding yellow OTUs. Each dot represents an individual. Results of the equal slopes and equal *y*-intercepts tests are shown. *p*-values > 0.05 were statistically non-significant (n.s.). Equal intercepts tests were not applicable (n.a.) whenever equal slopes hypotheses were rejected.

Figure 5. Pairwise comparisons of post-natal ontogenetic trajectories for OTUs in the *Delma australis*, *D. fraseri*, and *D. impar* species groups. Plots A-C show bivariate scaling relationships ln*Tail* on ln*SVL*, ln*Tail* on ln$\overline{BW}$, and ln$\overline{BW}$ on ln*SVL* for the *D. australis*/*D. hebesa* pair, plots

D-F exhibit scaling relationships for the *D. petersoni*/*D. fraseri* pair, and plots G-O display scaling relationships for the *D. impar* group pairs. In A-C, the yellow OTU (***) had a longer maximum *SVL* compared to the green OTU, but both OTUs had the same maximum $\overline{BW}$. In D-F, both OTUs had the same maximum *SVL* but the yellow OTU (*) had a larger maximum $\overline{BW}$ compared to the green OTU. In G-O, yellow OTUs had longer maximum *SVL* compared to corresponding green OTUs while green OTUs (**) had larger maximum $\overline{BW}$ than corresponding yellow OTUs. Each dot represents an individual. Results of the equal slopes and equal *y*-intercepts tests are shown. *p*-values > 0.05 were statistically non-significant (n.s.). Equal intercepts tests were not applicable (n.a.) whenever equal slopes hypotheses were rejected.

Figure 6. Pairwise comparisons of post-natal ontogenetic trajectories for the *Delma nasuta* species group. Plots A-DD show bivariate scaling relationships ln*Tail* on ln*SVL*, ln*Tail* on ln$\overline{BW}$, and ln$\overline{BW}$ on ln*SVL* for each OTU pair. In all plots, yellow OTUs exhibited longer maximum *SVL* compared to corresponding green OTUs. In A-AA, yellow OTUs had larger maximum $\overline{BW}$ compared to corresponding green OTUs. In BB-DD, the green OTU (**) had a larger maximum $\overline{BW}$ than the yellow OTU. Each dot represents an individual. Results of the equal slopes and equal *y*-intercepts tests are shown. *p*-values > 0.05 were statistically non-significant (n.s.). Equal intercepts tests were not applicable (n.a.) whenever equal slopes hypotheses were rejected.

Figure 7. Pairwise comparisons of post-natal ontogenetic trajectories for the *Delma tincta* species group. Plots A-I show bivariate scaling relationships ln*Tail* on ln*SVL*, ln*Tail* on ln$\overline{BW}$, and ln$\overline{BW}$ on ln*SVL* for each OTU pair. In plots A-C and G-I, yellow OTUs exhibited longer

maximum *SVL* and larger maximum $\overline{BW}$ than corresponding green OTUs, whereas in D-F both OTUs had the same maximum *SVL* but the yellow OTU (*) had a larger maximum $\overline{BW}$ compared to the green OTU. Each dot represents an individual. Results of the equal slopes and equal *y*-intercepts tests are shown. *p*-values > 0.05 were statistically non-significant (n.s.). Equal intercepts tests were not applicable (n.a.) whenever equal slopes hypotheses were rejected.

Figure 8. Pairwise comparisons of post-natal ontogenetic trajectories for the *Lialis* species group and two populations of *Pygopus lepidopodus*. Plots A-I show bivariate scaling relationships ln*Tail* on ln*SVL*, ln*Tail* on ln$\overline{BW}$, and ln$\overline{BW}$ on ln*SVL* for OTUs of the *Lialis* group, whereas plots J-L exhibit scaling relationships between two populations of *P. lepidopodus*. In all plots, yellow OTUs exhibited longer maximum *SVL* compared to corresponding green OTUs. In A-F and J-L, yellow OTUs had larger maximum $\overline{BW}$ compared to corresponding green OTUs. In G-I, the green OTU (**) had a larger maximum $\overline{BW}$ than the yellow OTU. Each dot represents an individua and "wet" and "dry" refer to *P. lepidopodus* populations that live in high and low rainfall biomes, respectively. Results of the equal slopes and equal *y*-intercepts tests are shown. *p*-values > 0.05 were statistically non-significant (n.s.). Equal intercepts tests were not applicable (n.a.) whenever equal slopes hypotheses were rejected.

Figure 9. Pairwise comparisons of post-natal ontogenetic trajectories for the *Pygopus nigriceps* species groups. Plots A-DD show bivariate scaling relationships ln*Tail* on ln*SVL*, ln*Tail* on ln$\overline{BW}$, and ln$\overline{BW}$ on ln*SVL* for OTUs of the *P. nigriceps* group. In all plots, yellow OTUs exhibited longer maximum *SVL* compared to corresponding green OTUs. In A-O, yellow OTUs

had larger maximum $\overline{BW}$ compared to corresponding green OTUs. In P-DD, green OTUs (**) had larger maximum $\overline{BW}$ than corresponding yellow OTUs. Each dot represents an individual and "wet" and "dry" refer to populations that live in high and low rainfall biomes, respectively. Results of the equal slopes and equal *y*-intercepts tests are shown. *p*-values > 0.05 were statistically non-significant (n.s.). Equal intercepts tests were not applicable (n.a.) whenever equal slopes hypotheses were rejected.

Figure 10. Test of the prediction that geometric similarity precedes evolutionary allometry during initial trait divergence using ln*Tail* on ln*SVL* pairwise comparisons. (A) Relative frequencies (prevalence) of trait divergence patterns during each divergence time interval using the full dataset. (B) Prevalence of trait divergence patterns during each divergence time interval using the reduced dataset. Note the full dataset consisted of all OTU pairs that had one OTU with a longer maximum *SVL* compared to the other OTU, whereas the reduced dataset consisted only of OTU pairs in which one of the OTUs was larger than the other OTU in both *SVL* and $\overline{BW}$ body size measures. GS = geometric similarity, EA = evolutionary allometry, and mya = millions of years ago. The term "pre-speciation" refers to the initial time of divergence between intraspecific populations, which is here assumed to have occurred more recently than two mya (i.e., the most recent known time of speciation for species included in this study). See Materials and Methods for definitions of each interpopulation/interspecies scaling pattern and Supplementary Tables 1-3 for source data.

Figure 11. Test of the prediction that geometric similarity precedes evolutionary allometry during initial trait divergence using ln*Tail* on $\overline{BW}$ pairwise comparisons. (A) Prevalence of trait divergence patterns during each divergence time interval using the full dataset. (B) Prevalence of trait divergence patterns during each divergence time interval using the reduced dataset. Note the full dataset consisted of all OTU pairs that had one OTU with a longer maximum *SVL* compared to the other OTU, whereas the reduced dataset consisted only of OTU pairs in which one of the OTUs was larger than the other OTU in both *SVL* and $\overline{BW}$ body size measures. GS = geometric similarity, EA = evolutionary allometry, and mya = millions of years ago. The term "pre-speciation" refers to the initial time of divergence between intraspecific populations, which is here assumed to have occurred more recently than two mya (i.e., the most recent known time of speciation for species included in this study). See Materials and Methods for definitions of each interpopulation/interspecies scaling pattern and Supplementary Tables 1, 4, and 5 for source data.

Figure 12. Test of the prediction that geometric similarity precedes evolutionary allometry during initial trait divergence using ln$\overline{BW}$ on ln*SVL* pairwise comparisons. (A) Prevalence of trait divergence patterns during each divergence time interval using the full dataset. (B) Prevalence of trait divergence patterns during each divergence time interval using the reduced dataset. Note the full dataset consisted of all OTU pairs that had one OTU with a longer maximum *SVL* compared to the other OTU, whereas the reduced dataset consisted only of OTU pairs in which one of the OTUs was larger than the other OTU in both *SVL* and $\overline{BW}$ body size measures. GS = geometric similarity, EA = evolutionary allometry, and mya = millions of years ago. The term "pre-speciation" refers to the initial time of divergence between intraspecific populations, which is here assumed to have occurred more recently than two mya (i.e., the most recent known time of

speciation for species included in this study). See Materials and Methods for definitions of each interpopulation/interspecies scaling pattern and Supplementary Tables 1, 6, and 7 for source data.

Figure 13. Test of the prediction that all allometric traits display geometric similarity (GS) during initial trait divergence. (A) Prevalence of GS-only scaling patterns (i.e., for ln*Tail* on ln*SVL*, ln*Tail* on ln$\overline{BW}$, and ln$\overline{BW}$ on ln*SVL*) using the full dataset. Each bar shows the prevalence of OTU pairs that only showed GS patterns (blue) vs. OTU pairs that did not exclusively exhibit GS patterns (yellow). (B) Prevalence of GS-only scaling patterns (i.e., for ln*Tail* on ln*SVL*, ln*Tail* on ln$\overline{BW}$, and ln$\overline{BW}$ on ln*SVL*) using the reduced dataset. Note the full dataset consisted of all OTU pairs that had one OTU with a longer maximum *SVL* compared to the other OTU, whereas the reduced dataset consisted only of OTU pairs in which one of the OTUs was larger than the other OTU in both *SVL* and $\overline{BW}$ body size measures. mya = millions of years ago. The term "pre-speciation" refers to the initial time of divergence between intraspecific populations, which is here assumed to have occurred more recently than two mya (i.e., the most recent known time of speciation for species included in this study). See Supplementary Tables 1, 8, and 9 for source data.

Figure 14. Strength of ontogenetic allometry and geometric similarity scaling patterns. Hypothetical log-log plots illustrate pairwise comparisons of ontogenetic trajectories for two populations (shown in green and blue) involving a trait that exhibits differing degrees of positive ontogenetic allometry. The ontogenetic allometric slopes for the two populations are shown in green and blue, whereas the interpopulation slope, α_i (of the dashed line connecting the adults of

both populations) is equal to 1.0 in all plots (i.e., geometric similarity). The trait shows differing strengths of positive ontogenetic allometry ranging from ontogenetic $\alpha = 1.1$ (weakest) to 1.4 (strongest) when the slope for isometry is assumed to equal 1.0. In each plot, the blue population underwent an 8% body size increase compared to the green population. This value of percent body size increase was chosen because it corresponds to the observed minimum amount of body size decrease/increase observed for pygopodid lizard populations that exhibited geometric similarity in locomotor-relevant traits.

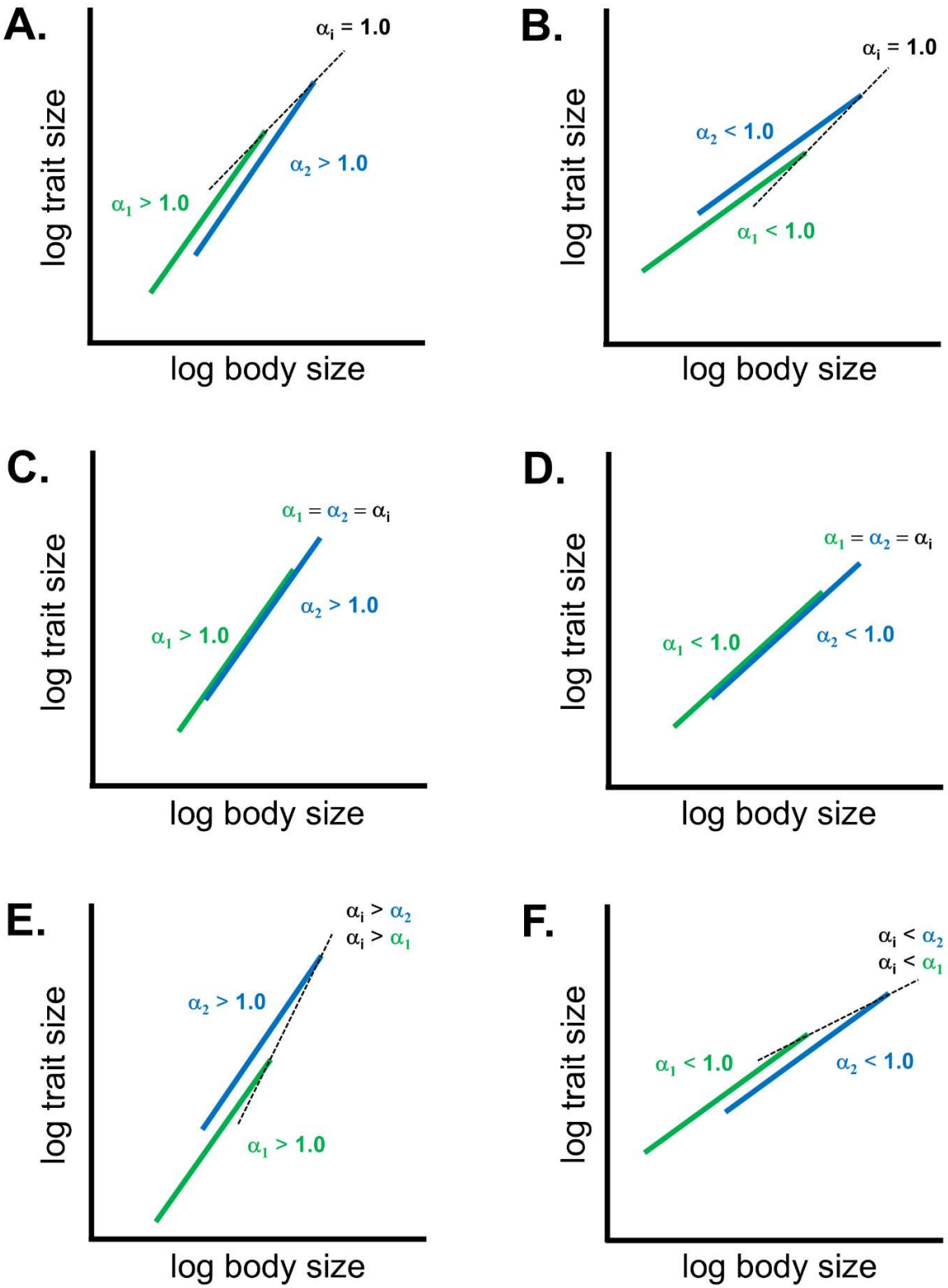
A.
α_i = 1.0
α_2 > 1.0
α_1 > 1.0
log trait size
log body size
B.
α_i = 1.0
α_2 < 1.0
α_1 < 1.0
log trait size
log body size
C.
$\alpha_1 = \alpha_2 = \alpha_i$
α_2 > 1.0
α_1 > 1.0
log trait size
log body size
D.
$\alpha_1 = \alpha_2 = \alpha_i$
α_1 < 1.0
α_2 < 1.0
log trait size
log body size
E.
α_i > α_2
α_i > α_1
α_2 > 1.0
α_1 > 1.0
log trait size
log body size
F.
α_i < α_2
α_i < α_1
α_1 < 1.0
α_2 < 1.0
log trait size
log body size

Figure 1.

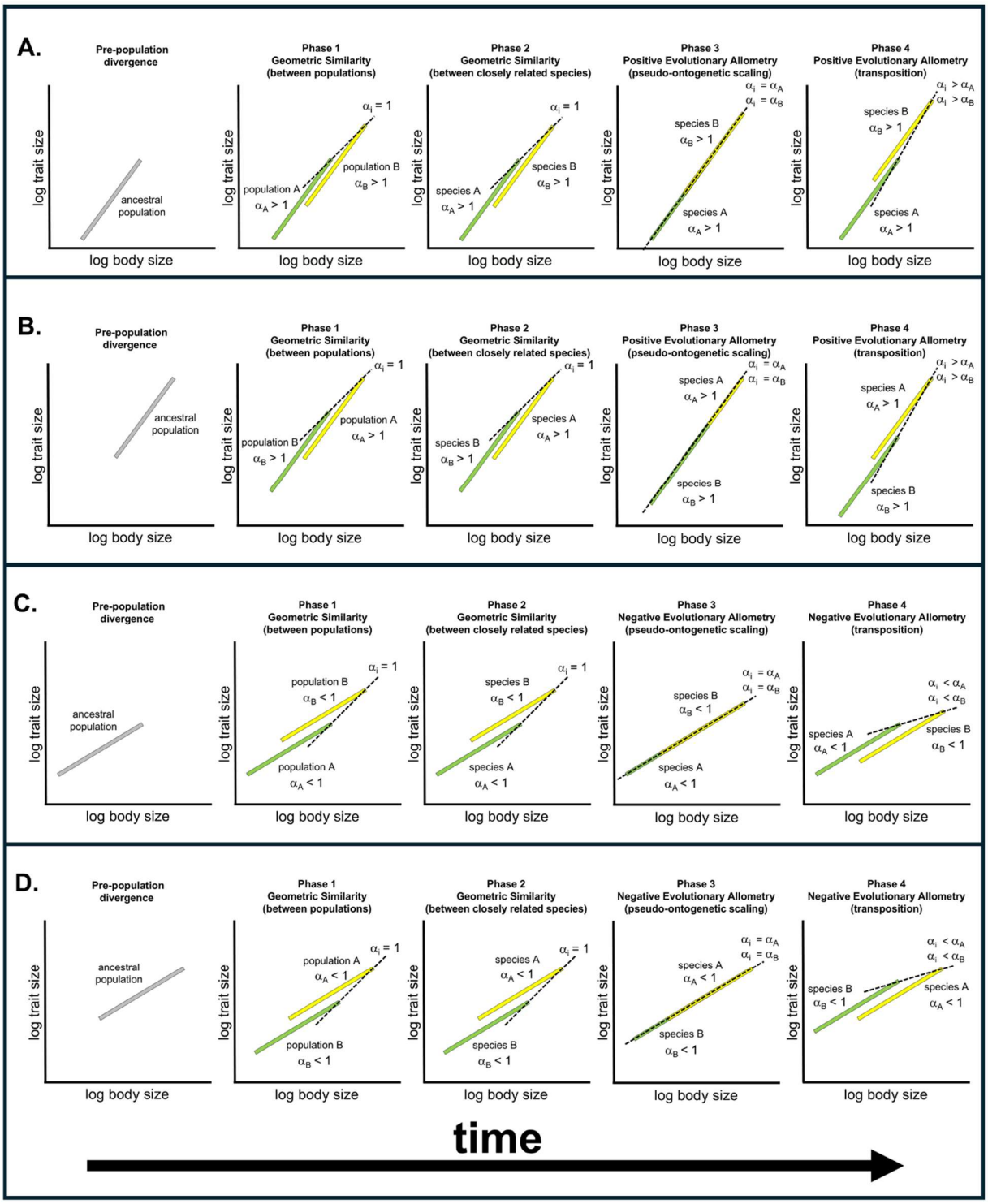
A.
Pre-population divergence
ancestral population
Phase 1 Geometric Similarity (between populations)
population A
population B
Phase 2 Geometric Similarity (between closely related species)
species A
species B
Phase 3 Positive Evolutionary Allometry (pseudo-ontogenetic scaling)
Phase 4 Positive Evolutionary Allometry (transposition)
B.
C.
Phase 3 Negative Evolutionary Allometry (pseudo-ontogenetic scaling)
Phase 4 Negative Evolutionary Allometry (transposition)
D.
log trait size
log body size
time

Figure 2.

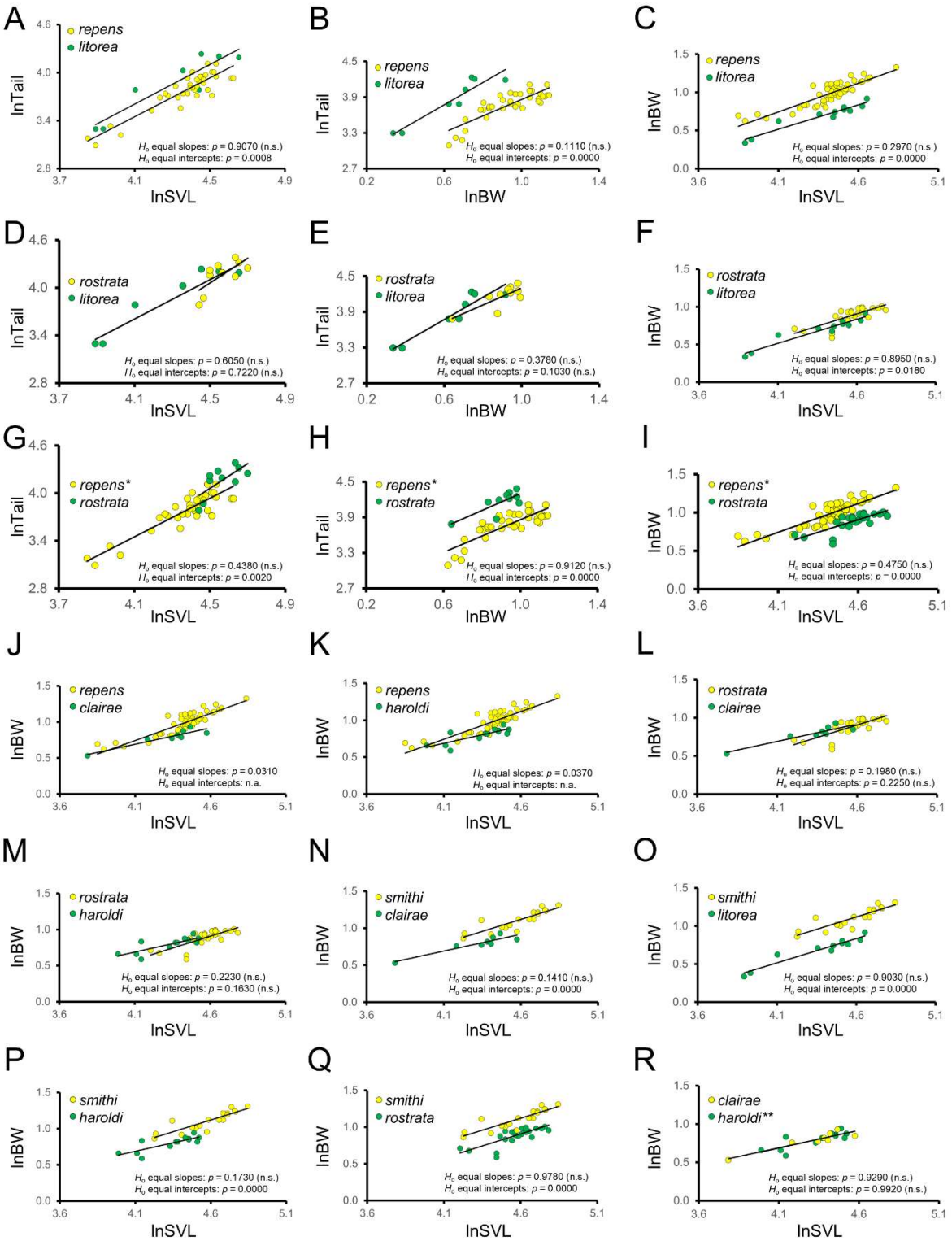
A
repens
litorea
lnTail
lnSVL
H_0 equal slopes: p = 0.9070 (n.s.)
H_0 equal intercepts: p = 0.0008
B
repens
litorea
lnTail
lnBW
H_0 equal slopes: p = 0.1110 (n.s.)
H_0 equal intercepts: p = 0.0000
C
repens
litorea
lnBW
lnSVL
H_0 equal slopes: p = 0.2970 (n.s.)
H_0 equal intercepts: p = 0.0000
D
rostrata
litorea
lnTail
lnSVL
H_0 equal slopes: p = 0.6050 (n.s.)
H_0 equal intercepts: p = 0.7220 (n.s.)
E
rostrata
litorea
lnTail
lnBW
H_0 equal slopes: p = 0.3780 (n.s.)
H_0 equal intercepts: p = 0.1030 (n.s.)
F
rostrata
litorea
lnBW
lnSVL
H_0 equal slopes: p = 0.8950 (n.s.)
H_0 equal intercepts: p = 0.0180
G
repens*
rostrata
lnTail
lnSVL
H_0 equal slopes: p = 0.4380 (n.s.)
H_0 equal intercepts: p = 0.0020
H
repens*
rostrata
lnTail
lnBW
H_0 equal slopes: p = 0.9120 (n.s.)
H_0 equal intercepts: p = 0.0000
I
repens*
rostrata
lnBW
lnSVL
H_0 equal slopes: p = 0.4750 (n.s.)
H_0 equal intercepts: p = 0.0000
J
repens
clairae
lnBW
lnSVL
H_0 equal slopes: p = 0.0310
H_0 equal intercepts: n.a.
K
repens
haroldi
lnBW
lnSVL
H_0 equal slopes: p = 0.0370
H_0 equal intercepts: n.a.
L
rostrata
clairae
lnBW
lnSVL
H_0 equal slopes: p = 0.1980 (n.s.)
H_0 equal intercepts: p = 0.2250 (n.s.)
M
rostrata
haroldi
lnBW
lnSVL
H_0 equal slopes: p = 0.2230 (n.s.)
H_0 equal intercepts: p = 0.1630 (n.s.)
N
smithi
clairae
lnBW
lnSVL
H_0 equal slopes: p = 0.1410 (n.s.)
H_0 equal intercepts: p = 0.0000
O
smithi
litorea
lnBW
lnSVL
H_0 equal slopes: p = 0.9030 (n.s.)
H_0 equal intercepts: p = 0.0000
P
smithi
haroldi
lnBW
lnSVL
H_0 equal slopes: p = 0.1730 (n.s.)
H_0 equal intercepts: p = 0.0000
Q
smithi
rostrata
lnBW
lnSVL
H_0 equal slopes: p = 0.9780 (n.s.)
H_0 equal intercepts: p = 0.0000
R
clairae
haroldi**
lnBW
lnSVL
H_0 equal slopes: p = 0.9290 (n.s.)
H_0 equal intercepts: p = 0.9920 (n.s.)

Figure 3.

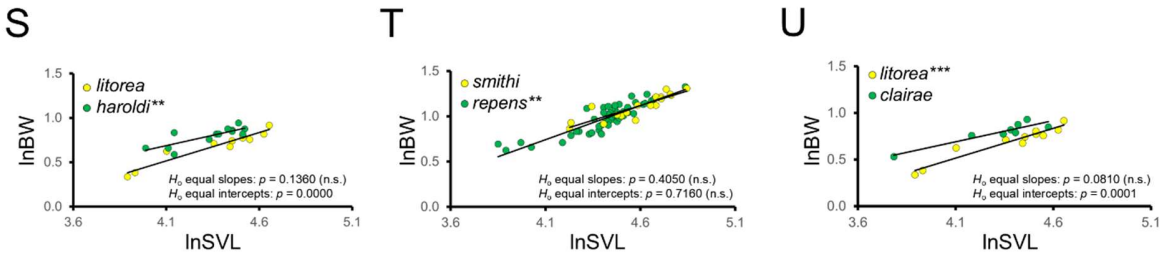

Figure 3 continued.

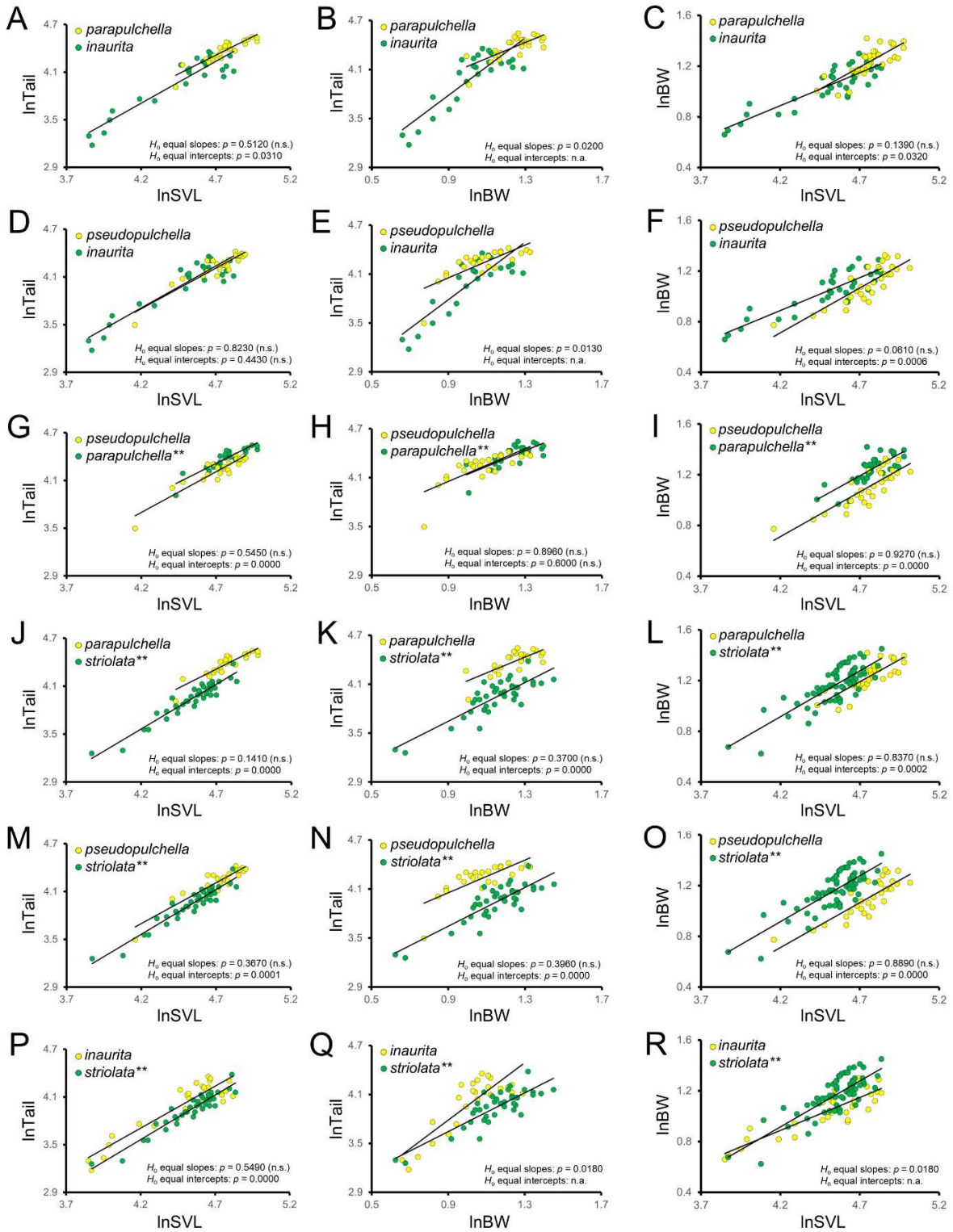
A
parapulchella
inaurita
lnTail
lnSVL
H_0 equal slopes: p = 0.5120 (n.s.)
H_0 equal intercepts: p = 0.0310
B
parapulchella
inaurita
lnTail
lnBW
H_0 equal slopes: p = 0.0200
H_0 equal intercepts: n.a.
C
parapulchella
inaurita
lnBW
lnSVL
H_0 equal slopes: p = 0.1390 (n.s.)
H_0 equal intercepts: p = 0.0320
D
pseudopulchella
inaurita
lnTail
lnSVL
H_0 equal slopes: p = 0.8230 (n.s.)
H_0 equal intercepts: p = 0.4430 (n.s.)
E
pseudopulchella
inaurita
lnTail
lnBW
H_0 equal slopes: p = 0.0130
H_0 equal intercepts: n.a.
F
pseudopulchella
inaurita
lnBW
lnSVL
H_0 equal slopes: p = 0.0610 (n.s.)
H_0 equal intercepts: p = 0.0006
G
pseudopulchella
parapulchella**
lnTail
lnSVL
H_0 equal slopes: p = 0.5450 (n.s.)
H_0 equal intercepts: p = 0.0000
H
pseudopulchella
parapulchella**
lnTail
lnBW
H_0 equal slopes: p = 0.8960 (n.s.)
H_0 equal intercepts: p = 0.6000 (n.s.)
I
pseudopulchella
parapulchella**
lnBW
lnSVL
H_0 equal slopes: p = 0.9270 (n.s.)
H_0 equal intercepts: p = 0.0000
J
parapulchella
striolata**
lnTail
lnSVL
H_0 equal slopes: p = 0.1410 (n.s.)
H_0 equal intercepts: p = 0.0000
K
parapulchella
striolata**
lnTail
lnBW
H_0 equal slopes: p = 0.3700 (n.s.)
H_0 equal intercepts: p = 0.0000
L
parapulchella
striolata**
lnBW
lnSVL
H_0 equal slopes: p = 0.8370 (n.s.)
H_0 equal intercepts: p = 0.0002
M
pseudopulchella
striolata**
lnTail
lnSVL
H_0 equal slopes: p = 0.3670 (n.s.)
H_0 equal intercepts: p = 0.0001
N
pseudopulchella
striolata**
lnTail
lnBW
H_0 equal slopes: p = 0.3960 (n.s.)
H_0 equal intercepts: p = 0.0000
O
pseudopulchella
striolata**
lnBW
lnSVL
H_0 equal slopes: p = 0.8890 (n.s.)
H_0 equal intercepts: p = 0.0000
P
inaurita
striolata**
lnTail
lnSVL
H_0 equal slopes: p = 0.5490 (n.s.)
H_0 equal intercepts: p = 0.0000
Q
inaurita
striolata**
lnTail
lnBW
H_0 equal slopes: p = 0.0180
H_0 equal intercepts: n.a.
R
inaurita
striolata**
lnBW
lnSVL
H_0 equal slopes: p = 0.0180
H_0 equal intercepts: n.a.

Figure 4.

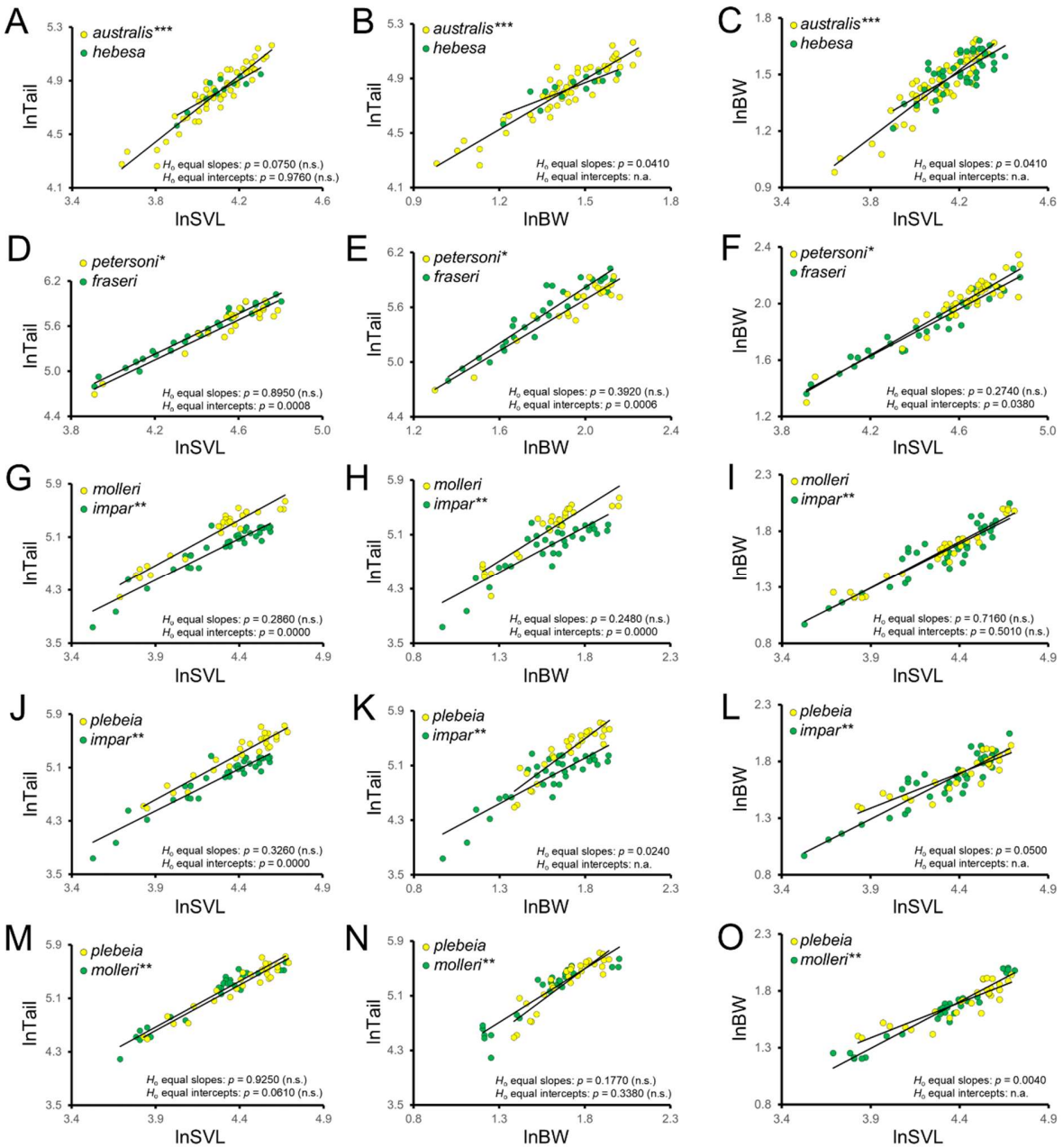
A
australis***
hebesa
lnTail
lnSVL
H_0 equal slopes: p = 0.0750 (n.s.)
H_0 equal intercepts: p = 0.9760 (n.s.)
B
australis***
hebesa
lnTail
lnBW
H_0 equal slopes: p = 0.0410
H_0 equal intercepts: n.a.
C
australis***
hebesa
lnBW
lnSVL
H_0 equal slopes: p = 0.0410
H_0 equal intercepts: n.a.
D
petersoni*
fraseri
lnTail
lnSVL
H_0 equal slopes: p = 0.8950 (n.s.)
H_0 equal intercepts: p = 0.0008
E
petersoni*
fraseri
lnTail
lnBW
H_0 equal slopes: p = 0.3920 (n.s.)
H_0 equal intercepts: p = 0.0006
F
petersoni*
fraseri
lnBW
lnSVL
H_0 equal slopes: p = 0.2740 (n.s.)
H_0 equal intercepts: p = 0.0380
G
molleri
impar**
lnTail
lnSVL
H_0 equal slopes: p = 0.2860 (n.s.)
H_0 equal intercepts: p = 0.0000
H
molleri
impar**
lnTail
lnBW
H_0 equal slopes: p = 0.2480 (n.s.)
H_0 equal intercepts: p = 0.0000
I
molleri
impar**
lnBW
lnSVL
H_0 equal slopes: p = 0.7160 (n.s.)
H_0 equal intercepts: p = 0.5010 (n.s.)
J
plebeia
impar**
lnTail
lnSVL
H_0 equal slopes: p = 0.3260 (n.s.)
H_0 equal intercepts: p = 0.0000
K
plebeia
impar**
lnTail
lnBW
H_0 equal slopes: p = 0.0240
H_0 equal intercepts: n.a.
L
plebeia
impar**
lnBW
lnSVL
H_0 equal slopes: p = 0.0500
H_0 equal intercepts: n.a.
M
plebeia
molleri**
lnTail
lnSVL
H_0 equal slopes: p = 0.9250 (n.s.)
H_0 equal intercepts: p = 0.0610 (n.s.)
N
plebeia
molleri**
lnTail
lnBW
H_0 equal slopes: p = 0.1770 (n.s.)
H_0 equal intercepts: p = 0.3380 (n.s.)
O
plebeia
molleri**
lnBW
lnSVL
H_0 equal slopes: p = 0.0040
H_0 equal intercepts: n.a.

Figure 5.

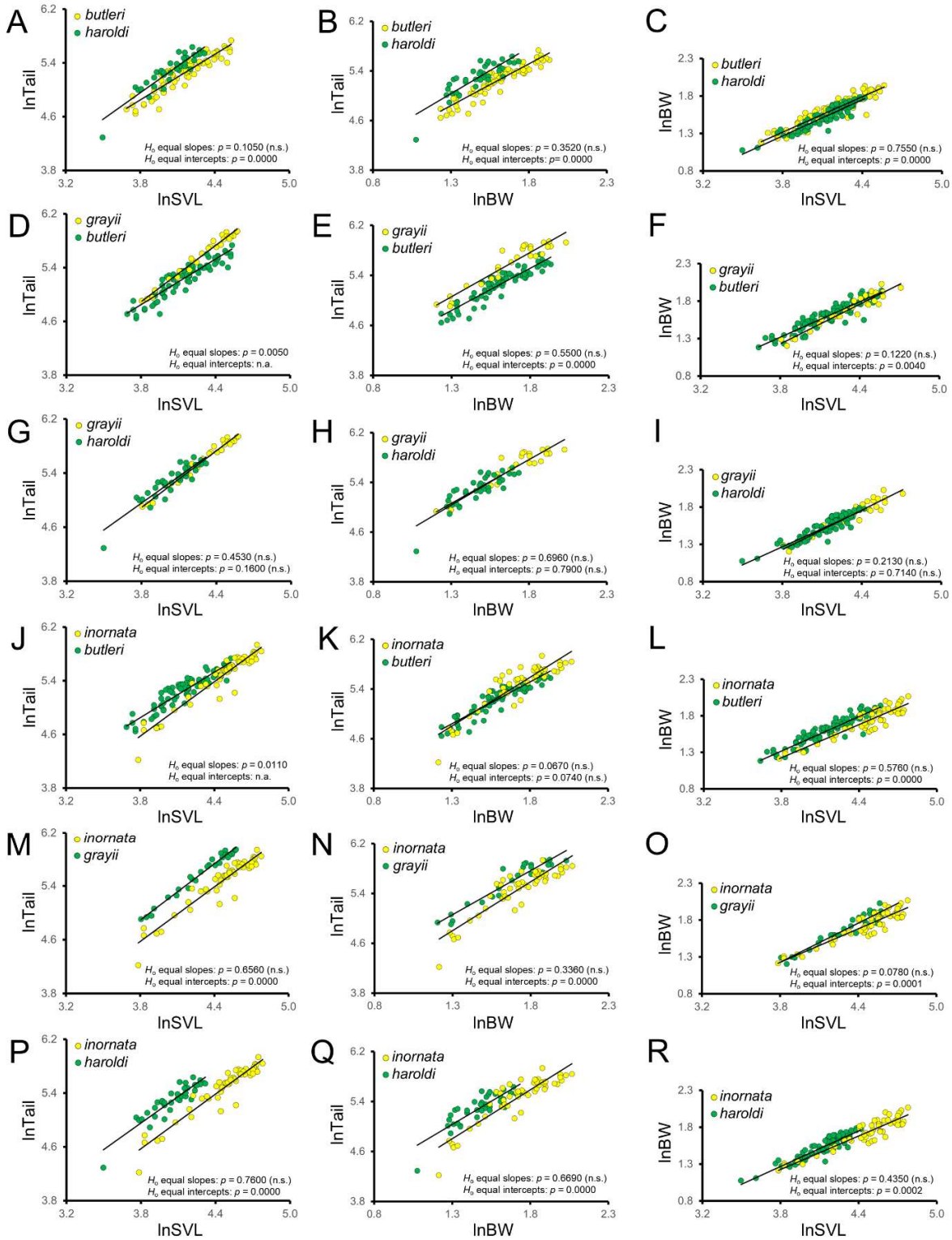
A
butleri
haroldi
lnTail
lnSVL
H_0 equal slopes: p = 0.1050 (n.s.)
H_0 equal intercepts: p = 0.0000
B
butleri
haroldi
lnTail
lnBW
H_0 equal slopes: p = 0.3520 (n.s.)
H_0 equal intercepts: p= 0.0000
C
butleri
haroldi
lnBW
lnSVL
H_0 equal slopes: p = 0.7550 (n.s.)
H_0 equal intercepts: p = 0.0000
D
grayii
butleri
lnTail
lnSVL
H_0 equal slopes: p = 0.0050
H_0 equal intercepts: n.a.
E
grayii
butleri
lnTail
lnBW
H_0 equal slopes: p = 0.5500 (n.s.)
H_0 equal intercepts: p = 0.0000
F
grayii
butleri
lnBW
lnSVL
H_0 equal slopes: p = 0.1220 (n.s.)
H_0 equal intercepts: p = 0.0040
G
grayii
haroldi
lnTail
lnSVL
H_0 equal slopes: p = 0.4530 (n.s.)
H_0 equal intercepts: p = 0.1600 (n.s.)
H
grayii
haroldi
lnTail
lnBW
H_0 equal slopes: p = 0.6960 (n.s.)
H_0 equal intercepts: p = 0.7900 (n.s.)
I
grayii
haroldi
lnBW
lnSVL
H_0 equal slopes: p = 0.2130 (n.s.)
H_0 equal intercepts: p = 0.7140 (n.s.)
J
inornata
butleri
lnTail
lnSVL
H_0 equal slopes: p = 0.0110
H_0 equal intercepts: n.a.
K
inornata
butleri
lnTail
lnBW
H_0 equal slopes: p = 0.0670 (n.s.)
H_0 equal intercepts: p = 0.0740 (n.s.)
L
inornata
butleri
lnBW
lnSVL
H_0 equal slopes: p = 0.5760 (n.s.)
H_0 equal intercepts: p = 0.0000
M
inornata
grayii
lnTail
lnSVL
H_0 equal slopes: p = 0.6560 (n.s.)
H_0 equal intercepts: p = 0.0000
N
inornata
grayii
lnTail
lnBW
H_0 equal slopes: p = 0.3360 (n.s.)
H_0 equal intercepts: p = 0.0000
O
inornata
grayii
lnBW
lnSVL
H_0 equal slopes: p = 0.0780 (n.s.)
H_0 equal intercepts: p = 0.0001
P
inornata
haroldi
lnTail
lnSVL
H_0 equal slopes: p = 0.7600 (n.s.)
H_0 equal intercepts: p = 0.0000
Q
inornata
haroldi
lnTail
lnBW
H_0 equal slopes: p = 0.6690 (n.s.)
H_0 equal intercepts: p = 0.0000
R
inornata
haroldi
lnBW
lnSVL
H_0 equal slopes: p = 0.4350 (n.s.)
H_0 equal intercepts: p = 0.0002

Figure 6.

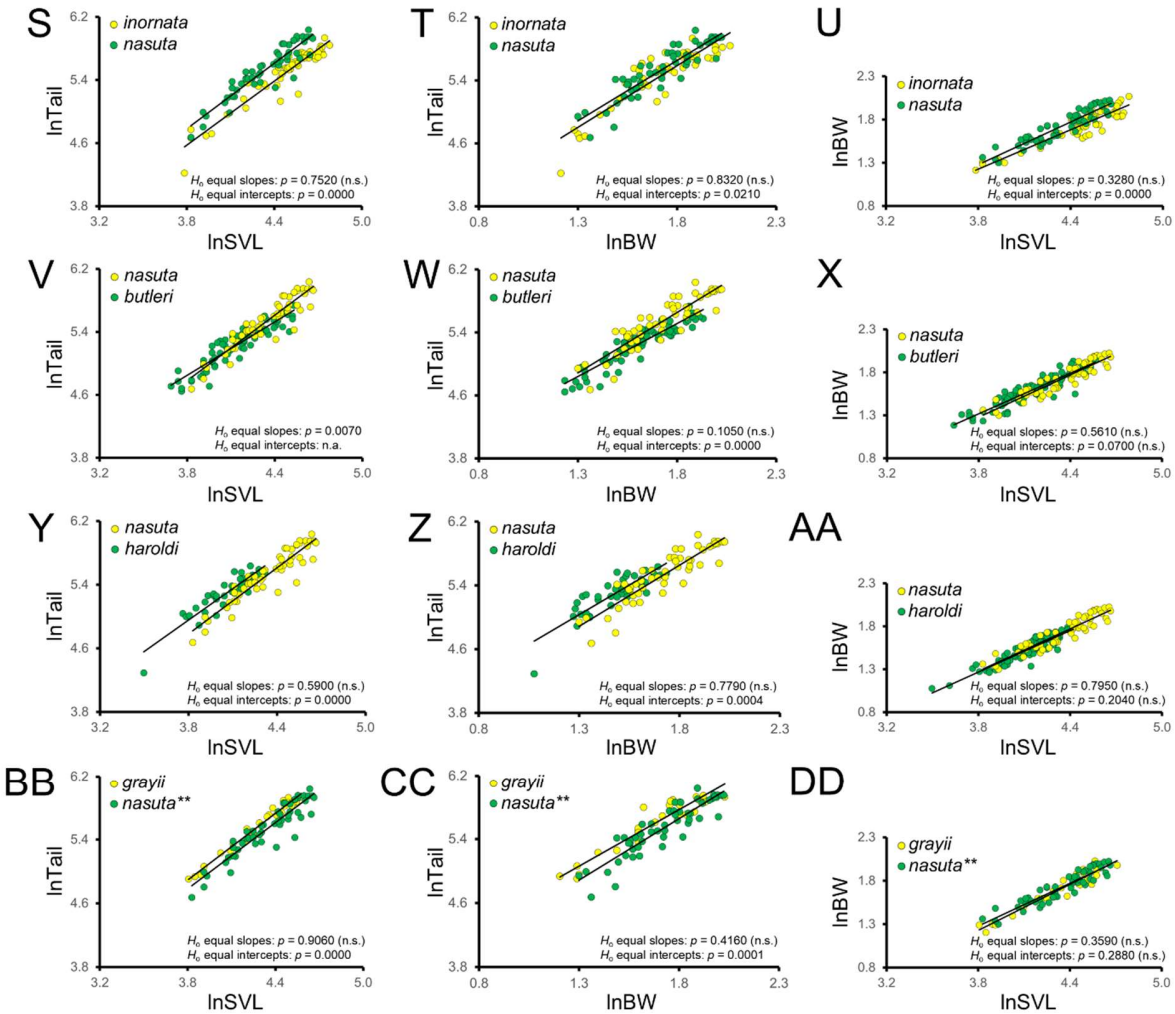

Figure 6 continued.

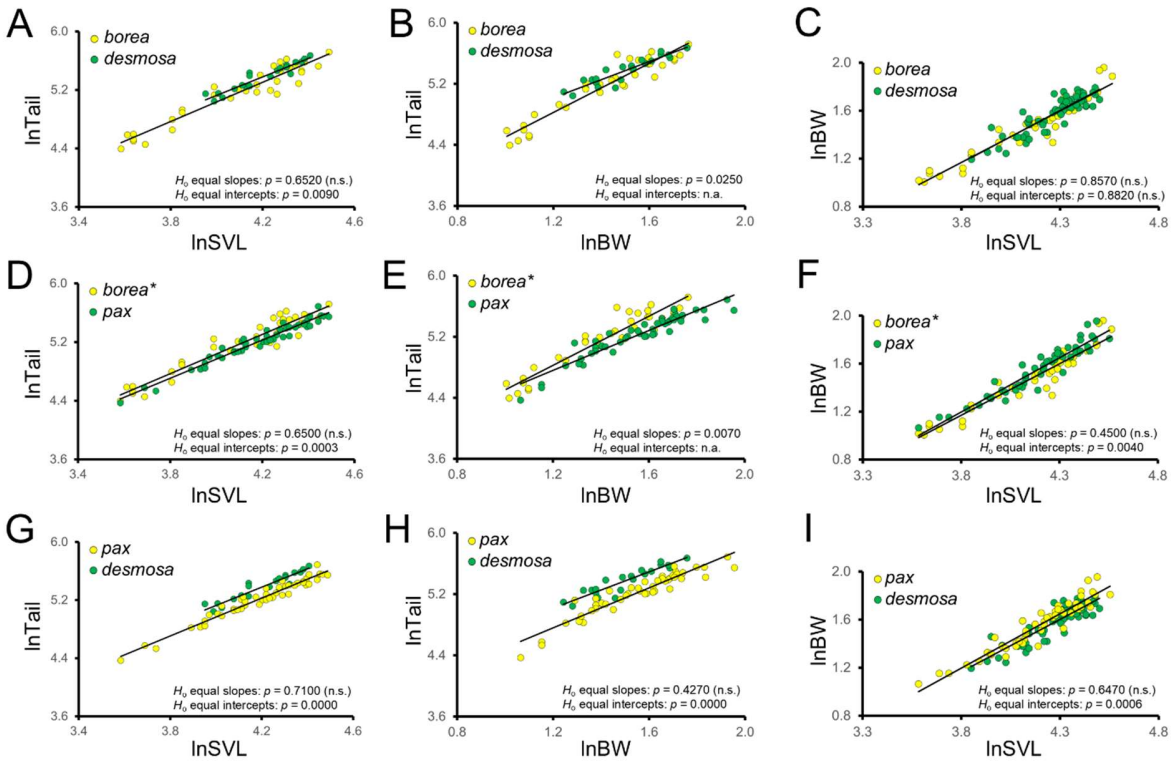
A
borea
desmosa
lnTail
lnSVL
H_0 equal slopes: p = 0.6520 (n.s.)
H_0 equal intercepts: p = 0.0090
B
borea
desmosa
lnTail
lnBW
H_0 equal slopes: p = 0.0250
H_0 equal intercepts: n.a.
C
borea
desmosa
lnBW
lnSVL
H_0 equal slopes: p = 0.8570 (n.s.)
H_0 equal intercepts: p = 0.8820 (n.s.)
D
borea*
pax
lnTail
lnSVL
H_0 equal slopes: p = 0.6500 (n.s.)
H_0 equal intercepts: p = 0.0003
E
borea*
pax
lnTail
lnBW
H_0 equal slopes: p = 0.0070
H_0 equal intercepts: n.a.
F
borea*
pax
lnBW
lnSVL
H_0 equal slopes: p = 0.4500 (n.s.)
H_0 equal intercepts: p = 0.0040
G
pax
desmosa
lnTail
lnSVL
H_0 equal slopes: p = 0.7100 (n.s.)
H_0 equal intercepts: p = 0.0000
H
pax
desmosa
lnTail
lnBW
H_0 equal slopes: p = 0.4270 (n.s.)
H_0 equal intercepts: p = 0.0000
I
pax
desmosa
lnBW
lnSVL
H_0 equal slopes: p = 0.6470 (n.s.)
H_0 equal intercepts: p = 0.0006

Figure 7.

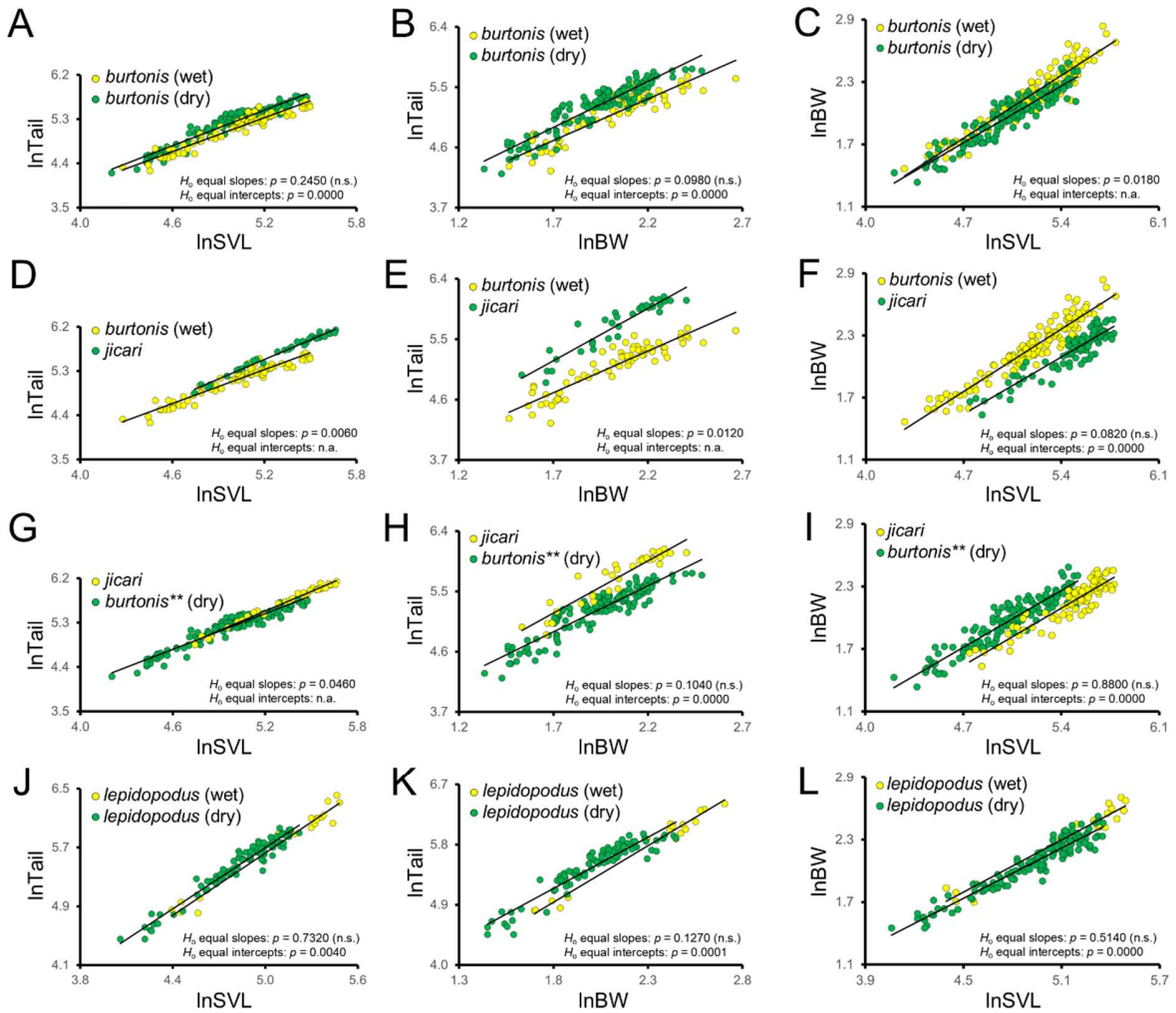
A
burtonis (wet)
burtonis (dry)
lnTail
lnSVL
H_0 equal slopes: p = 0.2450 (n.s.)
H_0 equal intercepts: p = 0.0000
B
burtonis (wet)
burtonis (dry)
lnTail
lnBW
H_0 equal slopes: p = 0.0980 (n.s.)
H_0 equal intercepts: p = 0.0000
C
burtonis (wet)
burtonis (dry)
lnBW
lnSVL
H_0 equal slopes: p = 0.0180
H_0 equal intercepts: n.a.
D
burtonis (wet)
jicari
lnTail
lnSVL
H_0 equal slopes: p = 0.0060
H_0 equal intercepts: n.a.
E
burtonis (wet)
jicari
lnTail
lnBW
H_0 equal slopes: p = 0.0120
H_0 equal intercepts: n.a.
F
burtonis (wet)
jicari
lnBW
lnSVL
H_0 equal slopes: p = 0.0820 (n.s.)
H_0 equal intercepts: p = 0.0000
G
jicari
burtonis** (dry)
lnTail
lnSVL
H_0 equal slopes: p = 0.0460
H_0 equal intercepts: n.a.
H
jicari
burtonis** (dry)
lnTail
lnBW
H_0 equal slopes: p = 0.1040 (n.s.)
H_0 equal intercepts: p = 0.0000
I
jicari
burtonis** (dry)
lnBW
lnSVL
H_0 equal slopes: p = 0.8800 (n.s.)
H_0 equal intercepts: p = 0.0000
J
lepidopodus (wet)
lepidopodus (dry)
lnTail
lnSVL
H_0 equal slopes: p = 0.7320 (n.s.)
H_0 equal intercepts: p = 0.0040
K
lepidopodus (wet)
lepidopodus (dry)
lnTail
lnBW
H_0 equal slopes: p = 0.1270 (n.s.)
H_0 equal intercepts: p = 0.0001
L
lepidopodus (wet)
lepidopodus (dry)
lnBW
lnSVL
H_0 equal slopes: p = 0.5140 (n.s.)
H_0 equal intercepts: p = 0.0000

Figure 8.

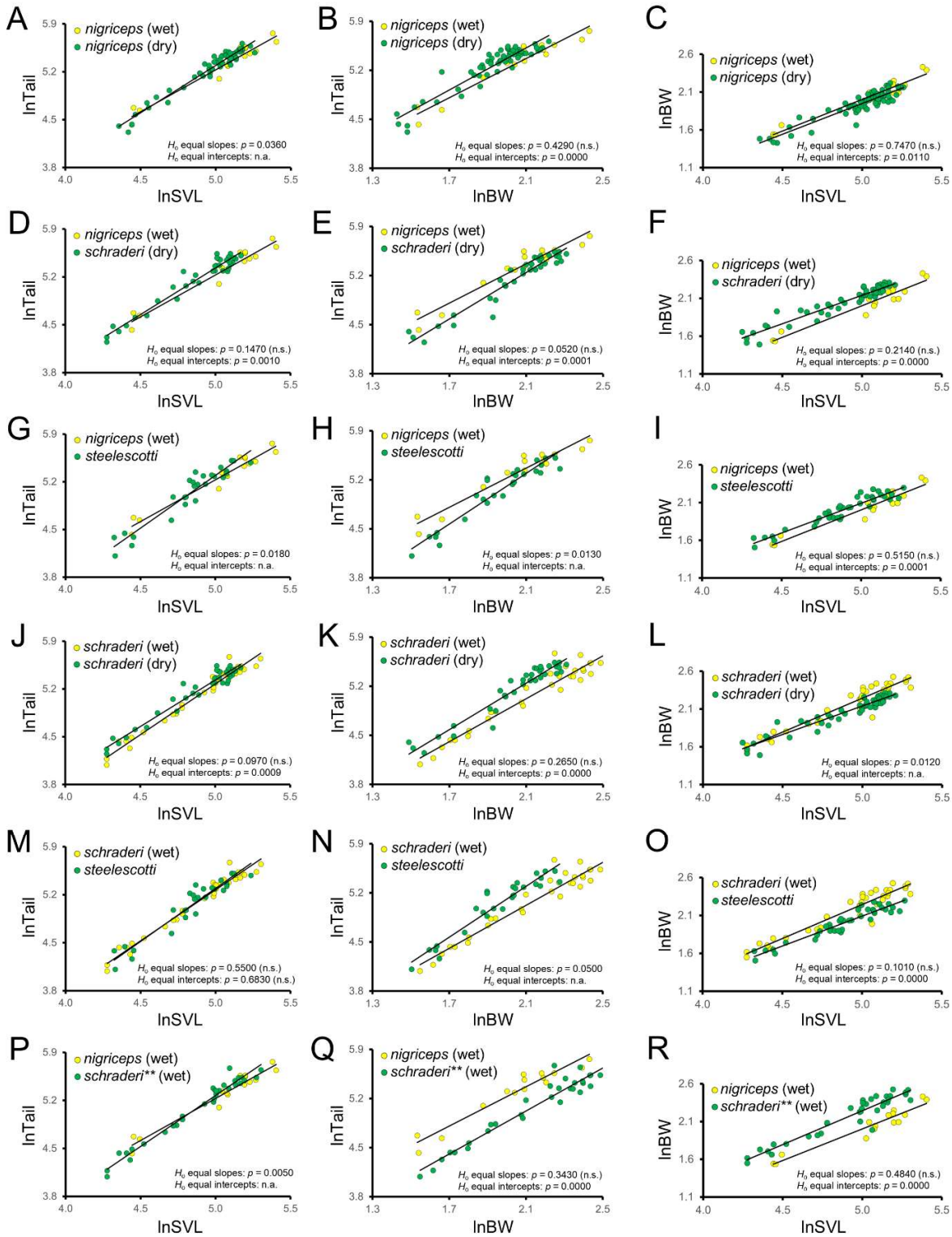
A
nigriceps (wet)
nigriceps (dry)
lnTail
lnSVL
H_0 equal slopes: p = 0.0360
H_0 equal intercepts: n.a.
B
nigriceps (wet)
nigriceps (dry)
lnTail
lnBW
H_0 equal slopes: p = 0.4290 (n.s.)
H_0 equal intercepts: p = 0.0000
C
nigriceps (wet)
nigriceps (dry)
lnBW
lnSVL
H_0 equal slopes: p = 0.7470 (n.s.)
H_0 equal intercepts: p = 0.0110
D
nigriceps (wet)
schraderi (dry)
lnTail
lnSVL
H_0 equal slopes: p = 0.1470 (n.s.)
H_0 equal intercepts: p = 0.0010
E
nigriceps (wet)
schraderi (dry)
lnTail
lnBW
H_0 equal slopes: p = 0.0520 (n.s.)
H_0 equal intercepts: p = 0.0001
F
nigriceps (wet)
schraderi (dry)
lnBW
lnSVL
H_0 equal slopes: p = 0.2140 (n.s.)
H_0 equal intercepts: p = 0.0000
G
nigriceps (wet)
steelescotti
lnTail
lnSVL
H_0 equal slopes: p = 0.0180
H_0 equal intercepts: n.a.
H
nigriceps (wet)
steelescotti
lnTail
lnBW
H_0 equal slopes: p = 0.0130
H_0 equal intercepts: n.a.
I
nigriceps (wet)
steelescotti
lnBW
lnSVL
H_0 equal slopes: p = 0.5150 (n.s.)
H_0 equal intercepts: p = 0.0001
J
schraderi (wet)
schraderi (dry)
lnTail
lnSVL
H_0 equal slopes: p = 0.0970 (n.s.)
H_0 equal intercepts: p = 0.0009
K
schraderi (wet)
schraderi (dry)
lnTail
lnBW
H_0 equal slopes: p = 0.2650 (n.s.)
H_0 equal intercepts: p = 0.0000
L
schraderi (wet)
schraderi (dry)
lnBW
lnSVL
H_0 equal slopes: p = 0.0120
H_0 equal intercepts: n.a.
M
schraderi (wet)
steelescotti
lnTail
lnSVL
H_0 equal slopes: p = 0.5500 (n.s.)
H_0 equal intercepts: p = 0.6830 (n.s.)
N
schraderi (wet)
steelescotti
lnTail
lnBW
H_0 equal slopes: p = 0.0500
H_0 equal intercepts: n.a.
O
schraderi (wet)
steelescotti
lnBW
lnSVL
H_0 equal slopes: p = 0.1010 (n.s.)
H_0 equal intercepts: p = 0.0000
P
nigriceps (wet)
schraderi** (wet)
lnTail
lnSVL
H_0 equal slopes: p = 0.0050
H_0 equal intercepts: n.a.
Q
nigriceps (wet)
schraderi** (wet)
lnTail
lnBW
H_0 equal slopes: p = 0.3430 (n.s.)
H_0 equal intercepts: p = 0.0000
R
nigriceps (wet)
schraderi** (wet)
lnBW
lnSVL
H_0 equal slopes: p = 0.4840 (n.s.)
H_0 equal intercepts: p = 0.0000

Figure 9.

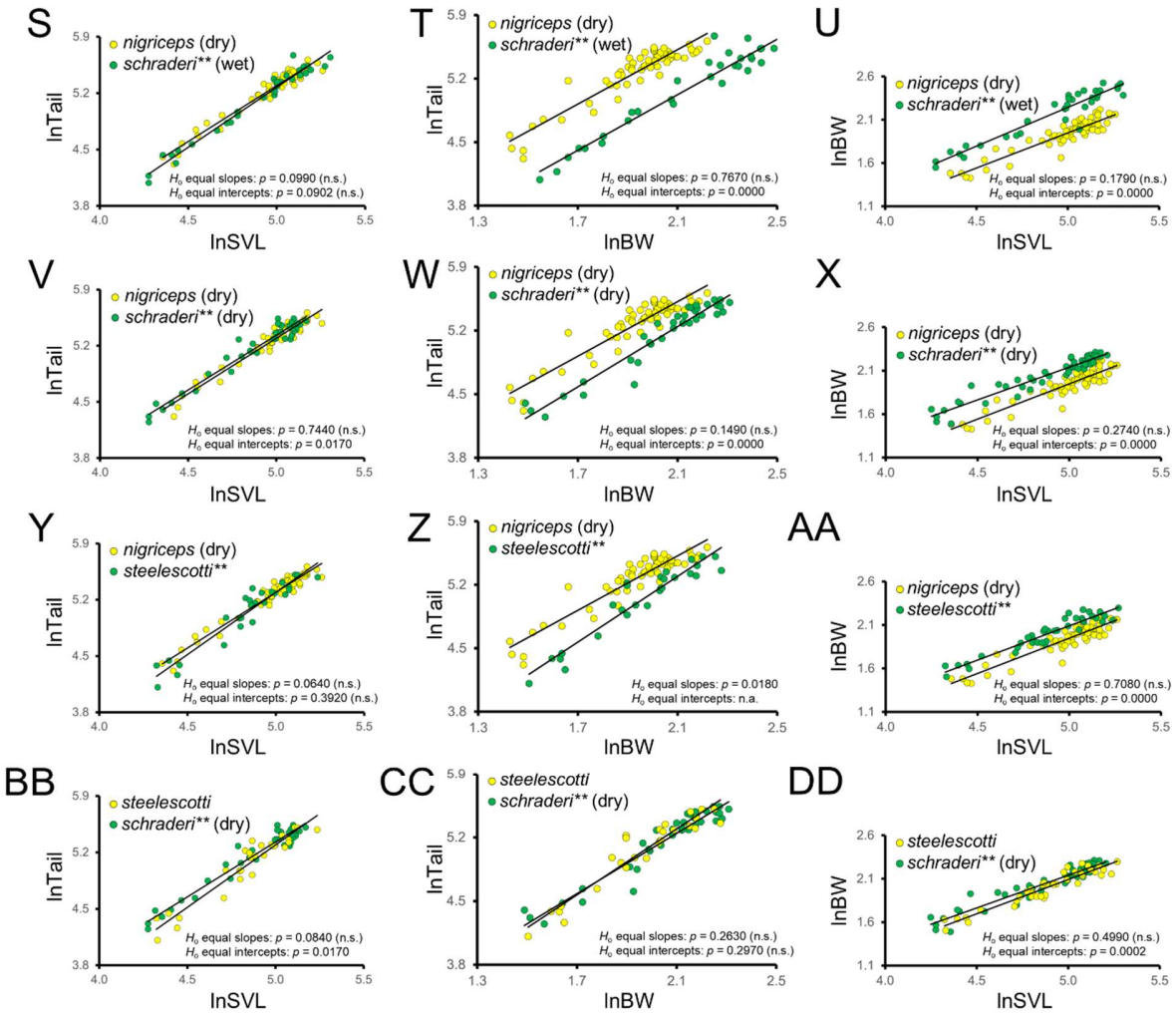

Figure 9 continued.

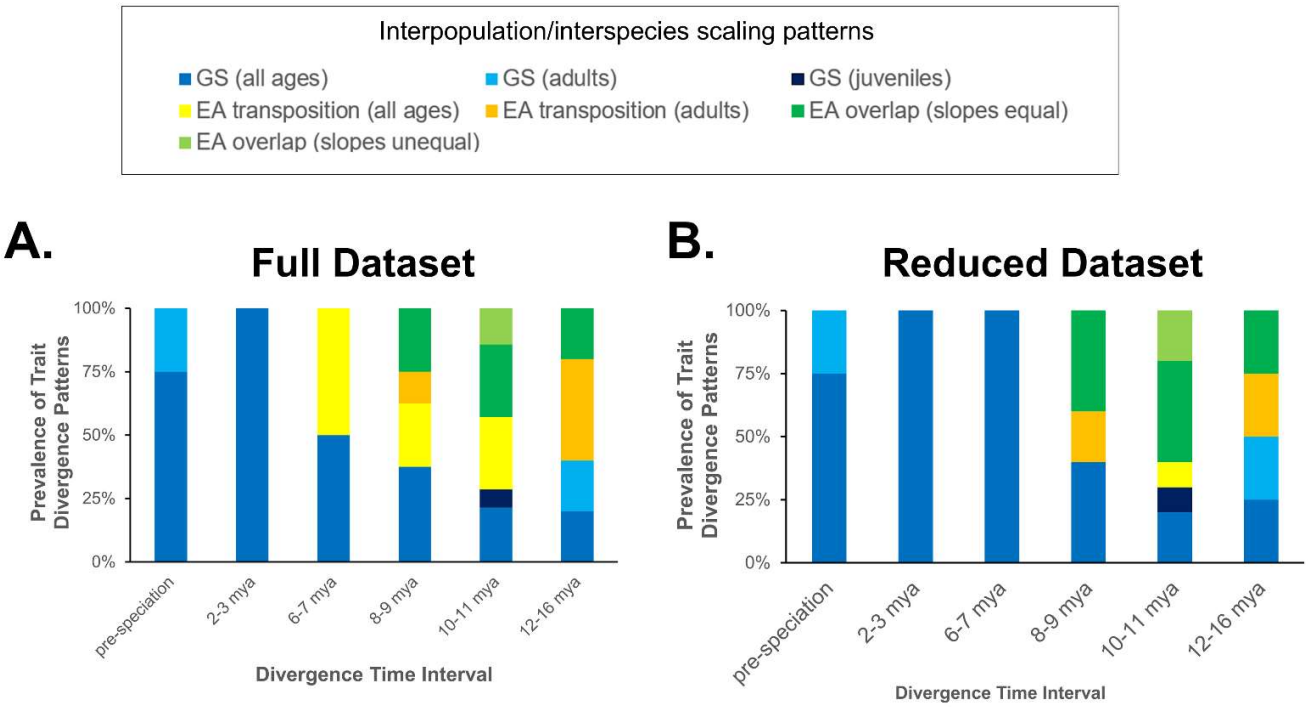
Interpopulation/interspecies scaling patterns
GS (all ages)
GS (adults)
GS (juveniles)
EA transposition (all ages)
EA transposition (adults)
EA overlap (slopes equal)
EA overlap (slopes unequal)
A.
Full Dataset
B.
Reduced Dataset
Prevalence of Trait Divergence Patterns
100%
75%
50%
25%
0%
pre-speciation
2-3 mya
6-7 mya
8-9 mya
10-11 mya
12-16 mya
Divergence Time Interval

Figure 10.

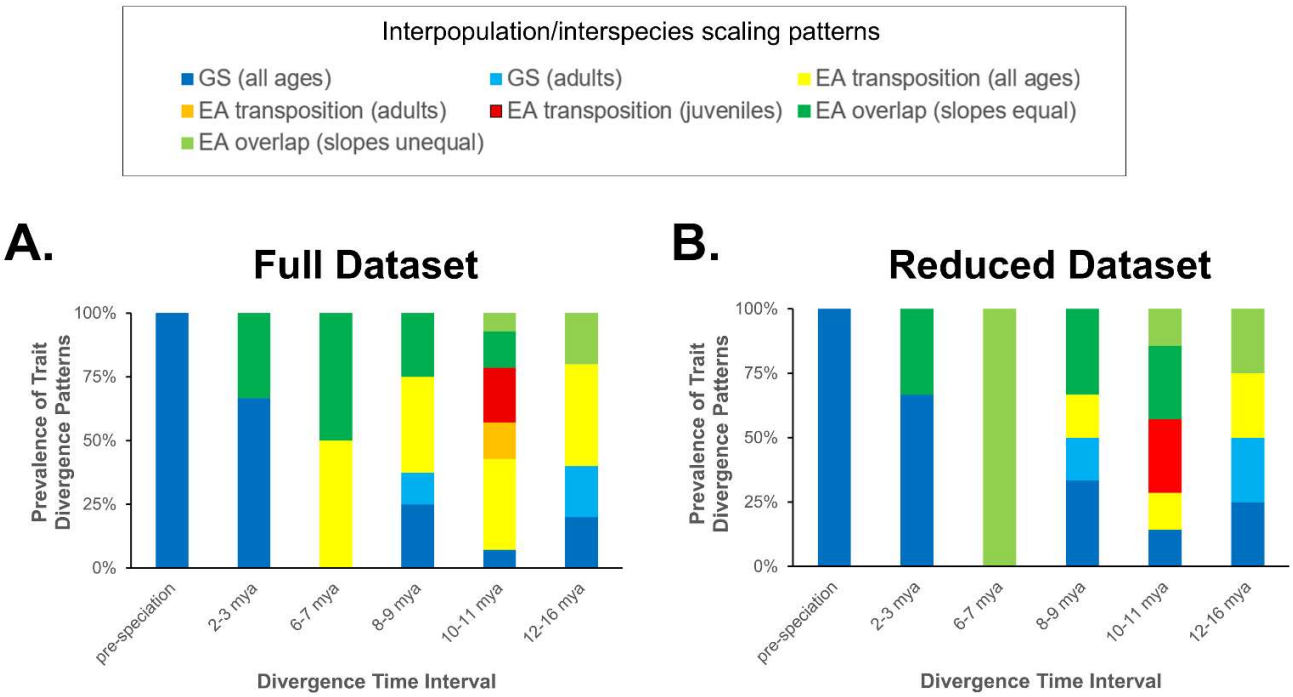
Interpopulation/interspecies scaling patterns
GS (all ages)
GS (adults)
EA transposition (all ages)
EA transposition (adults)
EA transposition (juveniles)
EA overlap (slopes equal)
EA overlap (slopes unequal)
A.
Full Dataset
B.
Reduced Dataset
Prevalence of Trait Divergence Patterns
100%
75%
50%
25%
0%
pre-speciation
2-3 mya
6-7 mya
8-9 mya
10-11 mya
12-16 mya
Divergence Time Interval

Figure 11.

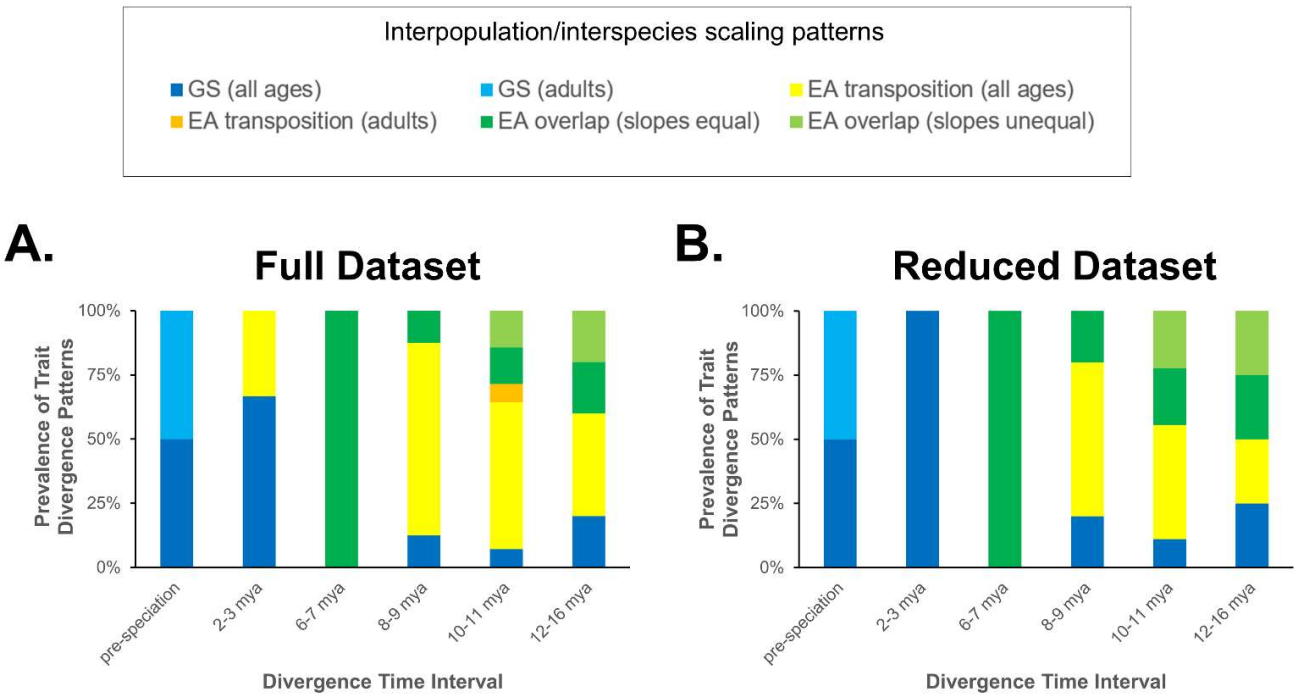
Interpopulation/interspecies scaling patterns
GS (all ages)
GS (adults)
EA transposition (all ages)
EA transposition (adults)
EA overlap (slopes equal)
EA overlap (slopes unequal)
A.
Full Dataset
B.
Reduced Dataset
Prevalence of Trait Divergence Patterns
100%
75%
50%
25%
0%
pre-speciation
2-3 mya
6-7 mya
8-9 mya
10-11 mya
12-16 mya
Divergence Time Interval

Figure 12.

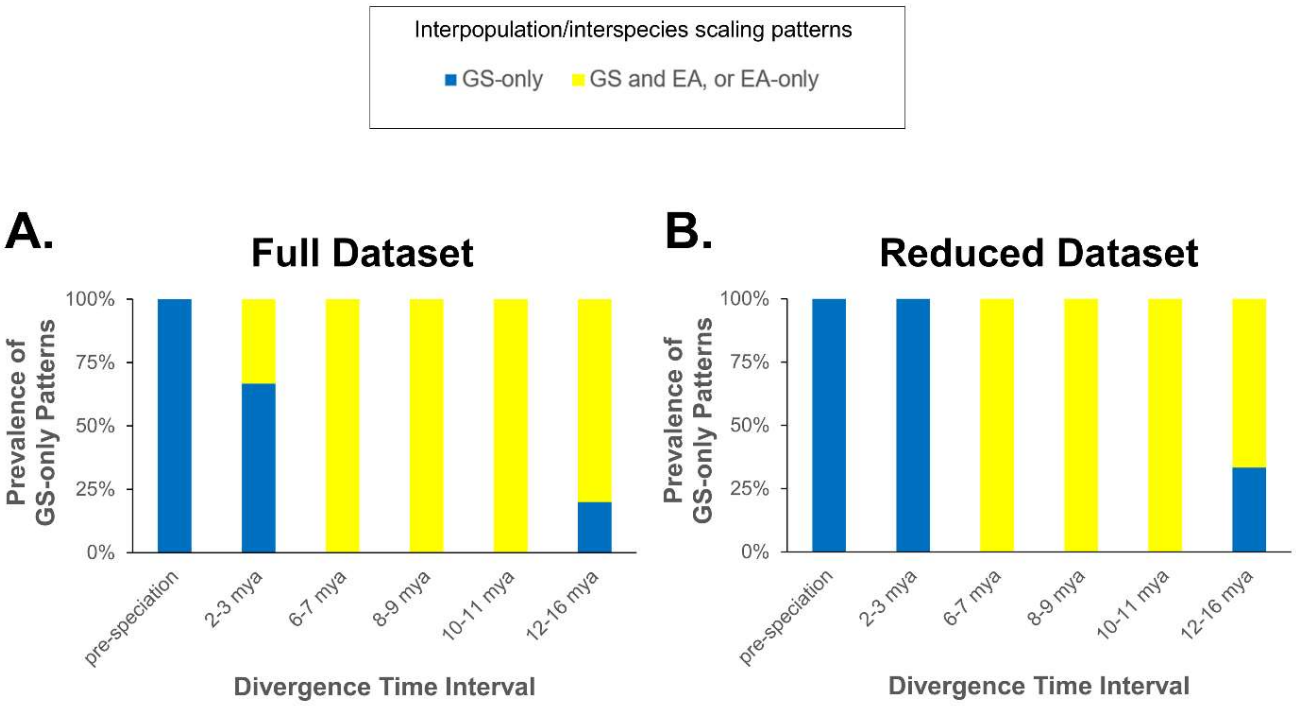
Interpopulation/interspecies scaling patterns
GS-only
GS and EA, or EA-only
A.
Full Dataset
Prevalence of GS-only Patterns
100%
75%
50%
25%
0%
pre-speciation
2-3 mya
6-7 mya
8-9 mya
10-11 mya
12-16 mya
Divergence Time Interval
B.
Reduced Dataset
Prevalence of GS-only Patterns
100%
75%
50%
25%
0%
pre-speciation
2-3 mya
6-7 mya
8-9 mya
10-11 mya
12-16 mya
Divergence Time Interval

Figure 13.

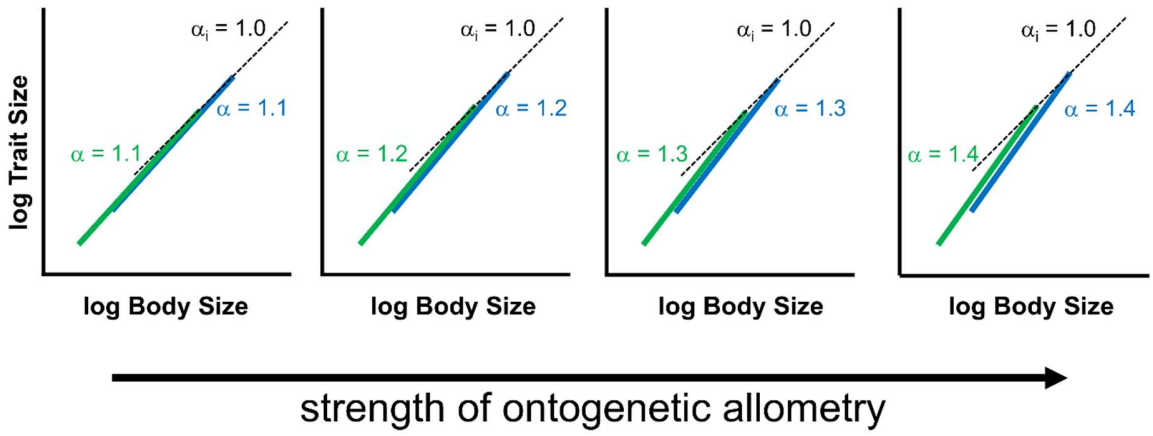
log Trait Size
α_i = 1.0
α = 1.1
α = 1.1
log Body Size
α_i = 1.0
α = 1.2
α = 1.2
log Body Size
α_i = 1.0
α = 1.3
α = 1.3
log Body Size
α_i = 1.0
α = 1.4
α = 1.4
log Body Size
strength of ontogenetic allometry

Figure 14.

Appendix 1

Using ontogenetic allometric trajectories to identify interpopulational trait scaling patterns in pygopodid lizards

A preliminary analysis of interpopulational scaling patterns for tail length and body size in pygopodid lizards was performed in June 2020 using the pairwise ontogenetic allometric trajectory approach (e.g., Kurtén 1954). In the dataset of Jennings (2002), one species of pygopodid lizard, *Pygopus lepidopodus*, was represented by samples taken from two geographically well-separated populations that differed in maximum body size. Samples of *P. lepidopodus* from the central east coast of Australia (hereafter "Eastern Population") attained larger body sizes—measured as snout-vent length (SVL)—compared to the specimens collected from the central coast of Western Australia (hereafter "Western Population"; Appendix 1—table 1). Post-natal allometric trajectories were estimated using linear regression of ln-transformed tail length (ln*Tail*) and ln-transformed snout-vent length (lnSVL) data separately for each population. The ln-transformed data points and regression lines were then plotted to show their relative positions in 2-D morphospace. The plot of the two *P. lepidopodus* populations showed overlapping trajectories during the juvenile growth stages but diverging trajectories during the adult growth stages of both populations (Appendix 1—figure 1). Given that the tail lengths of the lizards in both populations exhibited positive ontogenetic allometry (i.e., both slopes were greater than the isometric value of 1.0)—and thus fit the strong trend in pygopodid lizards (Jennings 2002), the Y-shaped scaling pattern suggests that the adults of each population diverged from each other in a manner that is consistent with geometric similarity. These results must be considered preliminary due to the low sample size in the Eastern population.

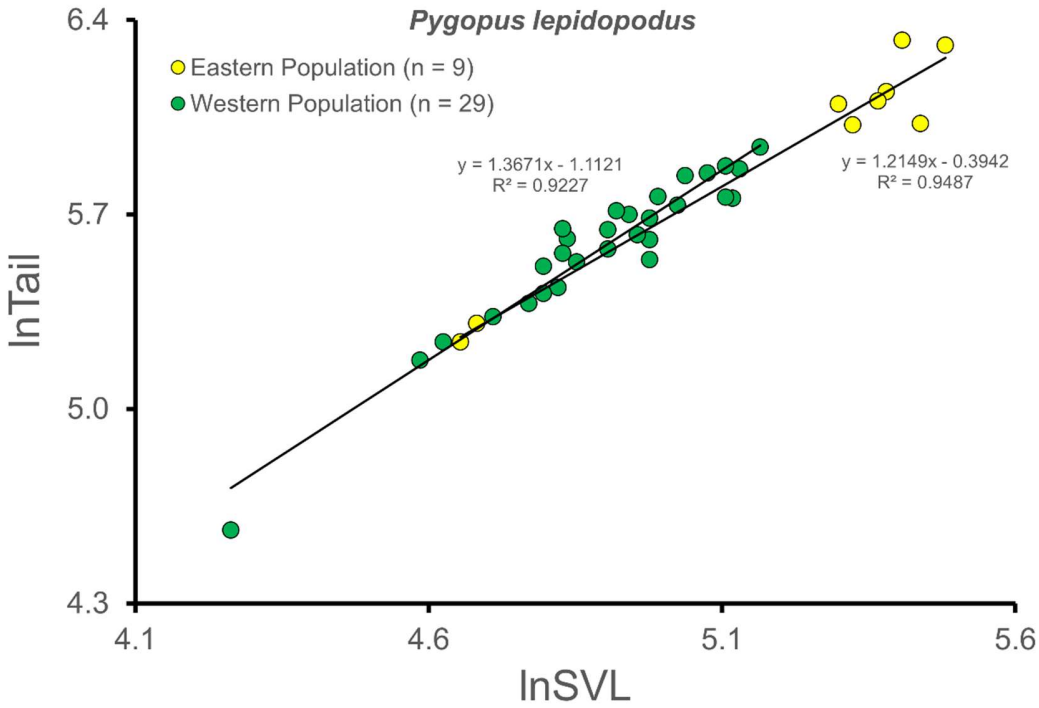

Appendix 1—figure 1. Pairwise comparison of post-natal ontogenetic allometric trajectories for two populations of *Pygopus lepidopodus*. This plot shows the bivariate scaling relationships of ln-transformed tail length (ln*Tail*) on ln-transformed snout-vent length (ln*SVL*) for each population. Individuals from the Eastern Population (yellow circles) exhibited larger maximum body sizes (measured as maximum SVL) compared to individuals in the Western Population (green circles). The least squares regression equations and R^2 values are also shown. Note that the slopes of both trajectories are greater than 1.0 (i.e., isometry) and thus both trajectories appear to show positive ontogenetic allometry. Source data are available in Appendix 1—table 1.

Appendix 1—table 1. Source data for Appendix 1—figure 1. All data for *Pygopus lepidopodus* were obtained from Jennings (2002). The "Eastern Population" refers to specimens from the states of New South Wales and Queensland, Australia, whereas the "Western Population" refers to specimens from the state of Western Australia. SVL = snout-vent length; Tail = tail length; AM = Australian Museum; QM = Queensland Museum; WBJ = William Bryan Jennings collection.

Population	**Source**	**Specimen #**	**SVL (mm)**	**Tail (mm)**
lepidopodus (Eastern population)	QM	45930	240	550
lepidopodus (Eastern Population)	QM	22531	230	415
lepidopodus (Eastern Population)	AM	R.139144	223	560
lepidopodus (Eastern Population)	AM	R.146628	217	465
lepidopodus (Eastern Population)	QM	24062	214	450
lepidopodus (Eastern Population)	QM	58779	205	413
lepidopodus (Eastern Population)	QM	6650	200	445
lepidopodus (Eastern Population)	AM	R.146229	108	202
lepidopodus (Eastern Population)	AM	R.141535	105	189
lepidopodus (Western Population)	WBJ	1837	175	381
lepidopodus (Western Population)	WBJ	2070	169	352
lepidopodus (Western Population)	WBJ	1864	167	317
lepidopodus (Western Population)	WBJ	2011	165	356
lepidopodus (Western Population)	WBJ	1841	165	318
lepidopodus (Western Population)	WBJ	1840	160	347
lepidopodus (Western Population)	WBJ	2112	154	344
lepidopodus (Western Population)	WBJ	1241	152	309
lepidopodus (Western Population)	WBJ	1565	147	319

lepidopodus (Western Population)	WBJ	1839	145	295
lepidopodus (Western Population)	WBJ	1836	145	273
lepidopodus (Western Population)	WBJ	1091	145	254
lepidopodus (Western Population)	WBJ	1872	142	278
lepidopodus (Western Population)	WBJ	1236	140	299
lepidopodus (Western Population)	WBJ	1021	137	303
lepidopodus (Western Population)	WBJ	1147	135	283
lepidopodus (Western Population)	WBJ	2471	135	264
lepidopodus (Western Population)	WBJ	1235	128	252
lepidopodus (Western Population)	WBJ	1418	126	274
lepidopodus (Western Population)	WBJ	1378	125	284
lepidopodus (Western Population)	WBJ	2312	125	260
lepidopodus (Western Population)	WBJ	2132	124	230
lepidopodus (Western Population)	WBJ	2103	121	248
lepidopodus (Western Population)	WBJ	2148	121	225
lepidopodus (Western Population)	WBJ	1880	118	217
lepidopodus (Western Population)	WBJ	1889	111	207
lepidopodus (Western Population)	WBJ	1099	102	189
lepidopodus (Western Population)	WBJ	1206	98	177
lepidopodus (Western Population)	WBJ	1810	71	96

Appendix 2

Using published data to identify interpopulational trait scaling patterns in pygopodid lizards

If a trait's ontogenetic allometric relationship is known for a monophyletic group of closely related species (i.e., species group or genus), then a simple test for geometric similarity can be applied to data consisting only of only two quantities for each operational taxonomic unit or "OTU" (i.e., population, subspecies, or species). The first quantity is the maximum known maximum body size or "maximum *X* value" of each OTU, where *X* is a measure of body size. The second quantity is the relative trait size ratio or "*Y*/*X*" value for each OTU, where *Y*/*X* represents relative trait size for a specific size-age class (e.g., adults only). If a positively allometric trait exhibits a geometric similarity pattern (Figure 1A), then the maximum *Y*/*X* (i.e., for adults) of the smaller OTU is expected to be a greater value than the maximum *Y*/*X* value for the larger OTU. If, on the other hand, a positively allometric trait displays ontogenetic scaling (Figure 1C) or evolutionary allometry via transposition patterns (Figure 1E), then the maximum *Y*/*X* value for the larger OTU will be greater than the maximum *Y*/*X* of the smaller OTU. Note that this test cannot discriminate between ontogenetic scaling and evolutionary allometry via transposition. In this case, the larger OTU is expected to have the larger maximum *Y*/*X* value of the two OTUs.

If a negatively allometric trait exhibits a geometric similarity pattern (Figure 1B), then the maximum *Y*/*X* (i.e., for adults) of the smaller OTU is expected to be a greater value than the maximum *Y*/*X* value for the larger OTU. Note, however, that in contrast to traits that exhibit

positive ontogenetic allometry, the maximum *Y*/*X* for a trajectory showing negative ontogenetic allometry is found early in post-natal development. Therefore, juveniles will have larger *Y*/*X* than adults along a given trajectory. However, this is not a complication provided that the *Y*/*X* values for a pair of OTUs represent a comparable size-age class. Accordingly, the *Y*/*X* of the larger species will be larger than the corresponding *Y*/*X* for the smaller species when the trait exhibits geometric similarity. If, on the other hand, a negatively allometric trait displays ontogenetic scaling (Figure 1D) or evolutionary allometry via transposition patterns (Figure 1F), then the *Y*/*X* value for the smaller OTU will be greater than the corresponding *Y*/*X* of the larger OTU. As before, this test cannot discriminate between ontogenetic scaling and evolutionary allometry via transposition.

Application of the test to published summary data for pygopodid lizards

Pygopodid lizards exhibited a strong trend of positive ontogenetic allometry for tail length when the natural log of tail length or "ln*tail*" was regressed against the natural log of snout-vent length or "lnSVL," a measure of body size (Jennings 2002). Using this information along with published estimates of maximum SVL and maximum relative tail length (maximum tail length as a percentage of SVL), it was possible to test several OTU pairs for geometric similarity using the above methodology. Because it was expected that very recently diverged conspecific populations (subspecies) or sister species would show tail divergence patterns consistent with geometric similarity, a search of the literature for appropriate pygopodid OTU pairs was conducted. The search yielded three pairs with the required data for this test. The first OTU pair (*Delma concinna concinna* vs. *D. c. major*) comprised two subspecies while the latter two pairs (*Delma haroldi* vs. *D. butleri* and *Pletholax gracilis* vs. *P. edelensis*) consisted of two very recently

diverged sister species according to phylogenetic studies (Brennan et al 2016; Skipwith et al. 2019; Keally et al. 2020). For each pairwise comparison, the OTU with the smaller maximum body size showed a relatively longer tail (**Appendix—table 1**). These results were therefore consistent with geometric similarity for the adult size-age classes in these species.

Appendix 2—table 1. Published estimates of maximum snout-vent length (SVL) and maximum relative tail length (tail length expressed as percentage of SVL) for three pygopodid lizard OTU pairs. OTU = operational taxonomic unit (i.e., subspecies or species). Note that *Aclys concinna concinna* and *A. c. major* (vis-à-vis Storr 1987) are now referred to as *Delma concinna concinna and D. c. major* (Jennings et al. 2003), while *Pletholax gracilis edelensis* (vis-à-vis Storr 1978) is now *Pletholax edelensis* (Keally et al. 2020).

pairwise comparison of comparable OTUs	OTU	maximum SVL (mm)	length of tail (% SVL)	source of data
Delma concinna concinna vs. *D. c. major*	*Delma concinna concinna*	101	450%	Storr 1987
Delma concinna concinna vs. *D. c. major*	*Delma concinna major*	112	438%	Storr 1987
Delma haroldi vs. *D. butleri*	*Delma haroldi*	75	369%	Storr 1987
Delma haroldi vs. *D. butleri*	*Delma butleri*	91	345%	Storr 1987
Pletholax gracilis vs. *P. edelensis*	*Pletholax gracilis*	83	346%	Storr 1978
Pletholax gracilis vs. *P. edelensis*	*Pletholax edelensis*	90	340%	Storr 1978

Appendix 3

Identifying interspecific trait scaling patterns between *Delma branchia* and *D. pax* of the Delma tincta species group using a combination of data from this study and a published study

Pepper et al. (2025) conducted a molecular and morphological study of the Delma tincta species group. We can use the testing framework described in Appendix 2 above to determine if *D. branchia* and *D. pax* exhibit patterns consistent with geometric similarity or evolutionary allometry. To perform the test, we can use snout-vent-length (snout-vent-length), head width at the ears (HeadW), and tail length (TailL) data for *D. branchia* in Appendix 4 of Pepper et al. (2025) with comparable data for *D. pax* in this paper. Note, that in this analysis, head width at the ears will be assumed to be the same as average body width because body width data were not available in Pepper et al. (2025). The results suggest that *D. pax* attains a greater maximum *SVL* than *D. branchia* and that the two species show geometric similarity for all three traits (Appendix 3—table 1).

Appendix 3—table 1. Estimates of maximum snout-vent length (*SVL*), maximum relative tail length (tail length expressed as percentage of *SVL*, maximum relative tail length (tail length expressed as a percentage of head width at the ear [HeadW], and HeadW as a percentage of *SVL*) for *Delma pax* and *Delma branchia*. OTU = operational taxonomic unit (i.e., species).

OTUs	maximum SVL (mm)	length of tail (% SVL)	length of tail (% head width at ear)	head width at ear (% SVL)	source of data
Delma pax	98	347%	5567%	8.8%	this study
Delma branchia	93	368%	5842%	7.2%	Pepper et al. 2025